2005-12-15

Electromagnetism in Gravitational Collapse

Craig Ernest Skinfill

Brigham Young University - Provo

ELECTROMAGNETISM IN AXISYMMETRIC GRAVITATIONAL

COLLAPSE

by

Craig Skinfill

A thesis submitted to the faculty of

Brigham Young University

in partial fulfillment of the requirements for the degree of

Master of Science

Department of Physics and Astronomy

Brigham Young University

April 2006

BRIGHAM YOUNG UNIVERSITY

GRADUATE COMMITTEE APPROVAL

of a thesis submitted by

Craig Skinfill

This thesis has been read by each member of the following graduate committee and by majority vote has been found to be satisfactory.

_____	_____
Date	Eric W. Hirschmann, Chair
_____	_____
Date	Ross L. Spencer
_____	_____
Date	Jean-Francois Van Huele

ABSTRACT

ELECTROMAGNETISM IN AXISYMMETRIC GRAVITATIONAL COLLAPSE

Craig Skinfill

Department of Physics and Astronomy

Master of Science

A numerical approach to including electromagnetism with general relativity is developed using `GRAXI` [1] as a starting point. We develop a mathematical model describing electromagnetism coupled to a scalar field in an evolving axisymmetric spacetime. As there are numerous formulations of electromagnetism, we evalute different formulations in a limited flat space case. The full curved space system is then developed, using the flat case as a guide to implementing electromagnetism. This model is then implemented using `GRAXI` as a code base.

ACKNOWLEDGMENTS

Contents

x

List of Figures

Chapter 1

Introduction

It is widely believed that some of the universe's most energetic phenomena such as gamma ray bursts, supernovae, jets, magnetars, neutron stars and accretion disks around black holes involve the interaction of strong gravitational and electromagnetic fields. A good understanding of these interactions is required to accurately understand these astrophysical processes. Currently, many of the models for these objects ignore general relativistic effects by using a Newtonian approach or, at best, assume a particular fixed black hole spacetime and then evolve electromagnetic fields on this gravitational background without accounting for the back reaction of the fields on the spacetime curvature.

Only by including both general relativity and electromagnetism can these objects be correctly modeled. This requires taking into account the effects of the electromagnetic field on the spacetime. This is a non-linear coupling between gravity and electromagnetism that increases the difficulty and challenge of understanding these energetic objects. By creating computer models that include electromagnetism and gravitation it becomes possible to begin to understand these objects and the complex interaction of these fields.

There is a long history of combining electromagnetism with general relativity. A few examples highlighting some of the challenges and importance of coupling gravity and electromagnetism are presented here. The Reissner-Nordstrom solution is that of a static, stationary, charged, non-rotating black hole. This should be compared with the Schwarzschild line element which describes a neutral non-rotating black hole. Additionally, there is a similar charged generalization called the Kerr-Newman black

hole for rotation Kerr black holes. The line element for Reissner-Nordstrom, a charged non-rotating black hole, generalizes the Schwarzschild solution by including terms involving the black holes's charge. In the limit that the charge is zero, the originial Schwarzschild solution is recovered. While this is an apparently trivial generalization, in reality this leads to a significantly different spacetime. The original Schwarzschild solution allows for a singularity surrounded by an event horizon. The inclusion of charge, however, leads to splitting the original Schwarzschild event horizon into two surfaces. This simple example shows the significant difference of adding electromagnetism to a fully relativistic system. For more details on the Reissner-Nordstrom solution see Chapter 18 of [2].

Another example of integrating electromagnetism with general relativity involves investigations into neutron star formation and evolution. The process of forming a neutron star and its behaviour are expected to be dictated, in large part, not just by the strong gravitational fields but also the electromagnetic fields which will exist in its vicinity. In addition to the material going into forming the star itself, the electromagnetic fields are expected to be strong enough to be a soure for the gravitational fields themselves.

Yet another example of new physics arising from the combination of electromagnetism and general relativity is the Blandford-Znajek mechanism [3], which is an electromagnetic realization of the Penrose process. The original idea behind the Penrose process is that with a rotating or Kerr black hole it is theoretically possible to extract energy from the black hole. The Blandford-Znajek mechanism does essentially the same thing by utilizing strong poloidal magnetic fields threading the black hole. To realize these magnetic fields requires that there be an accretion disk near the vicinity of the black hole. The conjecture is that there is a non-zero outgoing Poynting flux originating in the ergosphere of the rotating black hole. The original mechanism was suggested in an approximation due to the complexity of the combined Einstein-Maxwell equations. As a result, this process is still not completely understood and remains a topic of considerable debate in the formation and dynamics of material in the vicinity of astrophysical black holes. While this will not be the focus of this work,

it would be interesting to solve the full Einstein-Maxwell equations and get a better sense of this process and its significance astrophysically for energy extraction.

Within numerical relativity, there are also numerous examples of adding electromagnetism to Einstein's equation, but often the spacetime is fixed and only the matter and electromagnetic fields evolve. An example of this approach can be seen by Baumgarte and Shapiro[4, 5]. Initially they develop a generalized mathematical model for solving relativistic magnetohydrodynamics. Later they work to implement this model numerically but choose a fixed spacetime, namely the spherical collapse of a pressureless fluid to a black holer[5]. In other words, they decide to fix the spacetime as a forming black hole and allow for no dynamical change to the spacetime, asking only how the electromagnetic fields are affected.

While we are not developing a relativistic magnetohydrodynamic model, the work by Baumgarte and Shapiro does represent a common approach to dealing with the spacetime. By choosing a fixed spacetime some of the complexities are removed from the system. The only variables that need be evolved are those for the matter fields. Certainly, choosing a curved spacetime will change the resulting equations of motion for the matter fields, but by not evolving the spacetime the system of equations can be simplified substantially. In our case we would like to go beyond this and develop a model which includes an evolving spacetime.

These proceeding examples show some of the work to combine gravity and electromagnetism. They are in no way exhaustive, but demostrate some of the challenges and exciting possibilities of coupling general relativity and electromagnetism. In our case, however, one of our primary motivations for considering electromagnetism coupled to full general relativity stems from the discovery in the last fifteen years of critical behaviour at the threshold of black hole formation in gravitational collapse. This work was, in large part, initiated by Choptuik's discovery [6] that there is new unexpected behaviour in gravitational collapse. The particular example considered by Choptuik was that of general relativity coupled to a scalar field in spherical symmetry. When considering gravitational collapse in such a system, he found a power

law scaling relationship for the black hole mass, M_{BH}, in terms of parameters describing the initial scalar field data. If one takes some characteristics of the initial data, such as the amplitude, and parameterizes it with the paramter p, then there is a critical value called p^*. The significance 0f this critical valus is that for $p < p^*$, a black hole will not form and the evolution of this initial data for this simplified model will disperse to infinity, leaving behind flat space. On the other hand for $p > p^*$ gravitational collapse of this initial data will lead to the formation of a black hole of some mass. Mathematically, this can be expressed through the scaling law

$$M_{BH} \propto |p - p^*|^{\beta} \tag{1.1}$$

where, for the scalar field case, $\beta = 0.37$ and p^* is specific to the initial data. What is particularly unexpected about this scaling law is that its form holds for any p which describes the initial data. For instance, suppose the initial state of the system is an origin centered ring. p could be the initial amplitude, the initial radius, the "width" of the ring, etc. The critical parameter, p^*, will be different for different p's, but the scaling law is universal in the sense that the value of the scaling exponent, β, holds for any set of these parameters.

In addition to the scaling law there is also an unexpected and new symmetry for the evolution of the initial data characterized by p^*. In particular the solution exhibits self-similarity. In the originally considered scalar field case the self-similarity is discrete. This means that if one takes a snapshot of the solution at a given time and at a subsequent time but rescaled, one observes the same waveform. In addition, this critical solution in the language of dynamical systems serves as an intermediate attractor for nearby evolutions in initial data space. In other words, for initial data just slightly supercritical, *i.e.*, $p = p^* + \epsilon$, there is a period of time in which the evolution looks exactly like the discretely self-similar critical solution. After this time interval, the evolution eventually runs away to become a black hole solution. A similar thing happens for slightly subcritical initial data. This discovered behaviour at the threshold of black hole formation has generated considerable additional work [7, 8, 9, 10]. Indeed this critical behaviour has been found in a variety of spherically

symmetric systems. There is some work in axisymmetry and a few attempts in systems with no symmetry. So far, electromagnetism as a possible source for the gravitational collapse has not been considered. This is because in spherical symmetry there is no electromagnetic radiation. Therefore one must go to axisymmetry and solve the full set of Einstein-Maxwell equations. But if this could be done, it would amount to forming a black hole from light.

Subsequent chapters describe our attempt to develop a means of solving these axisymmetric Einstein-Maxwell equations. We simulate the full evolution of a spacetime with an electromagnetic field coupled to a scalar field in axisymmetry. An important feature of the code we develop is the evolution of the spacetime itself. While a dynamic spacetime adds a great deal of complexity and challenge, it is the only way to adequately study gravitational collapse. We are able to use an existing axisymmetric general relativity code, `GRAXI` [1], and add electromagnetism to it. In fact, one of our primary goals is to generalize `GRAXI` by including electromagnetism to provide for a foundation to study critical behaviour with electromagnetism.

The subsequent sections of this chapter provide additional background to orient ourselves in this larger work. Chapter 2 will be a discussion of a few flat space models without gravity, while Chapter 3 presents the full curved space model. The final chapter presents results on our numerical implementation. Appendices at the end include a primer on differential geometry and some of the more unwieldy equations in a single place.

1.1 General Relativity

Special relativity was developed by Einstein in 1905, and deals with observers in inertial frames without gravity. The Law of Inertia, Newton's first law, states that

Every body continues in its state of rest or of uniform motion in a straight line unless it is compelled to change that state by forces acting on it.[2]

Inertial frames are frames which are not accelerating and experience no net forces. Special relativity was initially developed to deal with inconsistencies between Newton's mechanics and Maxwell's electromagnetism.

General relativity expands on the special theory, by including a covariant description of gravity. According to general relativity, gravitation is caused by the curvature of spacetime due to the presence of mass and energy. In this theory, mass and energy are represented by the stress-energy tensor, which takes into account the relationship between energy and mass ($E = mc^2$). As a configuration of mass-energy changes, and as the stress-energy tensor evolves the very nature of spacetime changes as well. Essentially, spacetime itself becomes a dynamic entity and the Einstein equation governs its evolution (see 1.2).

Due to the dynamic nature of spacetime, the concept of a "straight" line needs to be reconsidered. In Euclidean geometry, a straight line is a curve that minimizes the distance between any two points. However, if we constrain ourselves to the surface of a sphere, such as the Earth, a straight line is no longer the minimal distance. For two points on the surface of a sphere, the minimal distance is a great circle. The generalized idea of a "straight" line, or minimal distance, is a *geodesic*. A geodesic is simply defined as a curve which "... extremizes the distance between two fixed points."[11] In the language of general relativity observers which are unaffected by external forces follow timelike geodesics (see Appendix A.2.2). Gravity thus becomes a consequence of a curved spacetime, rather then an external force.

The mathematical language in which the theory is expressed is called differential geometry.[1] This branch of geometry deals with calculus on arbitrary curved surfaces or spaces and accounts for non-Euclidean geometries. It is this non-Euclidean aspect that gives general relativity its most exciting predictions and possibilities.

1.2 Einstein's equation

Einstein's equation is deceptively simple in appearance:

$$G_{ab} = \frac{8\pi G}{c^4} T_{ab} \tag{1.2}$$

---

[1]Appendix A for a primer on differential geometry

This is a tensor equation relating the Einstein tensor, G_{ab}, and the stress-energy tensor, T_{ab} [2]. In this equation the Einstein tensor encodes the curvature and geometry of the spacetime manifold. The stress-energy tensor describes matter and energy. The stress-energy tensor is frequently seen outside of general relativity (for instance, fluid mechanics). The Einstein tensor is further defined as

$$G_{ab} = R_{ab} - \frac{1}{2}R\gamma_{ab} \tag{1.3}$$

where R_{ab} is the Ricci tensor, R is the Ricci scalar and γ_{ab} is the metric tensor of four dimensional spacetime. Often the metric is represented by the variable g_{ab}, but in anticipation of latter chapters, we will reserve the variable g_{ab} for the metric of a reduced three dimensional spacetime and γ_{ab} for the full 4-dimensional spacetime. These quantities are the geometric quantities in the Einstein equation.

In a four-dimensional spacetime, Einstein's equation is actually a system of 10 coupled, second-order, non-linear, partial differential equations for the components of the metric tensor. This complex set of equations leads to many of the difficulties and challenges of general relativity.

1.3 Our Model

The system we are studying is the gravitational collapse of electromagnetism and a scalar field ϕ in axisymmetry. GRAXI [1] was developed to study critical behaviour in axisymmetry and we intend to extend it by adding electromagnetism. In this way we can begin to expand the theoretical framework handled by GRAXI and test the results for cases with electromagnetism. In addition, we are also developing a general mathematical theory for handling electromagnetism in a curved axisymmetric spacetime. It is hoped that this will provide a framework and foundation for further development.

The action for this system of a scalar field and electromagnetism in curved space is the following

$$S = \int \sqrt{-\gamma}\, d^4x \left\{ R - \frac{a_0}{2}(\mathcal{D}_\mu \phi)(\mathcal{D}^\mu \phi)^* - \frac{a_1}{4}F_{\mu\nu}F^{\mu\nu} - a_2 V(\phi, \phi^*) \right\}. \tag{1.4}$$

---

[2]Note that G, in the coupling constant $8\pi G/c^4$, is the Universal Gravitational constant rather then the trace of the Einstein tensor.

Where we have made the following definitions

$$\mathcal{D}_\mu \phi = \nabla_\mu \phi - ieA_\mu \phi \tag{1.5}$$

$$F_{\mu\nu} = \nabla_\mu A_\nu - \nabla_\nu A_\mu = \mathcal{D}_\mu A_\nu - \mathcal{D}_\nu A_\mu \tag{1.6}$$

$$\phi = \phi_1 + i\phi_2 \tag{1.7}$$

We will refer to $\mathcal{D}_\mu$ as the gauge covariant derivative, defined by its action on the scalar field ϕ shown above. ∇_μ is the usual spacetime covariant derivative appropriate to the 4-metric $\gamma_{\mu\nu}$.[3] The constants a_0, a_1, and a_2 are included to allow us to tune the strength of the individual contributions to the action. Additionally, we can explore various subsets of this system by setting the appropriate constant to zero. For instance, we can remove the scalar field from the system by setting $a_0 = a_2 = 0$.

The Maxwell tensor, $F_{\mu\nu}$, is composed from the 4-vector gauge potential A_μ. In a relativistic formulation of electromagnetism the electromagnetic fields are represented as a single second rank antisymmetric tensor, $F_{\mu\nu}$, instead of two vector fields, $\vec{E}$ and $\vec{B}$. R is the Ricci scalar, and $V(\phi, \phi^*)$ is included to allow for a potential between the real and imaginary components of the scalar field. The square root of the determinant of the metric, γ, is included to ensure that we have a tensor density of weight $+1$. The Einstein equation for this system is derived by varying this action with respect to the metric. In addition, the equations of motion for the individual matter fields can be derived by varying the action with respect to the relevant matter fields.

1.4 $(2+1)+1$ decomposition

A set of evolution equations must be derived from the Einstein equations. The principle of general covariance states that physical laws should be invariant under a change of coordinates, including time. This is a fundamental principle in general relativity. Ideally, any means of extracting evolution equations should still conform to this principle. Because of time's role in relativity, namely as a coordinate in a 4 dimensional manifold or spacetime, this can be challenging. Singling out the

---

[3]See Appendix A.3.

time coordinate from the spatial coordinates seems inconsistent with the principles of general relativity and the ideas of general covariance. However, it is something we must do in order to get a meaningful evolution problem. The resulting set of equations should still be coordinate invariant, but may not be so in an obvious way.

One way to separate out the time coordinate is via the ADM decomposition (of Arnowitt, Deser and Misner) [12].[4] In the traditional ADM approach we distinguish a time-like direction normal to a family of purely spatial hypersurfaces on which we have an evolving reduced metric specific to the spatial hypersurface. This resulting reduced metric is purely spatial, and represents the spatial portion of the metric of the full spacetime. The vector field normal to the spatial hypersurfaces is chosen to be time-like. All of the various tensor quantities are projected into the spatial metric and along the time-like vector field. After doing this, we are able to define evolution equations as those equations with Lie derivatives along the time-like vector field.[5] A series of constraint equations are also formed as projections into the space-like metric that do not involve projections along the time-like vector. These constraint equations are conceptually similar to the $\nabla \cdot \vec{B} = 0$ equation in the Maxwell equations. The constraint equations do not involve "time derivatives", which in this case are derivatives projected along the time-like vector field. These equations are neccessary to describe consistent initial data for the general relativistic Cauchy problem.

Having described the traditional ADM decomposition, our approach is to modify the ADM decomposition because we are assuming the existence of an axisymmetric Killing vector.[6] There are two analytically equivalent "paths" to deriving the equations of motion from the action: vary with respect to the fields and then use the Killing vector to cancel terms in an adapted coordinate system, or, use the Killing vector to enforce the symmetry at the level of the action and then vary using the Euler-Langrange equations. Because we assume axisymmetry from the outset it is natural to consider the second option. In practice this leaves a three dimensional spacetime manifold on which we will then perform the ADM decomposition described above,

---

[4]This is a standard approach in numerical relativity, see page 146 of [11].

[5]See Appendix A.5

[6]See Appendix A.8 for a description of a Killing vector.

but now dividing out a time direction and spatial hypersurfaces which are only two dimensional.

1.5 Numerical approach

Once we have the appropriate equations in hand, we will use some standard techniques from numerical relativity. We use exclusively finite difference techniques on a finite two dimensional uniform grid. Our basic numerical approach for the time integration is to use an iterative Crank-Nicholson scheme. The traditional Crank-Nicholson scheme involves averaging terms with respect to time. For example, consider the simple one dimensional advection equation[7]

$$u_{,t} = cu_{,x} \tag{1.8}$$

where, u is our field and c is its constant velocity. The advection equation is a partial differential equation representing a propagating scalar field, u. The solution to the advection equation is

$$u = u(x,t) = V(x + ct) \tag{1.9}$$

where $V(x + ct)$ is an arbitrary function.

A difference equation is a discrete representation of a differential equation. Using the definition of the derivative,

$$\frac{\partial u}{\partial t} \equiv \lim_{h \to 0} \frac{u(t+h) - u(t)}{h} \tag{1.10}$$

we can approximate the partial derivative with a difference equation of using the above definition of a derivative,

$$\frac{\partial u}{\partial t} \approx \frac{u_i^{n+1} - u_i^n}{\delta t} \tag{1.11}$$

The notation is important, and in the case of u_i^n the superscript represents evaluating the function u at the "n^{th}" timestep while the subscript represents the "i^{th}" grid point. The size of the timestep is represented by the variable δt. In the case of u_i^{n+1}, the function is evaluated at the ith grid point and at the $n+1$ timestep. It is

---

[7]Note that here, and throughout, the "," represents partial differentiation, $i.e.$ $u_{,t} \equiv \frac{\partial u}{\partial t}$.

also possible, and sometimes desirable for stability purposes [13], to use alternative definitions of the derivative, such as a centered difference approximation as opposed to the "forward" difference approximation above.

$$\frac{\partial u}{\partial t} \equiv \lim_{h \to 0} \frac{u(t+h) - u(t-1)}{2h} \to \frac{u_i^{n+1} - u_i^{n-1}}{2\delta t}. \tag{1.12}$$

One advantage of the centered scheme is that it can be shown that this centered derivative is more accurate then the forward derivative defined in Eq. 1.11. The truncation error for the centered scheme is $\mathcal{O}(h^2)$ while the trunctation error of the forward derivative is only $\mathcal{O}(h)$. On the other hand, this scheme requires knowledge of points in the past, represented by u_i^{n-1} in Eq. 1.12.

Because we are often looking at evolution equations of a field on some sort of a time-space grid, one useful approach is to use forward differences in time and centered differences in space. This is often called FTCS or forward time centered space. The advection equation can be represented as a FTCS difference equation

$$\frac{u_i^{n+1} - u_i^n}{\delta t} = c \frac{u_{i+1}^n - u_{i-1}^n}{2\delta x}. \tag{1.13}$$

The Crank-Nicholson scheme is formed by taking a time average of the right-hand side at the n and $n+1$ time levels. This leads to

$$\frac{u_i^{n+1} - u_i^n}{\delta t} = c \left(\frac{u_{i+1}^{n+1} - u_{i+1}^n}{4\delta x} - \frac{u_{i-1}^{n+1} - u_{i-1}^n}{4\delta x} \right). \tag{1.14}$$

By solving Eq 1.14 for terms involving u^{n+1} we now have an equation that relates future values of u to the present (at the ith timestep) value of u. This resulting equation is

$$u_i^{n+1} - \frac{c\delta t}{4\delta x} \left(u_{i+1}^{n+1} - u_{i-1}^{n+1} \right) = u_i^n + \frac{c\delta t}{4\delta x} \left(u_i^n - u_i^n \right). \tag{1.15}$$

Notice, however, that there isn't a single term involving $n+1$. This is representable as a tridiagonal matrix equation[8] for u^{n+1} in terms of u^n. It is an example of an implicit scheme[13]. Such schemes for linear wave equations are unconditionally stable [13]. However, for a one-dimensional problem with a resolution of N points, an $N \times N$ matrix must be inverted at every time step.

---

[8]Due to the $i+1$, i and $i-1$ grid points

Because the traditional Crank-Nicholson involves inverting a matrix, which can be computationally very expensive and prone to error if the matrix is close to singular, we use an iterative approach. The new iterative difference equation is

$$^{(k+1)}u_i^{n+1} = u_i^n + \frac{c\delta t}{2}\left(\frac{^{(k)}u_{i+1}^{n+1} - ^{(k)}u_{i-1}^{n+1}}{2\delta x} - \frac{u_{i+1}^n - u_{i-1}^n}{2\delta x}\right). \tag{1.16}$$

where k represents the kth iteration. Essentially, at each time-step the algorithm solves the equations using the previous answer as a starting point, until the solutions converge to an answer, which generally happens within about 3 steps. The comparison algorithm involves taking a norm of the difference between iterations.

$$||^{(k+1)}u_i^{n+1} - ^{(k)}u_i^{n+1}|| \to \epsilon \tag{1.17}$$

If this is within some tolerance ϵ then the iterative algorithm ends and the last iteration is used as the result.

We use this iterative approach for solving the evolution equations of Einstein's system. However, there are also constraint equations that must be satisfied. The constraint equations are solved independent of the evolution equations at each time step of the evolution. The constraint equations are crucial for finding consistent initial data. Analytically, the constraint equations for general relativity should be satisfied automatically by the evolution equations. However, due to approximations and round-off error the constraints may not be satisfied throughout the numerical evolution. Solving these constraint equations provides an important check on the stability of the system. Unfortunately, solving the constraint equations tend to be numerically expensive.

It is possible to use the constraint equations to determine initial data, and then only solve the evolution equations. This is often refered to as *free evolution*. On the other hand, we can solve the constraint equations on each time step of the evolution and have a fully *constrained evolution*. A free evolution is computationally simple and faster, but at the risk of errors propagating because of round-off and approximations. While the constrained evolution involves significantly more computational resources. The constrained evolution will, because it solves the constraints on each time step, be more accurate.

As part of our computational infrastructure we use a tool called RNPL[14], which is an acronym for Rapid Numerical Prototype Language. This is a language for modeling systems of time-dependent partial differential equations. Rather than dealing with lower-level concerns like memory management, file I/O, etc., RNPL allows developers to focus on the actual equations that need to be modeled and expresses them in a specialized language. This language is used frequently in numerical relativity.

GRAXI[1], or **G**eneral **R**elativity **AXI**symmetry, is a code for numerical relativity in axisymmetry developed by Choptuik, Hirschmann, Liebling, and Pretorius[1]. GRAXI deals with scalar fields in axisymmetry, or spacetime with a single Killing vector with cylindrical-like symmetry. GRAXI was developed primarily to study critical behaviour in gravitational collapse of a scalar field in axisymmetry. By adding electromagnetism, we can generalize this and use it to study critical behaviour involving electromagnetism.

Chapter 2

Flat Space

While our ultimate aim is to study electromagnetism in full general relativity, it is nonetheless useful to get there by way of simpler, toy models. By developing and solving some simpler problems we would hope that we will learn some things that will be useful. One possibility is to consider the equations of axisymmetric scalar electrodynamics in flat space as a starting point. Rather then addressing the complex *curved* space problem, we can first look at this system in *flat* space. This gives us a few advantages: exposure and experience using RNPL and a chance to evaluate different formulations of electromagnetism to be used in curved space.

2.1 Equations for flat-space

To begin, we start with the action given in Eq. 1.4 and the associated definitions in Eqs. 1.5 - 1.7,

$$S = \int \sqrt{-\gamma}\, d^4x \left\{ R - \frac{a_0}{2}(\mathcal{D}_\mu \phi)(\mathcal{D}^\mu \phi)^* - \frac{a_1}{4} F_{\mu\nu} F^{\mu\nu} - a_2 V(\phi, \phi^*) \right\}. \qquad (2.1)$$

Here, we simplify it for flat space. The Ricci scalar, R, is a measure of curvature and we are choosing a spacetime that is flat therefore R vanishes. We can set $R = 0$ and γ then becomes appropriate to a flat space metric, usually depending at most on some coordinate choice. For this toy problem, we will also set $a_2 = 0$, implying that there is no potential between the complex components of the scalar field. The action now reduces to

$$S = \int \sqrt{-\gamma}\, d^4x \left\{ -\frac{a_0}{2}(\mathcal{D}_\mu \phi)(\mathcal{D}^\mu \phi)^* - \frac{a_1}{4} F_{\mu\nu} F^{\mu\nu} \right\}. \qquad (2.2)$$

The equations of motion are derived by using the Euler-Lagrange equations

$$\frac{\partial \mathcal{L}}{\partial \phi} - \nabla_a \left\{ \frac{\partial \mathcal{L}}{\partial (\nabla_a \phi)} \right\} = 0 \tag{2.3}$$

and varying with respect to ϕ, ϕ^* and A_μ. The variation with respect to ϕ^* gives

$$\nabla_a \nabla^a \phi = \nabla_a (ieA^a \phi) + ieA^a \mathcal{D}_a \phi \tag{2.4}$$

$$= 2ieA^a \nabla_a \phi + e^2 \phi A_a A^a + ie\phi \nabla_a A^a \tag{2.5}$$

and varying by ϕ would lead to the complex conjugate of this equation. For A_μ we must use Eqs. 1.5 and 1.6 to realize that while A_μ may not appear explicitly in this form of the action, it is nonetheless there. Expanding the action, to highlight the A_μ dependence, yields

$$S = \int \sqrt{-\gamma} \, d^4 x \left\{ -\frac{a_0}{2} (\nabla_\mu \phi - ieA_\mu \phi)(\nabla^\mu \phi - ieA^\mu \phi)^* \right.$$
$$\left. -\frac{a_1}{4} (\nabla_\mu A_\nu - \nabla_\nu A_\mu)(\nabla^\mu A^\nu - \nabla^\nu A^\mu) \right\}. \tag{2.6}$$

Varying with respect to A_μ leads to

$$\nabla_a F^{ab} = ie\frac{a_0}{a_1} \left[\phi^* \mathcal{D}^b \phi - \phi (\mathcal{D}^b \phi)^* \right] \tag{2.7}$$

$$= \frac{a_0}{a_1} \left[ie \left\{ \phi^* \nabla^b \phi - \phi \nabla^b \phi^* \right\} + 2e^2 \phi \phi^* A^b \right]. \tag{2.8}$$

Eqs. 2.4, 2.7 and the complex conjugate of 2.4 are the equations of motion for the flat space system, expressed covariantly.

At this point we have made no decision on the coordinates for this system. Because we are interested in axisymmetry, we choose a coordinate system in which the metric is

$$ds^2 = -dt^2 + d\rho^2 + \rho^2 d\varphi^2 + dz^2. \tag{2.9}$$

This is the standard metric of flat space in cylindrical coordinates. With this choice of coordinates the determinant is $\gamma = -\rho^2$, and the non-zero terms in the connection[1] are

$$\Gamma^\varphi{}_{\rho\varphi} = \frac{1}{\rho} \tag{2.10}$$

$$\Gamma^\rho{}_{\varphi\varphi} = -\rho \tag{2.11}$$

---

[1] See Appendix A.4

In addition to coordinate choices, we can, in electromagnetism, pick a gauge. For radiative problems a common choice is the Lorenz gauge,

$$\nabla_a A^a = 0. \tag{2.12}$$

With this set of assumptions and choices, the equation for ϕ, Eq. 2.4, simplifies to

$$\nabla_a \nabla^a \phi = 2ieA^a \nabla_a \phi + e^2 \phi A_a A^a \tag{2.13}$$

As we develop this system of equation, we will choose to work in an orthonormal basis, where the components of any vector, v_a, can be expressed as

$$v_{\hat{i}} = e_{\hat{i}}{}^a v_a \tag{2.14}$$

and where

$$\eta_{\hat{i}\hat{j}} = g_{ab} e_{\hat{i}}{}^a e_{\hat{j}}{}^b \tag{2.15}$$

is the Minkowski frame metric with signature +2. Given the coordinate choice from above, this leads to the following set of basis vectors

$$e_{\hat{t}}{}^a = (1, 0, 0, 0) \tag{2.16}$$

$$e_{\hat{\rho}}{}^a = (0, 1, 0, 0) \tag{2.17}$$

$$e_{\hat{\varphi}}{}^a = (0, 0, 1/\rho, 0) \tag{2.18}$$

$$e_{\hat{z}}{}^a = (0, 0, 0, 1). \tag{2.19}$$

This process of expanding with an orthonormal basis will also work with higher rank tensors. Applying this process to the Maxwell tensor leads to the following definitions

$$F_{\hat{\rho}\hat{t}} = E_\rho \tag{2.20}$$

$$F_{\hat{\varphi}\hat{t}} = \rho E_\varphi \tag{2.21}$$

$$F_{\hat{z}\hat{t}} = E_z \tag{2.22}$$

$$F_{\hat{\rho}\hat{\varphi}} = \rho B_z \tag{2.23}$$

$$F_{\hat{z}\hat{\rho}} = B_\varphi \tag{2.24}$$

$$F_{\hat{\varphi}\hat{z}} = B_\rho. \tag{2.25}$$

17

One of the values of expressing the vectors in this basis is to deal with regularity issues on the axis. The orthonormal basis absorbs some of the $1/\rho$ factors, and they are no longer a part of the evolution equations.

From this point on in this chapter on flat space, we will drop the hats on the components. It should now be understood that all components are expressed in an orthonormal basis as we have developed here.

2.2 EM formulations

One of the goals of this flat-space system is to evaluate different formulations of electromagnetism. Analytically, there are a large set of formulations that are consistent and complete. For instance, electromagnetism can be formulated exclusively with the scalar (φ) and 3-vector ($\vec{A}$) potential along with a gauge condition. On the other hand, one can also working strictly with the electric and magnetic fields, and not address the potential fields at all. These formulations are related by

$$\vec{E} \;=\; -\nabla\varphi - \frac{1}{c}\frac{\partial\vec{A}}{\partial t} \tag{2.26}$$

$$\vec{B} \;=\; \nabla\times\vec{A} \tag{2.27}$$

$$\nabla\cdot\vec{A} \;=\; -\frac{1}{c^2}\frac{\partial\varphi}{\partial t}. \tag{2.28}$$

Because we are forced to work with the finite-difference form of the equations, identifying a "better" formulation is crucial to a stable and usable numerical code. To this end, we will make the reasonable assumption that given a set of formulations in flat-space, unstable formulations will also be unusable in curved space. Also, we believe that a good formulation in flat space will at least hint at a good formulation in curved space.

We evaluated two approaches to electromagnetism. The first involving the full electric and magnetic fields. The other approach replaced the magnetic field with its definition with repect to the 3-vector potential. In the first approach all the spatial derivatives of the Maxwell fields are first order, while in the second case there are some second order spatial derivatives. By removing the magnetic field, in favour of A_μ, we reduced the number of constraint equations from five to one. These constraint

equations require a different technique to solve then the evolution equations. By removing constraint equations we can focus more attention on the solution to the evolution equations.[2]

In addition to the two approaches for electromagnetism, we also looked at two different substitutions with respect to the scalar field and its time derivative. Initially, we looked at defining a simple variable, $\pi = \phi_{,t}$, as the time derivative of the scalar field. This represented a sort of "velocity" of the scalar field. However, because terms involving $\mathcal{D}_a\phi$ seem to appear often we also tried another approach defining a new vector variable: $\Pi_a = \mathcal{D}_a\phi$. Combining these two sets of approaches leads to the four formulations we evaluated in flat space.

We expect that the conditions of curved space will further test the stability of any particular formulation. By showing that either there is a clear front-runner (and using that one) or that there isn't any significant difference, we can be more confident that any problems which arise in the curved space code are caused by the complex and evolving geometry and not from the choice of formulation for electromagnetism. We will primarily look at stability and convergence to evaluate the formulations. Convergence testing looks to determine if, in the limit as the computational grid becomes finer, the solutions are converging ro or diverging away from the continuum solution.

Because we will use a Crank-Nicholson scheme, the formulations will all be first-order in time. This is a consequence of our choice of using the Crank-Nicholson scheme. Again, the principal "variation" of the four formulations is the order of the spatial derivatives of the Maxwell and scalar fields.

2.2.1 Formulation A

To determine the evolution equations for the particular electromagnetic fields we must expand the covariant derivative, ∇_a and determine the divergence of F^{ab}, Eq. 2.7. The expanded divergence of F^{ab} is

$$\nabla_a F^{ab} = \partial_a F^{ab} + \Gamma^a_{da} F^{db} + \Gamma^b_{da} F^{ad} \tag{2.29}$$

---

[2]Evolution equations are equations involving time derivatives.

where Γ^a_{da} is the metric connection. The individual electromagnetic fields are found by selecting different values for the indices and then using Eqs. 2.20 - 2.25 to identify the component of F_{ab}. Starting with the time component so we choose $b = t$, we get

$$\nabla_a F^{at} = F^{\rho t}_{,\rho} + F^{\varphi t}_{,\varphi} + F^{zt}_{,z} + \frac{1}{\rho} F^{\rho t}. \tag{2.30}$$

Substituting the definitions from Eqs. 2.20 2.21 and 2.22 leads to

$$\nabla_a F^{at} = - \left[\frac{1}{\rho} (\rho E_\rho)_{,\rho} + E_{z,z} + \frac{1}{\rho} E_{\varphi,\varphi} \right] \tag{2.31}$$

when the terms involving E_ρ are combined. Using Eq. 2.29 to expand the left-hand side of Eq. 2.7 leads to

$$\frac{1}{\rho} (\rho E_\rho)_{,\rho} + E_{z,z} + \frac{1}{\rho} E_{\varphi,\varphi} = ie \frac{a_0}{a_1} \left[\phi^* \mathcal{D}_t \phi - \phi (\mathcal{D}_t \phi)^* \right] \tag{2.32}$$

Doing a similar thing for the spatial components, $b = \rho, z, \varphi$, we get three more equations

$$E_{\rho,t} = \frac{1}{\rho} B_{z,\varphi} - B_{\varphi,z} + ie \frac{a_0}{a_1} \left[\phi^* \mathcal{D}_\rho \phi - \phi (\mathcal{D}_\rho \phi)^* \right] \tag{2.33}$$

$$E_{\varphi,t} = B_{\rho,z} - B_{z,\rho} + ie \frac{a_0}{a_1} \left[\phi^* \mathcal{D}_\varphi \phi - \phi (\mathcal{D}_\varphi \phi)^* \right] \tag{2.34}$$

$$E_{z,t} = \frac{1}{\rho} (\rho B_\varphi)_{,\rho} - \frac{1}{\rho} B_{\rho,\varphi}$$
$$+ ie \frac{a_0}{a_1} \left[\phi^* \mathcal{D}_z \phi - \phi (\mathcal{D}_z \phi)^* \right] \tag{2.35}$$

These last three equations are the evolution equations for $\vec{E}$. It is interesting to note that Eq. 2.32 is equivalent to

$$\nabla \cdot \vec{E} = \zeta \tag{2.36}$$

where ζ is the charge density.[3] which leads to identifying the right hand side of Eq. 2.32 as the charge density of the system. The total charge of the system is, therefore,

$$Q = \int \zeta dv = \int ie \frac{a_0}{a_1} \left[\phi^* \mathcal{D}_t \phi - \phi (\mathcal{D}_t \phi)^* \right] dv \tag{2.37}$$

Because F_{ab} is defined as Eq. 1.6 it also satisfies $\partial_{[a} F_{bc]} = 0$, where

$$\partial_{[a} F_{bc]} = \frac{1}{3} \left(\partial_a F_{bc} + \partial_b F_{ca} + \partial_c F_{ab} \right). \tag{2.38}$$

---

[3] ζ is used instead of ρ, which is usually used to represent the charge density, to avoid confusion. We use ρ as the radial cooridinate in our coordinate system.

Using this extra relationship, the Maxwell equations for the magnetic field $\vec{B}$ can be derived as

$$0 = \frac{1}{\rho}(\rho B_\rho)_{,\rho} + B_{z,z} + \frac{1}{\rho}B_{\varphi,\varphi} \tag{2.39}$$

$$B_{\rho,t} = E_{\varphi,z} - \frac{1}{\rho}E_{z,\varphi} \tag{2.40}$$

$$B_{\varphi,t} = E_{z,\rho} - E_{\rho,z} \tag{2.41}$$

$$B_{z,t} = \frac{1}{\rho}E_{\rho,\varphi} - \frac{1}{\rho}(\rho E_\varphi)_{,\rho}. \tag{2.42}$$

This set of equations forms the other half of the Maxwell equations.

In order to be first-order in time for the scalar field, we define a variable for the time derivative of ϕ. This definition is

$$\pi \equiv \phi_{,t}. \tag{2.43}$$

Also, because the definition of $\mathcal{D}_a$ includes A_a we need to include and track the gauge potential. The final set of evolution equations for formulation A are

$$E_{\rho,t} = \frac{1}{\rho}B_{z,\varphi} - B_{\varphi,z} + \frac{a_0}{a_1}ie\left[\phi^*\phi_\rho - \phi\phi_\rho^* - 2ieA_\rho|\phi|^2\right] \tag{2.44}$$

$$E_{\varphi,t} = B_{\rho,z} - B_{z,\rho} + \frac{a_0}{a_1}ie\left[\phi^*\phi_\varphi - \phi\phi_\varphi^* - 2ieA_\varphi|\phi|^2\right] \tag{2.45}$$

$$E_{z,t} = \frac{1}{\rho}(\rho B_\varphi)_{,\rho} - \frac{1}{\rho}B_{\rho,\varphi} + \frac{a_0}{a_1}ie\left[\phi^*\phi_z - \phi\phi_z^* - 2ieA_z|\phi|^2\right] \tag{2.46}$$

$$B_{\rho,t} = E_{\varphi,z} - \frac{1}{\rho}E_{z,\varphi} \tag{2.47}$$

$$B_{\varphi,t} = E_{z,\rho} - E_{\rho,z} \tag{2.48}$$

$$B_{z,t} = \frac{1}{\rho}E_{\rho,\varphi} - \frac{1}{\rho}(\rho E_\varphi)_{,\rho} \tag{2.49}$$

$$A_{\rho,t} = A_{t,\rho} - E_\rho \tag{2.50}$$

$$A_{\varphi,t} = A_{t,\varphi} - E_\varphi \tag{2.51}$$

$$A_{z,t} = A_{t,z} - E_z \tag{2.52}$$

$$A_{t,t} = \frac{1}{\rho}(\rho A_\rho)_{,\rho} + \frac{1}{\rho}A_{\varphi,\varphi} + A_{z,z} \tag{2.53}$$

$$\phi_{,t} = \pi \tag{2.54}$$

$$\pi_{,t} = \frac{1}{\rho}(\rho\phi_{,\rho})_{,\rho} + \frac{1}{\rho^2}\phi_{,\varphi\varphi} + \phi_{,zz} - 2ie\left(-\phi_{,t}A_t + \phi_{,\rho}A_\rho + \frac{1}{\rho}\phi_{,\varphi}A_\varphi\right)$$
$$- e^2\left(-A_t^2 + A_\rho^2 + A_\varphi^2 + A_z^2\right)\phi. \tag{2.55}$$

21

While the constraint equations [4] are

$$\frac{1}{\rho} A_{\hat{z},\varphi} - A_{\hat{\varphi},z} - B_\rho = 0 \tag{2.56}$$

$$\frac{1}{\rho} (\rho A_{\hat{\varphi}})_{,\rho} - \frac{1}{\rho} A_{\hat{\rho},\varphi} - B_z = 0 \tag{2.57}$$

$$A_{\hat{\rho},z} - A_{\hat{z},\rho} - B_\varphi = 0 \tag{2.58}$$

$$\frac{1}{\rho}(\rho E_\rho)_{,\rho} + \frac{1}{\rho} E_{\varphi,\varphi} + E_{z,z} = \frac{a_0}{a_1} ie\left[\phi^*\phi_t - \phi\phi_t^* - 2ieA_t|\phi|^2\right] \tag{2.59}$$

$$\frac{1}{\rho}(\rho B_\rho)_{,\rho} + \frac{1}{\rho} B_{\varphi,\varphi} + B_{z,z} = 0. \tag{2.60}$$

This set of combined evolution and constraint equations are all first order in time. In addition, the Maxwell fields are all first order in space. The scalar field is second order in spatial derivatives. This amounts to the primary difference in the various formulations: to what order the spatial derivatives appear for the Maxwell fields and the scalar fields.

2.2.2 Formulation B

Formulation B uses the observation that terms involving $\mathcal{D}_a\phi$, the gauge co-variante derivative of ϕ, appear fairly frequently. This suggests making the following substitution

$$\Pi_a \equiv \mathcal{D}_a\phi = \partial_a\phi - ieA_a\phi. \tag{2.61}$$

This, in effect, replaces $\pi = \phi_{,t}$ as an evolved variable. In this formulation Π_a is now a 4-vector rather then a simple scalar as in formulation A. The individual components of the Π_μ vector are

$$\Pi_t = \phi_{,t} - ieA_t\phi \tag{2.62}$$

$$\Pi_\rho = \phi_{,\rho} - ieA_\rho\phi \tag{2.63}$$

$$\Pi_\varphi = \phi_{,\varphi} - ieA_\varphi\phi \tag{2.64}$$

$$\Pi_z = \phi_{,z} - ieA_z\phi. \tag{2.65}$$

---

[4]The constraint equations are equations with no time derivatives

Upon making this substitution, we can write the second order scalar field equation, Eq. 2.4, as

$$\nabla_a(\mathcal{D}^a\phi) = \nabla_a\Pi^a = ieA^a\Pi_a. \tag{2.66}$$

When written in component form, Eq. 2.66 becomes the evolution equation for Π_t

$$\Pi_{t,t} = \frac{1}{\rho}(\rho\Pi_\rho)_{,\rho} + (\frac{1}{\rho}\Pi_{\hat{\varphi}})_{,\varphi} + \Pi_{z,z} - ie(-A_t\Pi_t + A_\rho\Pi_\rho + A_{\hat{\varphi}}\Pi_{\hat{\varphi}} + A_z\Pi_z). \tag{2.67}$$

The evolution equations for the other components of Π_a and are found by taking time derivatives of the components of Π_a and using some of our other relations. For instance, for the Π_ρ component, on taking the time derivative of Eq. 2.63 we get

$$\Pi_{\rho,t} = \phi_{,t\rho} - ieA_\rho\phi_{,t} - ieA_{\rho,t}\phi. \tag{2.68}$$

Solving Eq. 2.62 for $\phi_{,t}$ and substituting into Eq. 2.68 along with Eq. 2.50 gives

$$\Pi_{\rho,t} = (\Pi_t + ieA_t\phi)_{,\rho} - ie\phi(A_{t,\rho} - ieA_\rho(\Pi_t + ieA_t\phi) - E_\rho) \tag{2.69}$$

$$= \Pi_{t,\rho} - ieA_\rho\Pi_t + ie(A_t\Pi_\rho + E_\rho\phi). \tag{2.70}$$

Following a similar approach the other equations become

$$\Pi_{\varphi,t} = \frac{1}{\rho}\Pi_{t,\varphi} - ieA_\varphi\Pi_t + ie(A_t\Pi_\varphi + E_\varphi\phi) \tag{2.71}$$

$$\Pi_{z,t} = \Pi_{t,z} - ieA_z\Pi_t + ie(A_t\Pi_z + E_z\phi). \tag{2.72}$$

The right-hand side of the other equations are changed by the substitution, but only marginally.

The final set of evolution equations for formulation B is

$$E_{\rho,t} = \frac{1}{\rho}B_{z,\varphi} - B_{\varphi,z} + \frac{ie}{2}\left[\phi^*\Pi_\rho - \phi\Pi_\rho^*\right] \tag{2.73}$$

$$E_{\varphi,t} = B_{\rho,z} - B_{z,\rho} + \frac{ie}{2}\left[\phi^*\Pi_\varphi - \phi\Pi_\varphi^*\right] \tag{2.74}$$

$$E_{z,t} = \frac{1}{\rho}(\rho B_\varphi)_{,\rho} - \frac{1}{\rho}B_{\rho,\varphi} + \frac{ie}{2}\left[\phi^*\Pi_z - \phi\Pi_z^*\right] \tag{2.75}$$

$$B_{\rho,t} = E_{\varphi,z} - \frac{1}{\rho}E_{z,\varphi} \tag{2.76}$$

$$B_{\varphi,t} = E_{z,\rho} - E_{\rho,z} \tag{2.77}$$

23

$$B_{z,t} = \frac{1}{\rho} E_{\rho,\varphi} - \frac{1}{\rho}(\rho E_\varphi)_{,\rho} \tag{2.78}$$

$$\phi_{,t} = \Pi_t + ieA_t\phi \tag{2.79}$$

$$\Pi_{t,t} = \frac{1}{\rho}(\rho\Pi_\rho)_{,\rho} + (\frac{1}{\rho}\Pi_\varphi)_{,\varphi} + \Pi_{z,z}$$
$$-ie(-A_t\Pi_t + A_\rho\Pi_\rho + A_\varphi\Pi_\varphi + A_z\Pi_z)\phi \tag{2.80}$$

$$\Pi_{\rho,t} = \Pi_{t,\rho} - ieA_\rho\Pi_t + ie(A_t\Pi_\rho + E_\rho\phi) \tag{2.81}$$

$$\Pi_{\varphi,t} = \frac{1}{\rho}\Pi_{t,\varphi} - ieA_\varphi\Pi_t + ie(A_t\Pi_\varphi + E_\varphi\phi) \tag{2.82}$$

$$\Pi_{z,t} = \Pi_{t,z} - ieA_z\Pi_t + ie(A_t\Pi_z + E_z\phi) \tag{2.83}$$

$$A_{\rho,t} = A_{t,\rho} - E_\rho \tag{2.84}$$

$$A_{\varphi,t} = A_{t,\varphi} - E_\varphi \tag{2.85}$$

$$A_{z,t} = A_{t,z} - E_z \tag{2.86}$$

$$A_{t,t} = \frac{1}{\rho}(\rho A_\rho)_{,\rho} + \frac{1}{\rho}A_{\varphi,\varphi} + A_{z,z}. \tag{2.87}$$

The constraint equations for this formulation are now

$$\frac{1}{\rho}A_{z,\varphi} - A_{\varphi,z} - B_\rho = 0 \tag{2.88}$$

$$\frac{1}{\rho}(\rho A_\varphi)_{,\rho} - \frac{1}{\rho}A_{\rho,\varphi} - B_z = 0 \tag{2.89}$$

$$A_{\rho,z} - A_{z,\rho} - B_\varphi = 0 \tag{2.90}$$

$$\frac{1}{\rho}(\rho E_\rho)_{,\rho} + \frac{1}{\rho}E_{\varphi,\varphi} + E_{z,z} = \frac{ie}{2}\left[\phi^*\Pi_t - \phi\Pi_t^*\right] \tag{2.91}$$

$$\frac{1}{\rho}(\rho B_\rho)_{,\rho} + \frac{1}{\rho}B_{\varphi,\varphi} + B_{z,z} = 0. \tag{2.92}$$

While this formulation of evolution and constraint equations is first order in time, as are the other fomulations, spatially it is completely first order for the Maxwell fields and the scalar field. This formulation contains the largest number of fields to manage.

2.2.3 Formulation C

The constraint equations are always an important subset of the equations, but they can often be difficult to solve numerically. The evolution equations are hyperbolic equations and the constraint equations are elliptic [15]. The numerical techniques used

to solve hyperbolics are very different than those used to solve elliptics. Combining them into a single code can therefore be a challenge. Further, the constraint equations represent consistency equations for the initial data. Theoretically, if those equations are satisfied at the initial time, they should be satisfied through the entire evolution. Unfortunately, due to numerical errors from approximations and round-off, this is not always the case. One then must make a choice of how the constraints are to be solved. One can do what is called free evolution, where the constraints are explicitly satisfied on only the initial time slice and then are no more than monitored throughout the course of the evolution. As mentioned, numerical errors can yield fields then that no longer satisfy the constraints after some time. An alternative is to do constrained evolution. As the name suggests, one solves the constraint equations for some of the fields at every time. Solving the constraints on each time step is computationally expensive, but provides an important check of the code. One can also imagine doing some combination of these two extremes and then having what is known as a partially constrained evolution. In the flat space case presented in this chapter, we do a free evolution for the electromagnetic fields. However, in the curved case presented later we actually do a constrained evolution of the general relativity constraint equations.

An entirely different approach is to try to remove the constraints from the set of equations to be solved for. One way to do this in electromagnetism is to write the Maxwell equations only in terms of the gauge potential. If one does this, however, the resulting equations are second order in space and time. As we do not want a second order in time system, we can only take a step in this direction by eliminating the magnetic field. By using

$$\vec{B} = \nabla \times \vec{A} \tag{2.93}$$

we can remove all references to $\vec{B}$ and reduce the set of constraints to a single equation. The substitutions are

$$B_\rho = \frac{1}{\rho} A_{z,\varphi} - A_{\varphi,z} \tag{2.94}$$

$$B_z = \frac{1}{\rho} (\rho A_\varphi)_{,\rho} - \frac{1}{\rho} A_{\rho,\varphi} \tag{2.95}$$

$$B_\varphi = A_{\rho,z} - A_{z,\rho}. \tag{2.96}$$

The remaining constraint equation is now

$$\frac{1}{\rho}(\rho E_\rho)_{,\rho} + E_{z,z} = \frac{ie}{2}\left[\phi^* \Pi_t - \phi \Pi_t^*\right] \tag{2.97}$$

which is simply Gauss's Law. The evolution equations are now

$$E_{\rho,t} = \frac{1}{\rho^2}(\rho A_\varphi)_{,\rho\varphi} - \frac{1}{\rho^2}A_{\rho,\varphi\varphi} - A_{\rho,zz} + A_{z,\rho z} + \frac{ie}{2}\left[\phi^* \Pi_\rho - \phi \Pi_\rho^*\right] \tag{2.98}$$

$$E_{\varphi,t} = \frac{1}{\rho}A_{z,\varphi z} - A_{\varphi,zz} - \left(\frac{1}{\rho}(\rho A_\varphi)_{,\rho}\right)_{,\rho} + \left(\frac{1}{\rho}A_{\rho,\varphi}\right)_{,\rho}$$
$$+ \frac{ie}{2}\left[\phi^* \Pi_\varphi - \phi \Pi_\varphi^*\right] \tag{2.99}$$

$$E_{z,t} = \frac{1}{\rho}(\rho A_{\rho,z})_{,\rho} - \frac{1}{\rho}(\rho A_{z,\rho})_{,\rho} - \frac{1}{\rho^2}A_{z,\varphi\varphi} + \frac{1}{\rho}A_{\varphi,z\varphi}$$
$$+ \frac{ie}{2}\left[\phi^* \Pi_z - \phi \Pi_z^*\right] \tag{2.100}$$

$$\phi_{,t} = \Pi_t + ieA_t\phi \tag{2.101}$$

$$\Pi_{t,t} = \frac{1}{\rho}(\rho\Pi_\rho)_{,\rho} + (\frac{1}{\rho}\Pi_\varphi)_{,\varphi} + \Pi_{z,z}$$
$$- ie(-A_t\Pi_t + A_\rho\Pi_\rho + A_\varphi\Pi_\varphi + A_z\Pi_z)\phi \tag{2.102}$$

$$\Pi_{\rho,t} = \Pi_{t,\rho} - ieA_\rho\Pi_t + ie(A_t\Pi_\rho + E_\rho\phi) \tag{2.103}$$

$$\Pi_{\varphi,t} = \frac{1}{\rho}\Pi_{t,\varphi} - ieA_\varphi\Pi_t + ie(A_t\Pi_\varphi + E_\varphi\phi) \tag{2.104}$$

$$\Pi_{z,t} = \Pi_{t,z} - ieA_z\Pi_t + ie(A_t\Pi_z + E_z\phi) \tag{2.105}$$

$$A_{\rho,t} = A_{t,\rho} - E_\rho \tag{2.106}$$

$$A_{\varphi,t} = A_{\varphi,\varphi} - E_\varphi \tag{2.107}$$

$$A_{z,t} = A_{t,z} - E_z \tag{2.108}$$

$$A_{t,t} = \frac{1}{\rho}(\rho A_\rho)_{,\rho} + \frac{1}{\rho}A_{\varphi,\varphi} + A_{z,z}. \tag{2.109}$$

In this set of equations there are second-order spatial derivatives of the Maxwell fields. Note that, in addition, there are a few mixed ρ and z derivatives. The scalar field still appear as first-order spatially. This set reduces the number of equations by six, three evolution and three constraint. By reducing the number of constraint equations there are fewer equations to solve on each time step.

2.2.4 Formulation D

The final formulation goes back to the treatment of the time derivative of ϕ seen in formulation A. We again define π to be $\pi = \phi_{,t}$, rather then using the vector Π_a. The Maxwell fields are treated as in formulation C. Therefore, formulation D is fully second-order (spatially) in the Maxwell and scalar fields. The evolution equations for this set look like the following

$$
\begin{aligned}
E_{\rho,t} &= \frac{1}{\rho^2}\left(\rho A_\varphi\right)_{,\rho\varphi} - \frac{1}{\rho^2}A_{\rho,\varphi\varphi} - A_{\rho,zz} + A_{z,\rho z} \\
&\quad + \frac{a_0}{a_1} ie\left[\phi^*\phi_\rho - \phi\phi_\rho^* - 2ieA_\rho|\phi|^2\right] \tag{2.110}
\end{aligned}
$$

$$
\begin{aligned}
E_{\varphi,t} &= \frac{1}{\rho}A_{z,\varphi z} - A_{\varphi,zz} - \left(\frac{1}{\rho}\left(\rho A_\varphi\right)_{,\rho}\right)_{,\rho} + \left(\frac{1}{\rho}A_{\rho,\varphi}\right)_{,\rho} \\
&\quad + \frac{a_0}{a_1} ie\left[\phi^*\phi_\varphi - \phi\phi_\varphi^* - 2ieA_\varphi|\phi|^2\right] \tag{2.111}
\end{aligned}
$$

$$
\begin{aligned}
E_{z,t} &= \frac{1}{\rho}\left(\rho A_{\rho,z}\right)_{,\rho} - \frac{1}{\rho}\left(\rho A_{z,\rho}\right)_{,\rho} - \frac{1}{\rho^2}A_{z,\varphi\varphi} + \frac{1}{\rho}A_{\varphi,z\varphi} \\
&\quad + \frac{a_0}{a_1} ie\left[\phi^*\phi_z - \phi\phi_z^* - 2ieA_z|\phi|^2\right] \tag{2.112}
\end{aligned}
$$

$$
A_{\rho,t} = A_{t,\rho} - E_\rho \tag{2.113}
$$

$$
A_{\varphi,t} = A_{t,\varphi} - E_\varphi \tag{2.114}
$$

$$
A_{z,t} = A_{t,z} - E_z \tag{2.115}
$$

$$
A_{t,t} = \frac{1}{\rho}\left(\rho A_\rho\right)_{,\rho} + \frac{1}{\rho}A_{\varphi,\varphi} + A_{z,z} \tag{2.116}
$$

$$
\phi_{,t} = \pi \tag{2.117}
$$

$$
\begin{aligned}
\pi_{,t} &= \frac{1}{\rho}(\rho\phi_{,\rho})_{,\rho} + \frac{1}{\rho^2}\phi_{,\varphi\varphi} + \phi_{,zz} - 2ie\left(-\phi_{,t}A_t + \phi_{,\rho}A_\rho + \frac{1}{\rho}\phi_{,\varphi}A_\varphi\right) \\
&\quad - e^2\left(-A_t^2 + A_\rho^2 + A_\varphi^2 + A_z^2\right)\phi. \tag{2.118}
\end{aligned}
$$

Again, there is a single constraint equation

$$
\frac{1}{\rho}(\rho E_\rho)_{,\rho} + E_{z,z} = \frac{ie}{2}\left[\phi^*\phi_t - \phi\phi_t^* - 2ieA_t|\phi|^2\right] \tag{2.119}
$$

for this formulation.

2.3 Data

The four formulations we studied are summarized below

$$(A) \quad \vec{E}, \, \vec{B}, \, A_\mu, \, \pi$$

$$(B) \quad \vec{E}, \, \vec{B}, \, A_\mu, \, \Pi_\mu$$

$$(C) \quad \vec{E}, \, A_\mu, \, \Pi_\mu$$

$$(D) \quad \vec{E}, \, A_\mu, \, \pi.$$

For each set, the code was run for 400 timesteps at a base resolution of 32x64, and then tested for convergence. The convergence test compares runs of increasing resolution. Based on an ideal convergence factor of 4, a residual is calculated for the fields of each formulation. With the residual, a quantitative "score" can be given to each formulation. Figures 2.1, 2.2, 2.3 and 2.4 show the convergence tests for each of the formulations. The convergence test "evolves" over time, and this evolution is displayed in the figures. Regions where the data is closer to 4 represents periods of time where the fields appear to be converging.

The figures show convergence tests for ϕ and the components of A_μ for all four formulations. These fields where chosen because, regardless of the choice, they will exist in each formulation. Convergence tests are a means of measuring overall tendency of the system to "converge" to the continuum limit. Each formulation is run on increasingly finer grids, and then tested for convergence. Schematically this is

$$\frac{||u_{4h} - u_{2h}||}{||u_{2h} - u_h||} \rightarrow 4 \tag{2.120}$$

where "u_h" is a solution to the finite difference equation with a grid spacing h, and $||..||$ is a norm. Ideally the solutions should converge to 4 due to the second-order nature of the Crank-Nicholson scheme used. Often the convergence test will show variation around 4, but the convergence should show a tendency towards 4.

Using the least squares fitting algorithm for a data set involves finding a curve which minimizes the sum of the residuals. Residuals are the square difference between the fitting curve and the corresponding data point. This can be shown mathematically as

$$R = \Sigma_i \left[y_i - 4 \right]^2. \tag{2.121}$$

Using this least squares approach as an idea, we can determine the sum of the residuals from the data set of each convergence test and the curve $x = 4$. This gives us a means
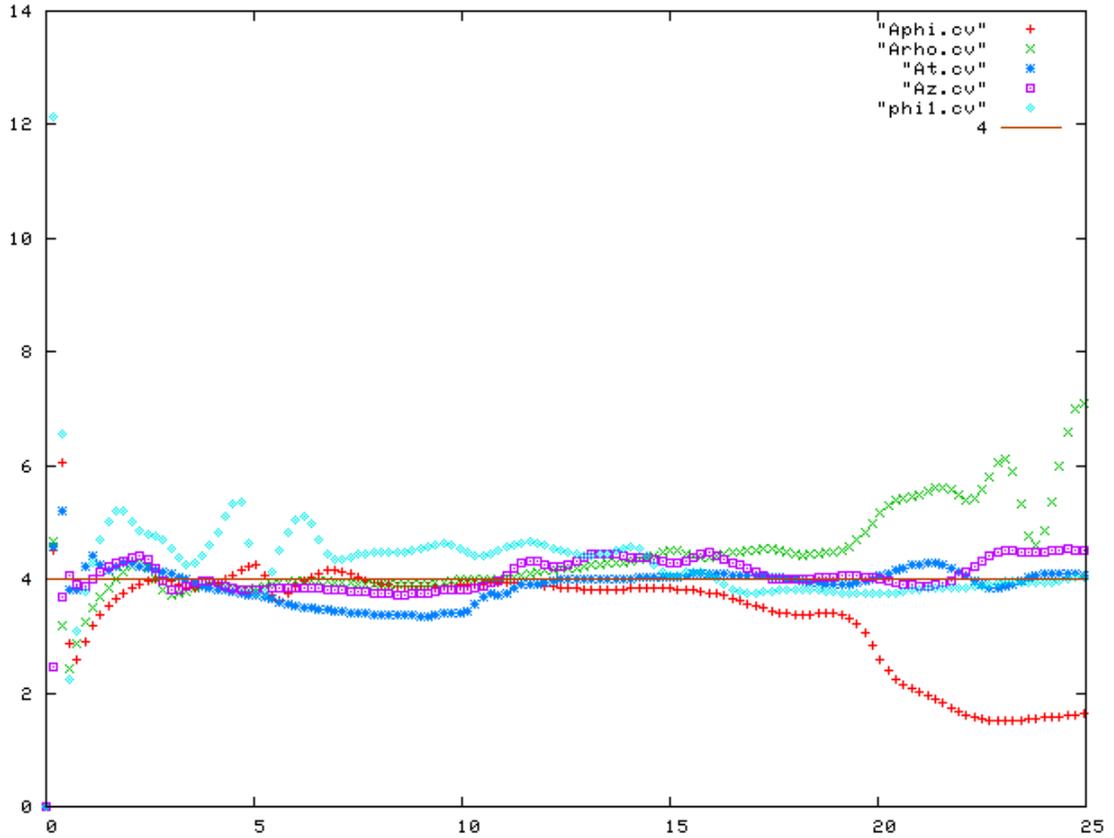
Figure 2.1: Convergence tests for the scalar field ϕ and the components of the vector A_μ in formulation A. Many of the fields show a convergence factor around 4, the ideal convergence. However, near the end of the run a few fields, A_ρ and A_ϕ in particular, seem to begin to move away from 4. The vertical axis is the "convergence factor" while the horizontal axis is time.

of measuring how far a giving convergence test is from the theoretical convergence of 4. The Table 2.3 shows the residuals, normalized by the number of timesteps (400), for the 5 fields. The sum for each formulation is included, as well.

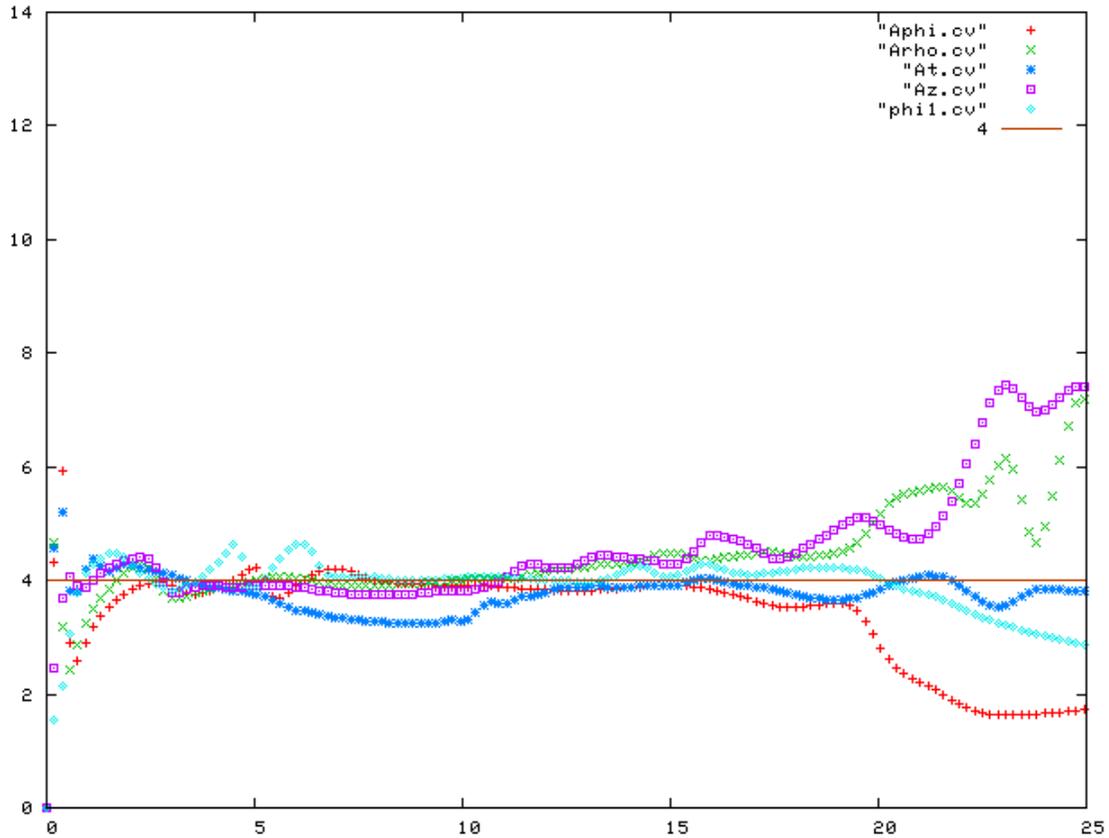|	A_ϕ	A_ρ	A_z	A_t	ϕ	Σ
A	0.43339	0.2790175	0.07205	0.0696125	0.3118575	1.1659275
B	0.3832925	0.2897425	0.0856925	0.50619	0.11161	1.3765275
C	0.572655	0.2843125	0.184725	0.176525	0.31118	1.5293975
D	0.2033475	0.30134	0.2387775	0.2524225	0.275705	1.2715925

Figure 2.2: Convergence tests for the scalar field ϕ and the components of the vector A_μ in formulation B. This formulation shows much more variation from 4 then formulation A, see Figure 2.1. In this formulation, all of the fields appear to be departing from four near the end of the run. The vertical axis is the "convergence factor" while the horizontal axis is time.
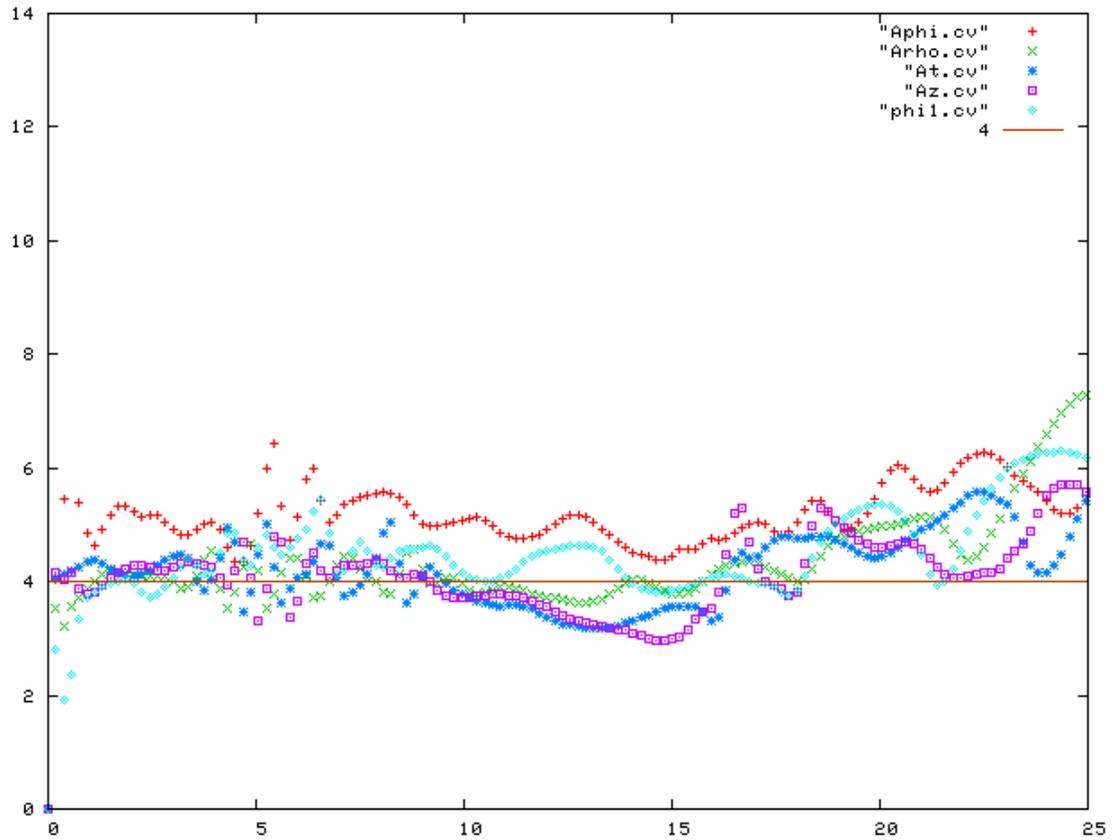
Figure 2.3: Convergence tests for the scalar field ϕ and the components of the vector A_μ in formulation C. Like formulation B, Figure 2.2, this formulation appears to be much more "noisy" then formulation A. There is much more variation from four in this formulation. Its interesting to notice that all of the fields appear to be about four, at the end of the run. Formulation C performed the worst, when compared to the analysis of the residuals. The vertical axis is the "convergence factor" while the horizontal axis is time.
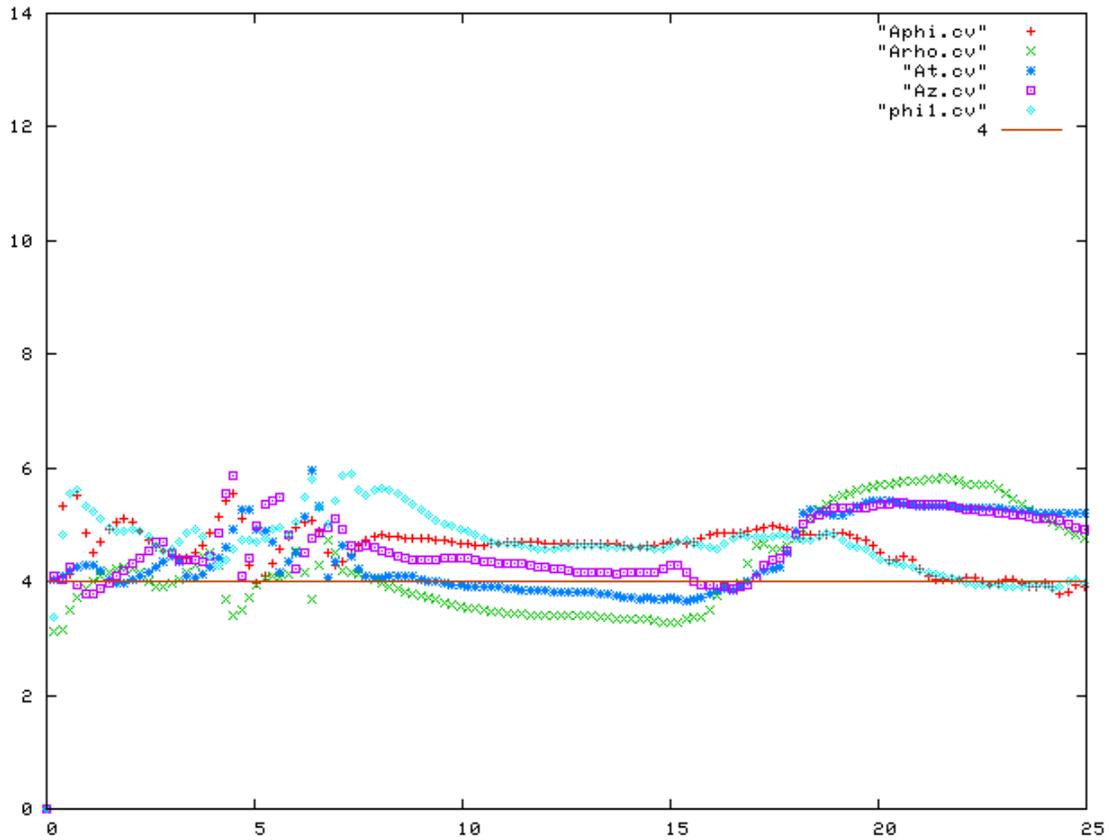
Figure 2.4: Convergence tests for the scalar field ϕ and the components of the vector A_μ in formulation D. This formulation shows some trend towards convergence in the middle of the run. A_φ and ϕ appear to be very close to four at the end of the run, while the other fields show some movement towards four. It may be useful to test this formulation with more timesteps to see if the other fields will settle into four as well. The vertical axis is the "convergence factor" while the horizontal axis is time.

2.4 Results

From an analytic perscpective, there is no difference between these formulations. All are equivalent. The question here is the numerical one of which formulation is better. All appear stable for short times. Convergence tests show that each formulation has some strengths but overall they are similar. Based on the analysis of the residuals of the five common fields, formulation A is slightly better. From a runtime perspective, formulation C tends to run a bit faster, by at most a factor of about 2. We attribute this to the fact that this formulation has the fewest fields. Unfortunately, formulation C performs poorly with regard to the residuals. With regard to the curved space system, we choose formulation A.

Chapter 3

Curved Space

Our goal is to produce a fully evolving system for gravitational collapse with electromagnetism. As noted in the introduction, many astrophysical phenomena involve an interaction between electromagnetism and gravitation. While many are accurately modeled using Newtonian gravity, the more physically accurate models require general relativity and its dynamic spacetime. In this chapter we will begin by deriving the equations of motion for a fully evolving spacetime. We will also consider issues associated with regularity and examine some possible model problems as subsets of the full equations.

3.1 Equations of Motion

To derive the equations of motion we start with the action. We assume, from the start, axisymmetry with this symmetry expressed by a Killing vector. We can decompose the action along the Killing vector to reduce the action from four dimensions to three. Once the action is decomposed, we use the standard variational approach with the Euler-Lagrange equations. The variation will produce the basic equations of motion. In order to develop evolution equations we need a notion of time, and we can use the ADM decomposition to decompose the equations of motion into evolution and constraint equations. Finally, coordinate choices and the enforcement of regularity will produce the final, regularized set of equations. The complete set of equations derived by this process is presented in Appendix B.2. Subsets of these equations are used to develop the numerical code.

3.1.1 Killing vector

Our first step to deriving the equations of motion is to reduce the action from four dimensions to three by using the axisymmetric Killing vector. We begin with the full four dimensional action, Eq. 1.4,

$$S = \int \sqrt{-\gamma}\, d^4x \left\{ R - \frac{a_0}{2}(\mathcal{D}_\mu \phi)(\mathcal{D}^\mu \phi)^* - \frac{a_1}{4}F_{\mu\nu}F^{\mu\nu} - a_2 V(\phi, \phi^*) \right\}. \qquad (3.1)$$

Recall that $\mathcal{D}_\mu \phi$ is the gauge covariant derivative of ϕ defined in Eq. 1.5. F_{ab} is the Maxwell tensor and $V(\phi, \phi^*)$ is a generic potential.[1] We assume from the outset that we have axisymmetry. This symmetry is invariantly defined by the existance of a Killing vector. Using a coordinate system adapted to the Killing vector allows us to write the Killing vector as as $X^\mu = \left(\frac{\partial}{\partial\varphi}\right)^\mu$.

We can exploit the symmetry to reduce the problem from a four dimensional spacetime to a three dimensional spacetime. While this will generally introduce new fields, which, in the 4-dimensional manifold are tensor components in the direction of the Killing vector, the reduced, three dimensional system can be easier to deal with then the full four dimensional system.

It is not necessary to decompose the action first. It is possible to follow a variational approach, and then use the Killing vector to decompose the resulting equations of motion. While both approaches are analytically equivalent, applying the Killing vector first leads to an interesting insight. We will see that taking this approach allows us to introduce a scalar twist in the place of a second rank tensor. Making this replacement is apparent when the Killing vector is applied before the varying the action.

In order to begin the Killing vector decomposition, we first define the following auxiliary fields:

$$s^2 = X_\mu X^\mu \qquad (3.2)$$

$$Y_\mu = \frac{X_\mu}{s^2} \qquad (3.3)$$

$$Z_{\mu\nu} = \partial_\mu Y_\nu - \partial_\nu Y_\mu \qquad (3.4)$$

---

[1]See Section 1.3 for a full explaination of these fields and the action.

Y_μ is the rescaled Killing vector an s is the norm of the Killing vector. Z_{ab} is a second-rank antisymmetric tensor with a form similar to the the Maxwell tensor, F_{ab} (Eq. 1.6), but only in three dimensions rather then four. Z_{ab} will play a role later as we decompose the action. It will appear as another tensor in the action, which looks, in form, like the Maxwell tensor. This approach is actually very similar to the Kaluza-Klein approach to integrating general relativity and electromagnetism [16].

With these fields we can now construct a projection operator. This operator will allow us to decompose any four dimensional tensor into a three dimensional tensor and scalar (the component along the Killing vector). The metric can also be decomposed into a three dimensional metric of the reduced spacetime and a portion along the Killing vector. By contracting this new three dimensional metric with any tensor, say T, we can determine the projection of T onto the reduced spacetime. Therefore, the reduced metric acts as a "projection operator" for any tensor. The operator will project tensors in the full four dimensional spacetime into the reduced (axisymmetric) three dimensional spacetime by removing components lying along the Killing vector. This projection operator is defined as

$$
\begin{align}
{}^3g_{\mu\nu} &= {}^4\gamma_{\mu\nu} - s^2 Y_\mu Y_\nu \tag{3.5} \\
&= {}^4\gamma_{\mu\nu} - Y_\mu X_\nu \tag{3.6}
\end{align}
$$

where ${}^4\gamma_{\mu\nu}$ is the metric of the original four dimensional spacetime.[2] ${}^3g_{\mu\nu}$ will be the metric of this new reduced three dimensional spacetime. The inverse operator is defined simply as

$$
{}^3g^{\mu\nu} = {}^4\gamma^{\mu\nu} - Y^\mu X^\nu. \tag{3.7}
$$

We perform a tensor contraction on each index of every tensor with this projection operator. For example, projecting the vector ${}^4V^\mu$ leads to

$$
\begin{align}
{}^3g^\mu{}_\nu \, {}^4V^\nu &= {}^4\gamma^\mu{}_\nu \, {}^4V^\nu - Y_\nu X^\mu \, {}^4V^\nu \tag{3.8} \\
&= {}^4V^\nu - \frac{X^\nu}{s^2} V_\varphi. \tag{3.9}
\end{align}
$$

---

[2]The preceeding superscripted 4 identifies the dimensionality of the tensor.

Alternatively, every vector can be decomposed along the Killing vector and orthogonal to the Killing vector. First, recall that any tensor can be written as a contraction with the metric,

$$^4V_\mu = \gamma_\mu{}^\nu V_\nu. \tag{3.10}$$

Using this property of the metric and Eq. 3.6, the vector $^4V^\mu$ can be decomposed to

$$^4V_\mu \;=\; ^4\gamma_\mu{}^\nu\, ^4V_\nu = {}^3g_\mu{}^\nu\, ^4V_\nu + Y_\mu\left(X^\nu\, ^4V_\nu\right) \tag{3.11}$$

$$= \; ^3V_\mu + Y_\mu V_\varphi \tag{3.12}$$

where $^3V_\mu$ are the components of V_μ that lie within the three dimensional axisymmetric spacetime, and V_φ is the component of the vector V_μ along the direction of the Killing vector. From the perscpective of the reduced three dimensional spacetime V_φ acts as a true scalar. With respect to the 4-dimensional spacetime V_φ is a component of a vector. The symmetry allows for the change of perspective.

Decomposing a second-rank tensor is a little more involved, but follows a similar pattern. For a given tensor, $T_{\mu\nu}$, we contract each index with a seperate projection operator

$$^3g^\mu{}_\alpha\, ^3g^\nu{}_\beta\, ^4T_{\mu\nu} \;=\; \left(^4\gamma^\mu{}_\alpha - Y^\mu X_\alpha\right)\left(^4\gamma^\nu{}_\beta - Y^\nu X_\beta\right){}^4T_{\mu\nu} \tag{3.13}$$

$$= \left(^4\gamma^\mu{}_\alpha\, ^4\gamma^\nu{}_\beta - {}^4\gamma^\mu{}_\alpha Y^\nu X_\beta - Y^\mu X_\alpha\, ^4\gamma^\nu{}_\beta + Y^\nu X_\beta Y^\mu X_\alpha\right){}^4T_{\mu\nu} \tag{3.14}$$

$$= \; ^4T_{\alpha\beta} - {}^4T_{\alpha\varphi}Y_\beta - {}^4T_{\varphi\beta}Y_\alpha + {}^4T_{\varphi\varphi}Y_\alpha Y_\beta \tag{3.15}$$

Like the vector above, a second rank tensor can also be decompsed along and orthagonal to the Killing vector, as

$$^4T_{\mu\nu} \;=\; \gamma_\mu{}^\lambda\gamma_\nu{}^\omega T_{\lambda\omega} \tag{3.16}$$

$$= \left(^3g_\mu{}^\lambda + Y_\mu X^\lambda\right)\left(^3g_\nu{}^\omega + Y_\nu X^\omega\right) T_{\lambda\omega} \tag{3.17}$$

$$= \; ^3g_\mu{}^\lambda\, ^3g_\nu{}^\omega T_{\lambda\omega} + {}^3g_\mu{}^\lambda Y_\nu X^\omega T_{\lambda\omega} + {}^3g_\nu{}^\omega Y_\mu X^\lambda T_{\lambda\omega} + Y_\mu X^\lambda Y_\nu X^\omega T_{\lambda\omega} \tag{3.18}$$

$$= \; ^3T_{\mu\nu} + Y_\nu\, ^3g_\mu{}^\lambda T_{\lambda\varphi} + Y_\mu\, ^3g_\nu{}^\omega T_{\varphi\omega} + Y_\mu Y_\nu T_{\varphi\varphi}. \tag{3.19}$$

Tensors of higher rank, as well as mixed tensors, will follow a similar process. Scalars, as zero rank tensors, are not affected by the projections or decompositions.

In the case of the action, we need to determine the effect of the projection on each of the terms. The decomposition of the gauge covariant derivative operator $\mathcal{D}_\mu$ is

$$
\begin{align}
{}^4\mathcal{D}_\mu &= \gamma_\mu{}^\lambda {}^4\mathcal{D}_\lambda \tag{3.20} \\
&= \left(g_\mu{}^\lambda + Y_\mu X^\lambda \right) {}^4\mathcal{D}_\lambda \tag{3.21} \\
&= {}^3\mathcal{D}_\mu + Y_\mu \nabla_\varphi - i e Y_\mu A_\varphi \tag{3.22} \\
&= {}^3\mathcal{D}_\mu - i e Y_\mu A_\varphi \tag{3.23}
\end{align}
$$

where ${}^3\mathcal{D}_\mu$ is the gauge covariant derivative operator in the 3-space of the hypersurfaces. The term involving ∇_φ is zero due to the axisymmetry.[3] The term in the action involving ${}^4\mathcal{D}_\mu$ can now be written

$$
({}^4\mathcal{D}_\mu \phi)({}^4\mathcal{D}^\mu \phi)^* = ({}^3\mathcal{D}_\mu \phi)({}^3\mathcal{D}^\mu \phi)^* + \frac{e^2}{s^2} A_\varphi^2 |\phi|^2. \tag{3.24}
$$

The electromagnetic fields following the same decomposition become

$$
\begin{align}
{}^4A_\mu &= {}^3A_\mu + Y_\mu A_\varphi \tag{3.25} \\
{}^4F_{\mu\nu} &= {}^3F_{\mu\nu} + X^\omega Y_\nu {}^3\nabla_\mu A_\omega - X^\lambda Y_\mu {}^3\nabla_\nu A_\lambda \tag{3.26} \\
{}^4F_{\mu\nu}{}^4F^{\mu\nu} &= {}^3F^{\mu\nu} \left({}^3F_{\mu\nu} + 2Y_\nu {}^3\nabla_\mu A_\varphi \right) \notag \\
&\quad + \frac{2}{s^2} {}^3\nabla^\mu A_\varphi \left({}^3\nabla_\mu A_\varphi - Y_\mu {}^3\nabla_\varphi A_\varphi \right). \tag{3.27}
\end{align}
$$

The derivative operator ${}^3\nabla_\mu$ is the covariant derivative defined relative to the reduced axisymmetric spacetime. The final terms to decompose are the Ricci scalar and the metric determinant, they are

$$
\begin{align}
\sqrt{-{}^4\gamma} &= s\sqrt{-{}^3g} \tag{3.28} \\
{}^4R &= {}^3R - \frac{2}{s} {}^3\nabla_\mu {}^3\nabla^\mu s - \frac{s^2}{4} Z_{\mu\nu} Z^{\mu\nu}. \tag{3.29}
\end{align}
$$

---

[3]Note, A_φ is the φ component of the vector A_μ in the full 4-dimensional manifold, but in the reduced 3-manifold A_φ acts completely like a true 3-scalar.

Making all of these substitutions into the action results in

$$
\begin{aligned}
S \;=\; & \int s\sqrt{-^3g}\,d^4x \Big\{ {}^3R - \frac{2}{s}\,{}^3\nabla_\mu\,{}^3\nabla^\mu s - \frac{s^2}{4}Z_{\mu\nu}Z^{\mu\nu} - a_2 V(\phi,\phi^*) \\
& - \frac{a_0}{2}\Big[(^3\mathcal{D}_\mu\phi)(^3\mathcal{D}^\mu\phi)^* + \frac{e^2}{s^2}A_\varphi^2|\phi|^2 \Big] \\
& - \frac{a_1}{4}\Big[{}^3F^{\mu\nu}\big({}^3F_{\mu\nu} + 2Y_\nu\,{}^3\nabla_\mu A_\varphi \big) + \frac{2}{s^2}\,{}^3\nabla^\mu A_\varphi \big({}^3\nabla_\mu A_\varphi - Y_\mu\,{}^3\nabla_\varphi A_\varphi \big) \Big] \Big\}.
\end{aligned}
\tag{3.30}
$$

The action appears to be much more complex then the original and but this is the effect of separating out the components along the Killing vector from those in the reduced spacetime.

3.1.2 Euler-Lagrange Equation

With the action now decomposed with respect to the Killing vector, we can proceed with a standard variational approach in order to get the equations of motion with respect to the fields. In particular, we will vary the action with respect to the following fields: $^3A_\mu$, A_φ, s, Y_μ, ϕ, ϕ^*, and $^3g_{\mu\nu}$ by using the Euler-Lagrange equation

$$
\frac{\partial \mathcal{L}}{\partial \phi} - {}^3\nabla_a \left\{ \frac{\partial \mathcal{L}}{\partial(^3\nabla_a\phi)} \right\} = 0.
\tag{3.31}
$$

As an example the Euler-Lagrange equation for $^3A_\mu$ leads to

$$
s\sqrt{-^3g}\,\frac{a_0 ie}{2}\phi\left({}^3\mathcal{D}^\mu\phi \right)^* - {}^3\nabla_\nu\left(s\sqrt{-^3g}\,\frac{a_1}{2}\,{}^3F^{\mu\nu} \right) = 0.
\tag{3.32}
$$

For ϕ the equation leads to

$$
s\sqrt{-^3g}\left(\frac{a_0}{2}ieA_\mu\left({}^3\mathcal{D}^\mu\phi \right)^* + \frac{e^2}{s^2}A_\varphi^2\phi^* - a_2\frac{\partial V}{\partial\phi} \right) + {}^3\nabla_\mu\left(s\sqrt{-^3g}\,\frac{a_0}{2}\left({}^3\mathcal{D}^\mu\phi \right)^* \right) = 0,
\tag{3.33}
$$

which on simplification becomes the equation of motion for the ϕ^* field. Varying with ϕ^* will lead to the conjugate of this equation which is the equation of motion for ϕ. The set of equations derived from the action are

$$
0 \;=\; {}^3\nabla^a(^3\mathcal{D}_a\phi) + \frac{1}{s}\,{}^3\nabla^a s\,{}^3\mathcal{D}_a\phi - ieA^a\,{}^3\mathcal{D}_a\phi - \frac{e^2}{s^2}A_\varphi^2\phi - \frac{2a_2}{a_0}\frac{\partial V}{\partial\phi^*}
\tag{3.34}
$$

$$
\begin{aligned}
0 \;=\; & {}^3\nabla_a\,{}^3\nabla^a s - \frac{s^3}{4}Z_{ab}Z^{ab} + \frac{a_0}{2}\frac{e^2}{s}A_\varphi^2|\phi|^2 + \frac{a_2}{2}sV \\
& - \frac{a_1}{8}s\Big[(^3F_{ab} + A_\varphi Z_{ab})(^3F^{ab} + A_\varphi Z^{ab}) - \frac{2}{s^2}\,{}^3\nabla_a A_\varphi\,{}^3\nabla^a A_\varphi \Big]
\end{aligned}
\tag{3.35}
$$

40

$$0 = {}^3\nabla_a\,{}^3\nabla^a A_\varphi - {}^3\nabla^a A_\varphi \Big[\frac{1}{s}\,{}^3\nabla_a s\Big] - \frac{a_0}{a_1}e^2\,A_\varphi|\phi|^2 - \frac{s^2}{2}Z_{ab}({}^3F^{ab} + A_\varphi Z^{ab}) \quad (3.36)$$

$$0 = {}^3\nabla_a\Big[s^3 Z^{ab} + a_1 s A_\varphi({}^3F^{ab} + A_\varphi Z^{ab})\Big] \quad (3.37)$$

$$0 = {}^3\nabla_a\Big[s({}^3F^{ab} + A_\varphi Z^{ab})\Big] + \frac{a_0}{a_1}\frac{ie}{2}\,s\Big[\phi\,({}^3\mathcal{D}^b\phi)^* - \phi^*\,({}^3\mathcal{D}^b\phi)\Big] \quad (3.38)$$

$$\begin{aligned}
{}^3R_{ab} =\ & \frac{1}{s}\,{}^3\nabla_a\,{}^3\nabla_b s + \frac{s^2}{2}\,Z_{ac}Z_b{}^c \\
& + \frac{a_0}{4}\Big[{}^3\mathcal{D}_a\phi\,({}^3\mathcal{D}_b\phi)^* + {}^3\mathcal{D}_b\phi\,({}^3\mathcal{D}_a\phi)^*\Big] + \frac{a_2}{2}\,g_{ab}V \\
& + \frac{a_1}{2}\Big[({}^3F_{ac} + A_\varphi Z_{ac})({}^3F_b{}^c + A_\varphi Z_b{}^c) - \frac{1}{4}g_{ab}({}^3F_{cd} + A_\varphi Z_{cd})({}^3F^{cd} + A_\varphi Z^{cd})\Big] \\
& + \frac{a_1}{2}\frac{1}{s^2}\Big[{}^3\nabla_a A_\varphi\,{}^3\nabla_b A_\varphi - \frac{1}{2}g_{ab}\,{}^3\nabla_c A_\varphi\,{}^3\nabla^c A_\varphi\Big].
\end{aligned} \quad (3.39)$$

A useful simplification is to remove Z_{ab} by using Eq. 3.37. Because Eq. 3.37 is a total divergence we can introduce a potential, w, as

$$ {}^3\epsilon_{abc}\,{}^3\nabla^c w = s(s^2 + a_1 A_\varphi^2)Z_{ab} + a_1\,sA_\varphi\,{}^3F_{ab}. \quad (3.40)$$

By solving Eq. 3.40 for Z_{ab} we can elimate Eq. 3.37 as it is satisfied identically. The set of equations with Z_{ab} removed is

$$0 = {}^3\nabla^a({}^3\mathcal{D}_a\phi) + \frac{1}{s}\,{}^3\nabla^a s\,{}^3\mathcal{D}_a\phi - ieA^a\,{}^3\mathcal{D}_a\phi - \frac{e^2}{s^2}A_\varphi^2\phi - \frac{2a_2}{a_0}\frac{\partial V}{\partial \phi^*} \quad (3.41)$$

$$\begin{aligned}
0 =\ & {}^3\nabla_a\,{}^3\nabla^a s - \frac{s^3}{4}\frac{1}{d^2}\Big[{}^3w_{ab} - a_1 sA_\varphi\,{}^3F^{ab}\Big]^2 + \frac{a_0}{2}\frac{e^2}{s}A_\varphi^2|\phi|^2 + \frac{a_2}{2}\,sV \\
& - \frac{a_1}{8}s\Big[\frac{1}{d^2}({}^3F_{ab}\,s^3 + A_\varphi\,{}^3w_{ab})^2 - \frac{2}{s^2}\,{}^3\nabla_a A_\varphi\,{}^3\nabla^a A_\varphi\Big]
\end{aligned} \quad (3.42)$$

$$\begin{aligned}
0 =\ & {}^3\nabla_a\,{}^3\nabla^a A_\varphi - {}^3\nabla_a A_\varphi\Big[\frac{1}{s}\,{}^3\nabla^a s\Big] - \frac{a_0}{a_1}A_\varphi|\phi|^2 \\
& - \frac{s^2}{2}\frac{1}{d^2}\Big[{}^3w_{ab} - a_1 sA_\varphi\,{}^3F_{ab}\Big]\Big[{}^3F^{ab}\,s^3 + A_\varphi\,{}^3w^{ab}\Big]
\end{aligned} \quad (3.43)$$

$$0 = {}^3\nabla_a\,{}^3\nabla^a w - \frac{1}{d}\,{}^3\nabla^a w\cdot{}^3\nabla_a d + \frac{a_1}{2}\,{}^3\epsilon_{abc}\,{}^3F^{ab}\cdot d\,{}^3\nabla^c\Big[\frac{s\,A_\varphi}{d}\Big] \quad (3.44)$$

$$0 = {}^3\nabla_a\Big[\frac{s}{d}({}^3F^{ab}\,s^3 + A_\varphi\,{}^3w^{ab})\Big] + \frac{a_0}{a_1}\frac{ie}{2}\,s\Big[\phi({}^3\mathcal{D}^b\phi)^* - \phi^*({}^3\mathcal{D}^b\phi)\Big] \quad (3.45)$$

$$\begin{aligned}
{}^3R_{ab} =\ & \frac{1}{s}\,{}^3\nabla_a\,{}^3\nabla_b s + \frac{s^2}{2}\frac{1}{d^2}\Big[{}^3w_{ac} - a_1 sA_\varphi\,{}^3F_{ac}\Big]\Big[{}^3w_b{}^c - a_1 sA_\varphi\,{}^3F_b{}^c\Big] \\
& + \frac{a_0}{4}\Big[{}^3\mathcal{D}_a\phi\,({}^3\mathcal{D}_b\phi)^* + {}^3\mathcal{D}_b\phi\,({}^3\mathcal{D}_a\phi)^*\Big] + \frac{a_2}{2}\,g_{ab}V \\
& + \frac{a_1}{2}\frac{1}{d^2}\Big[({}^3F_{ac}\,s^3 + A_\varphi\,{}^3w_{ac})({}^3F_b{}^c\,s^3 + A_\varphi\,{}^3w_b{}^c) - \frac{1}{4}g_{ab}({}^3F_{cd}\,s^3 + A_\varphi\,{}^3w_{cd})^2\Big] \\
& + \frac{a_1}{2}\frac{1}{s^2}\Big[{}^3\nabla_a A_\varphi\,{}^3\nabla_b A_\varphi - \frac{1}{2}g_{ab}\,{}^3\nabla_c A_\varphi\,{}^3\nabla^c A_\varphi\Big]
\end{aligned} \quad (3.46)$$

41

where $d = s(s^2 + a_2 A_\varphi^2)$. Removing Z_{ab} replaced a second-rank tensor equation with a scalar equation, which is a dramatic simplification

3.1.3   2+1 decomposition

The next step in deriving the equations of motion is the $2+1$ decomposition[4]. This decomposition follows the pattern of the $3+1$ ADM decomposition mentioned in the introduction [12]. This decomposition will give us a notion of a "time derivative" to which we can associate evolution and constraint equations. The $2+1$ decomposition produces a family of 2-dimensional spacelike hypersurfaces and the extrinsic curvature tensor details how those hypersurfaces are embedded within the larger spacetime and how the embedding evolves. The next two subsections will develop the mathematics of the $2+1$ decomposition and the extrinsic curvature tensor. Finally, the last subsection will decompose the equations of motion along the $2 + 1$ split.

Spatial Hypersurfaces

The system we are developing does not contain a timelike Killing vector, so we must use some other approach to single out time. To begin with we will make an arbitrary decision, that a scalar field, t, exists and that $t = constant$ identifies non-intersecting spatial hypersurfaces. Our only requirement on t is that the unit normal vector n_a to t is a future pointing timelike vector field.

Each of the hypersurfaces identified by t contains a coordinate system which can be chosen to be related by a shift vector, β^a. This vector represents the deviation of coordinates from one surface to another. Finally, we can write t^a, the tangent vector, in terms of the shift vector and the unit normal to the hypersurface,

$$t^a = \alpha n^a + \beta^a \tag{3.47}$$

where n^a is the unit normal to the hypersurfaces. The unit normal, n_a, is constructed as

$$n_a = \alpha \, t_{,a} \tag{3.48}$$

---

[4]Most of the presentation here is derived from Chapters 3 and 4 of [11].

and α is the normalization. The normalization α is often refered to as the *lapse* and will be instrumental in the analysis of the numerical implementation and in studying critical behaviour for this system. The shift vector β^a is defined only on the resulting two dimensional spatial hypersurfaces. We can now define a "time derivative" to be the Lie derivative along t^a. This approach still maintains the covariant nature of general relativity, while allowing us to define a time derivative to be used to find evolution equations.

Like the decomposition with respect to the Killing vector[5] we can write the 3-dimensional spacetime metric as

$$^3g_{ab} = h_{ab} - n_a n_b \tag{3.49}$$

where h_{ab} is the induced metric of the final two dimensional spatial hypersurface. h_{ab} can be viewed as a "projection operator" which projects a tensor onto the hypersurfaces. The covariant derivative relative to this new metric h_{ab} is simply the projection of the 3-dimensional covariant derivative

$$^2\nabla_a = h^b{}_a {}^3\nabla_b \tag{3.50}$$

and is equivalent to the covariant derivative relative to h_{ab}.

We can now define a time derivative of a tensor,T, as the Lie derivative along the vector t_a,

$$\dot{T} = \mathcal{L}_t T. \tag{3.51}$$

Extrinsic Curvature Tensor

The extrinsic curvature tensor describes how a hypersurface is embedded in the larger spacetime. To derive it we must look at the covariant derivative of a vector field tangent to the hypersurface. Taking a tangent vector field , V^a, we can evaluate the components of its covariant derivative. There are, in principle, components of $h^a{}_d {}^3\nabla_a V^b$ normal to the hypersurface. By expressing $h^a{}_d {}^3\nabla_a V^b$ as

$$h^a{}_d {}^3g^b{}_c {}^3\nabla_a V^c \tag{3.52}$$

---

[5]See Section 3.1.1

43

and expanding the 3-metric by Eq. 3.49, we have

$$h^a{}_d{}^3\nabla_a V^b = h^a{}_d \left(h^b{}_c - n^b n_c \right) {}^3\nabla_a V^c. \tag{3.53}$$

This equation is now

$$h^a{}_d{}^3\nabla_a V^b = h^a{}_d h^b{}_c{}^3\nabla_a V^c - h^a{}_d n^b n_c{}^3\nabla_a V^c. \tag{3.54}$$

The first term of Eq. 3.54 are the componets tangent to the hypersurface, while the second is normal. Because V^a was chosen to be a tangent vector it is orthogonal to n_a, $V^a n_a = 0$, and $n_c{}^3\nabla_a V^c$ can be rewritten as

$${}^3\nabla_a \left(n_c V^c \right) - V^c{}^3\nabla_a n_c \tag{3.55}$$

by using the product rule. The first term is zero from the definition of V^a as a tangent vector. The resulting second term of Eq. 3.54 is now

$$h^a{}_d n^b V^c{}^3\nabla_a n_c. \tag{3.56}$$

Expressing n_c as ${}^3g^e{}_c n_e$ gives us

$$h^a{}_d n^b V^c{}^3g^e{}_c{}^3\nabla_a n_e \tag{3.57}$$

because the metric commutes with the covariant derivative. Expanding the metric term using Eq. 3.49 leads to

$$h^a{}_d n^b V^c \left(h^e{}_c - n^e n_c \right){}^3\nabla_a n_e = h^a{}_d n^b V^c \left(h^e{}_c{}^3\nabla_a n_e - n^e n_c{}^3\nabla_a n_e \right). \tag{3.58}$$

The second term, $-h^a{}_d n^b V^c n^e n_c{}^3\nabla_a n_e$, is identically zero. This follows from

$$n^e \nabla_a n_e = 0 \tag{3.59}$$

because n_a is a unit vector. We can now define a quantity called the *extrinsic* curvature tensor, K_{ab}, as

$$K_{ab} \equiv -h_a{}^c h_b{}^{d\,3}\nabla_c n_d. \tag{3.60}$$

Using Eq. 3.60, Eq. 3.54 can be expressed as

$$h^a{}_d{}^3\nabla_a V^b = h^a{}_d h^b{}_c{}^3\nabla_a V^c - V^c K_{cd} n^b. \tag{3.61}$$

44

The extrinsic curvature describes how the spatial slices are embedded in the 3-dimensional spacetime and how that embedding evolves.

The important relations derived in the $2 + 1$ decomposition are

$$h_{ab} = {}^3 g_{ab} + n_a n_b \tag{3.62}$$

$$n^a n_a = -1 \tag{3.63}$$

$$K_{AB} = -h_a{}^c h_b{}^{d3} \nabla_c n_d = {}^3 \nabla_a n_b \tag{3.64}$$

$$\partial_t h_{AB} = -2\alpha K_{AB} + \Delta_A \beta_B + \Delta_A \beta_B \tag{3.65}$$

$$\partial_t K_{AB} = (\beta^{C2} \nabla_C K_{AB} + K_{AC}{}^2 \nabla_B \beta^C + K_{BC}{}^2 \nabla_A \beta^C)$$
$$+ \alpha[K K_{AB} + {}^{(2)} R_{AB}] - 2\alpha K_{AC} K_B{}^C - {}^2\nabla_A{}^2\nabla_B \alpha - \alpha {}^3 R_{AB} \tag{3.66}$$

Our final set of equations expressed in the $2 + 1$ decomposition is in Appendix B.1.

3.1.4   Coordinate choices and conditions

The Einstein equation contains 10 equations for 10 unknowns. However, the Einstein tensor must also satisfy the contracted *Bianchi* identities $\nabla_b G^{ab} \equiv 0$ which constrains the tensor components such that they are no longer independent. This apparent over-determined system for the metric components is "solved" by the additional coordinate freedom which the metric possesses. This fixes the problem of over-determinacy by allowing for an arbitrary choice of coordinates and coordinate transformations. In general, this means that we are at liberty to make four coordinate choices. Here, because of the symmetry we can make three. We will choose the maximal slicing condition, which specifies the trace of the extrinsic curvature tensor, K_{ab}, to be zero. Mathematically this states that

$$K \equiv K_{ab} h^{ab} = 0. \tag{3.67}$$

This is a condition on the time component. The maximal slicing condition is a singularity avoiding coordinate choice.

A conformal coordinate transformation leads to a metric of the form

$$g_{ab} = a^2 \delta_{ab}. \tag{3.68}$$

Which relates the metric to the flat space metric, δ_{ab}, and a scalar field a. The final coordinate choice is a "conformal" choice for h_{ab}

$$h_{ab} = a^2 \delta_{ab}. \tag{3.69}$$

Where now δ_{ab} is the a flat 2-dimensional metric. This coordinate choice leads to equally scaled ρ and z coordinates.

3.1.5 Regularity conditions

An important aspect of developing a set of equations that can be solved numerically in the presence of a symmetry is the existence of regularity conditions. Because of our choice of a coordinate system adapted to the symmetry we have a so-called symmetry axis, namely where $\rho = 0$. At such points there is no reason physical quantities should be anything but finite and well behaved. The fields representing physical quantities should be "regular." However the equations may appear to be singular at symmetry points such as $\rho = 0$. For example, the Laplacian expressed in cylindrical coordinates in flat space is

$$\nabla^2 f = \frac{1}{\rho} \frac{\partial}{\partial \rho} \left(\rho \frac{\partial f}{\partial \rho} \right) + \frac{\partial^2 f}{\partial z^2}. \tag{3.70}$$

At first glance it would appear that the first term diverges as $\rho \to 0$ because of the $1/\rho$ prefactor. Of course, this is not what happens. Instead, the ρ derivative of f is exactly equal to zero at $\rho = 0$, or $(f_{,\rho})|_{\rho=0} = 0$. But in the numerical or discrete case, enforcing the finiteness of this limit as $\rho \to 0$ can be difficult. There are tricks that can be used to help enforce regularity at the descrete level, but at a minimum one must know that $\partial f / \partial \rho = 0$ as $\rho \to 0$. In fact, we can turn the argument around and insist that the system be regular at $\rho = 0$ and use this to determine the behaviour of physical fields near $\rho = 0$.

More specifically, many of the equations that arise in our current model involve terms that include negative powers of ρ. These terms, in general, look like

$$\frac{1}{\rho^n} f(\rho, z, t) \tag{3.71}$$

and will have problems as $\rho \to 0$. Since it is simply our choice of coordinate system that introduces these terms, we expect that in the limit as ρ approaches 0 the entire term should either go as a positive power of ρ or as a constant. That is mathematically,

$$\lim_{\rho \to 0} \frac{1}{\rho^n} f(\rho, z, t) \sim \rho^m \tag{3.72}$$

where m is an integer and $m \geq 0$. If we had chosen Cartesian-like coordinates, these terms would not contain the negative powers of ρ. In order to ensure that the final equations which we will try to solve are regular, we will make a series of substitutions for the various fields based on the behaviour of those fields and the equations near the axis.

Determining the functional behaviour of different tensor fields near the axis is accomplished in the following way: One imagines writing tensor quantities, such as the metric or assorted vector fields, in Cartesian-like coordinates where everything will be manifestly regular. One then assumes the existence of a symmetry (in our case axisymmetry) and enforces it with repect to these tensor quantities through the equation

$$\mathcal{L}_X A = 0, \tag{3.73}$$

where A is any tensor quantity, such as a vector, metric, etc. This equation states that the Lie derivative of the tensor is zero in the direction of the symmetry defined by the Killing vector X_μ. Assuming the Killing vector is known, this amounts to solving a set of first order, linear, partial differential equations for the components of the unknown tensor. These components will not be solved for completely (that's what the Einstein equations are for) but we will get information about the functional dependence of those components on the coordinates in the presence of the symmetry. Once that is known we transform back to the coordinate system adapted to the Killing vector. We then have the functional dependence of the tensor components in the coordinate system we are interested in using.

Each of the components of the various tensor quantities must be evaluated and their regularity behaviour determined. The fields of interest are the metric, the Maxwell tensor F_{ab}, the 4-vector potential A_a, Z_{ab} (defined in Eq. 3.4), and Y_a (the

rescaled Killing vector). These are either second rank tensors or vectors. A simplified approach is to consider an arbitrary second rank symmetric and anti-symmetric tensor, and an arbitrary vector. Any second rank tensor can be decomposed into a symmetric and anti-symmetric part

$$T_{ab} = S_{ab} + A_{ab} = \frac{1}{2}(T_{ab} + T_{ba}) + \frac{1}{2}(T_{ab} - T_{ba}) \tag{3.74}$$

which allows us to use the result for the arbitrary symmetric and antisymmetric tensors.

Consider an arbitrary covariant vector A_ν. The regularity conditions require the following ρ behaviour

$$
\begin{aligned}
A_t &= f_1 \\
A_\rho &= \rho f_2 \\
A_z &= f_3 \\
A_\phi &= \rho^2 f_4.
\end{aligned}
$$

Where $f_n = f_n(t, \rho^2, z)$ simply represents a function which is constant in ρ along the axis. This means that the t and z components will act as a constant on the axis, while the ρ and ϕ components will be zero on the axis.

For arbitrary second-rank symmetric and antisymmetric tensors, S_{ab} and A_{ab} respectively, the regularity conditions require

$$
\begin{aligned}
S_{tt} &= f_1 & S_{t\rho} &= \rho f_2 \\
S_{tz} &= \rho f_3 & S_{t\phi} &= \rho^2 f_4 \\
S_{\rho\rho} &= f_5 & S_{\rho z} &= \rho f_6 \\
S_{\rho\phi} &= \rho^3 f_7 & S_{zz} &= f_8 \\
S_{z\phi} &= \rho^2 f_9 & S_{\phi\phi} &= \rho^2 f_5 + \rho^4 f_{10} \\
A_{t\rho} &= \rho g_1 & A_{tz} &= \rho g_2 \\
A_{t\phi} &= \rho^2 g_3 & A_{\rho z} &= \rho g_4 \\
A_{\rho\phi} &= \rho g_5 & A_{z\phi} &= \rho^2 g_6.
\end{aligned}
$$

Again, f_n and g_n are general functions of the coordinates which are constant in ρ along $\rho = 0$. The final set of regularity substitutions are the following:

$$s = \rho a e^{\rho \bar{\sigma}} \tag{3.75}$$

$$a = \psi^2 \tag{3.76}$$

$$\psi = \bar{\psi} e^{\frac{\rho \bar{\sigma}}{2}} \tag{3.77}$$

$$A_\varphi = s^2 A_{\hat{\varphi}} \tag{3.78}$$

$$P = s^2 P_{\hat{p}} \tag{3.79}$$

$$\tilde{K}_{\mu\nu} = a^2 K_{\mu\nu}. \tag{3.80}$$

3.2 Two reduced models

In order to study this system we will choose two different sets of initial data. At first we will restrict ourselves to only varying the initial data of the electromagnetic fields. Also, we restrict ourselves to cases without rotation.

Primarily, as we study these fields, we are looking at the behaviour of the ADM lapse, α, defined in Section 3.1.3. The lapse comes from the ADM decomposition as the time component of the time-like vector n^a. The lapse is a measure of time for a local observer. In flat space the lapse will be identically one, meaning that all observers measure the passage of time to be exactly the same. However, in the presence of strong gravitational fields general relativity predicts that the measurement of time will be dilated. In other words, distant observers will measure time slowing down in these strong fields. We are searching for strong fields, so we expect that the lapse will collapse, or tend towards zero, in the presence of a strong gravitational field. As we look at different configurations, we can look primarily at the behaviour of the lapse throughout the evolution. Regions where the lapse starts to drop will represent regions of strong gravity. In cases where α returns to values near 1, the system is dispersive where the matter fields disperse off the grid.

There are other approaches to determining strong gravitational fields. For instance, searching for apparant horizans and event horizans. Also, evaluating the

geodesics within the spacetime will lead to geometric information strong gravitational fields. As a first attempt to study this system, we will continue to use the lapse.

3.2.1 Toroidal fields

Consider first the case that only A_ϕ is non zero. All the equations are simplified by setting the terms involving ${}^2E^z, {}^2E^\rho$, and ${}^2F^z_\rho$ to zero. As well, we can set the other components of the vector A_μ to zero. In the process of this simplification, we discovered that the scalar field and electromagnetic fields are coupled such that we must set the coupling parameter, e, between electromagnetism and the scalar field to zero in order to guarantee that those fields aren't sourced later in the evolution. Because e represents the coupling strength between F_{ab} and the scalar field, it makes sense that e would need to be zero to insure that the other components of F_{ab} are not sourced. Choosing only $A_\phi \neq 0$ corresponds to toroidal electromagnetic fields.

3.2.2 Poloidal fields

The second case we will consider is to set $A_\phi = 0$ and allow the corresponding electromagnetic fields on the 3-manifold to be non-zero. Again, we need to set e, the coupling constant between the scalar field and the electromagnetic fields, to zero. Setting e to zero is still required to insure we do not source the A_μ fields. Setting e to anything else will couple all the electromagnetic fields, ${}^2E^z, {}^2E^\rho, {}^2F^z_\rho$, and A_μ, to both components of the complex scalar field. This configuration only allows for poloidal electromagnetic fields.

Chapter 4

Results

In this chapter we present results of the numerical implementation of adding electromagnetism to `GRAXI`, which we will call `GREMAXI`. While there is a large set of possible initial data, we restrict our attention to toroidal fields (only $A_\varphi \neq 0$). This is the simplest case with electromagnetism, the other case involve multiple fields instead of just one.

4.1 Initial data sets

This section is a review of four sets of initial data for the A_φ field. The form of A_φ for the initial data is a generalized gaussian,

$$A_\varphi = A_0 \exp\left(\frac{\sqrt{(\rho - \rho_0)^2 + \beta_0 (z - z_0)^2} - r_0}{\delta_0}\right)^2. \tag{4.1}$$

The various parameters with the subscripted zero allow the initial data to be tuned. For instance, varying the β_0 parameter leads to oblate or prolate profiles, while changing r_0 produces rings of different radius. These six parameters lead to a six parameter space to explore for the initial data of the A_φ field. In Sections 4.1.1 - 4.1.3 we look at the evolution of the system with initial data of various combinations of a few of these parameters. Additionally, the initial data is time-symmetric (*i.e.* the "velocity" of the A_φ field is initially zero, along with the extrinsic curvature components).

Primarily, there are two results of the evolution of the fields from the initial data: gravitational collapse or dispersion. If the initial fields are strong enough, a portion of the matter fields will begin to collapse under gravity. This is, in fact, what we expect by including general relativity. The matter fields, being either the

scalar field or the various Maxwell related fields, will cause the spacetime to curve. This region of strong curvature will attact the matter fields and cause the density to increase until a black hole forms. In a dispersive case, the matter fields will propogate away leaving behind flat space. It is common to see some curvature, and some change in the ADM lapse, but eventually the matter fields will disperse.

The ADM lapse is our monitor for the evolution of the spacetime and to determine if the system is leading towards collapse or dispersion. If, through the evolution, the lapse tends towards one, then the system is dispersive. While if the lapse decreases then the system is interpreted to be collapsing. The lapse is not the only way to measure the gravitational field. It is also possible to look at the evolution of the extrinsic curvature tensor, or the scalar field resulting from the 2-dimensional conformal transformation, or other geometric quantities derived from the metric.

Based on the results of `GRAXI` we expect to see some "ringing-down" of the minimum value of the ADM lapse. Until a critical point is reached and the lapse collapses completely, or the lapse returns to one. The first case signifies a gravitational collapse and the second is dispersion.

4.1.1 Initial data: origin centered gaussian

$$A_\varphi = A_0 \exp\left(\sqrt{\rho^2 + z^2}\right)^2 \tag{4.2}$$

We start by choosing an initial data set consisting only of A_ϕ as an origin-centered Gaussian with various starting amplitudes. Figure 4.1 shows an example of this initial profile. This became our original test problem for the entire system. A few mistakes in the translation from algebraic equations to numerical code were caught while studying this initial data set. As well, a minus sign mistake showed up in the equation for the lapse. Once these bugs where fixed, the code appeared to run well and accurately.

Early simulations of origin centered Gaussians worked very well for weak amplitudes. For larger amplitudes, which are the more interesting cases and where we expect the gravitational field to be strong and perhaps lead to black hole formation,
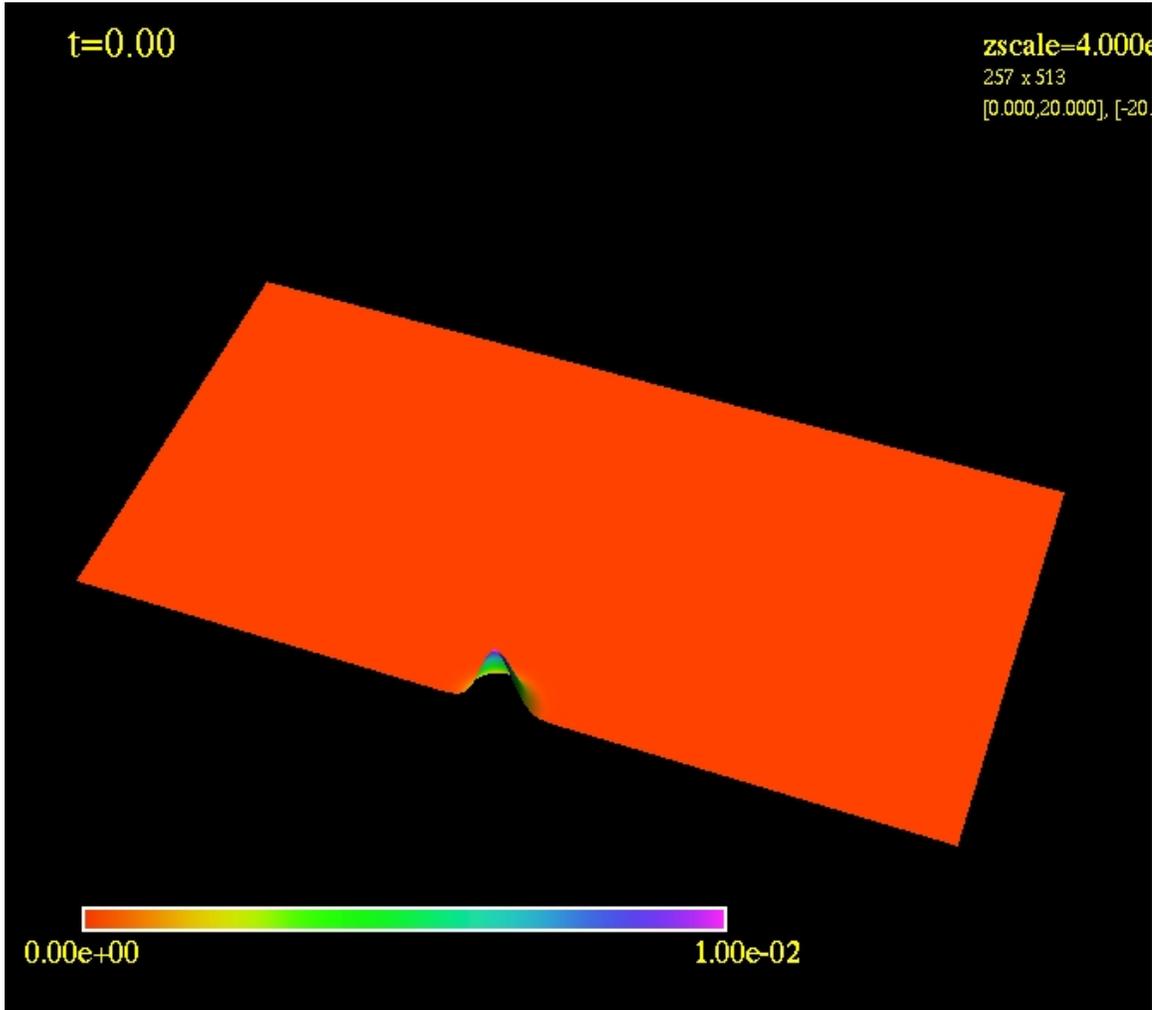
Figure 4.1: Initial data profile where the field is centered on the origin, with Gaussian fall-off. The field is highly concentrated at the origin. The colourmap scale runs from 0 to 1, and is the amplitude of the field.

we started to encountered problems. Even for amplitudes within a range where dispersion was expected to ultimately take place, we found that the code would crash. We concluded that there was some instability that caused components of the extrinsic curvature to grow without bound and hence stop the evolution. Figure 4.2, displays three sets of data. The first, labeled as "alpha", is the minimal value of the lapse for an evolution where $A_0 = 0.9$. The small dip in the beginning of the evolution shows some curvature of the spacetime, but which returns to flat space within about twenty-five timesteps. This evolution proceeds to appear dispersive until around timestep 125 where suddenly, and rapidly, the lapse plummets to values less then 0.1. Looking again at Figure 4.2, the other two fields are the minimum and maximum values of the A_ϕ field. The important thing to notice is that all the matter fields have dispersed, indicated by the minimum and maximum data sets at zero, and yet the lapse collapses anyhow. This should not signify gravitational collapse, as there is nothing to cause the collapse. The source of the collapse seems to be an instability in the numerical code itself. Figure 4.3 is a similar plot of the maximum and minumum values of the extrinsic curvature, labeled as "kzz krr" in the figure. This figure, Figure 4.3, also shows a large jump around the same timestep as the lapse, again signifying a numerical instability.

To test for problems in the code, we can set $A_0 = 0$ and recover `GRAXI`. Taking the same initial data, with all the electromagnetism field set to zero, and comparing data from a run of `GRAXI` and this code where the same. However, after setting a run of `GRAXI` to run for two-hundred timesteps, which is beyond which any interesting dynamics happened, the same numerical stabilty showed up. This appears to actually be in `GRAXI` itself, but it happens at much later time then in `GREMAXI`. Electromagnetism, apparently, brings this instabilty much closer to the beginning of the evolution, but doesn't necessarily cause it.

4.1.2 Initial data: origin centered ring

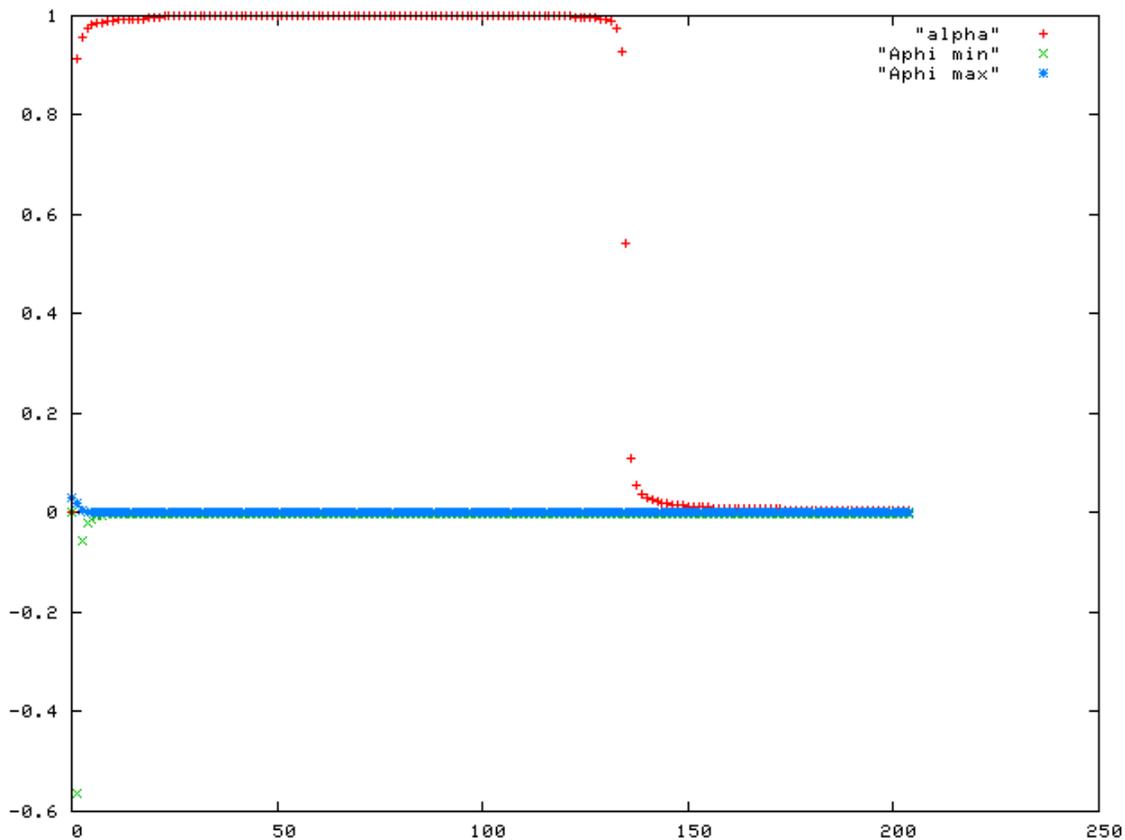$$A_\varphi = A_0 \exp\left(\sqrt{\rho^2 + z^2} - 5.0\right)^2 \tag{4.3}$$

Figure 4.2: This figure dispays two sets of information, the minimum value of the evolution of the ADM lapse and the max/min of the evolution of the A_φ field. The initial data for this evolution is, $A_0 = 0.9$. Until timestep 125 this appears to be a simple dispersive case, until the lapse crashes to values below 0.1. A collapse of the lapse can signify the formation of a black hole, but A_φ has propogated out of the region. With no matter to form the black hole it seems unlikely that a hole is forming. Figure 4.3 displays the maximum and minimum values of the extrinsic curvature tensor, which also shows a sharp discontinuty around the same timestep that the lapse crashes. Based on the behaviour of the lapse and the extrinsic curvature tensor there appears to be a numerical instability in the code.
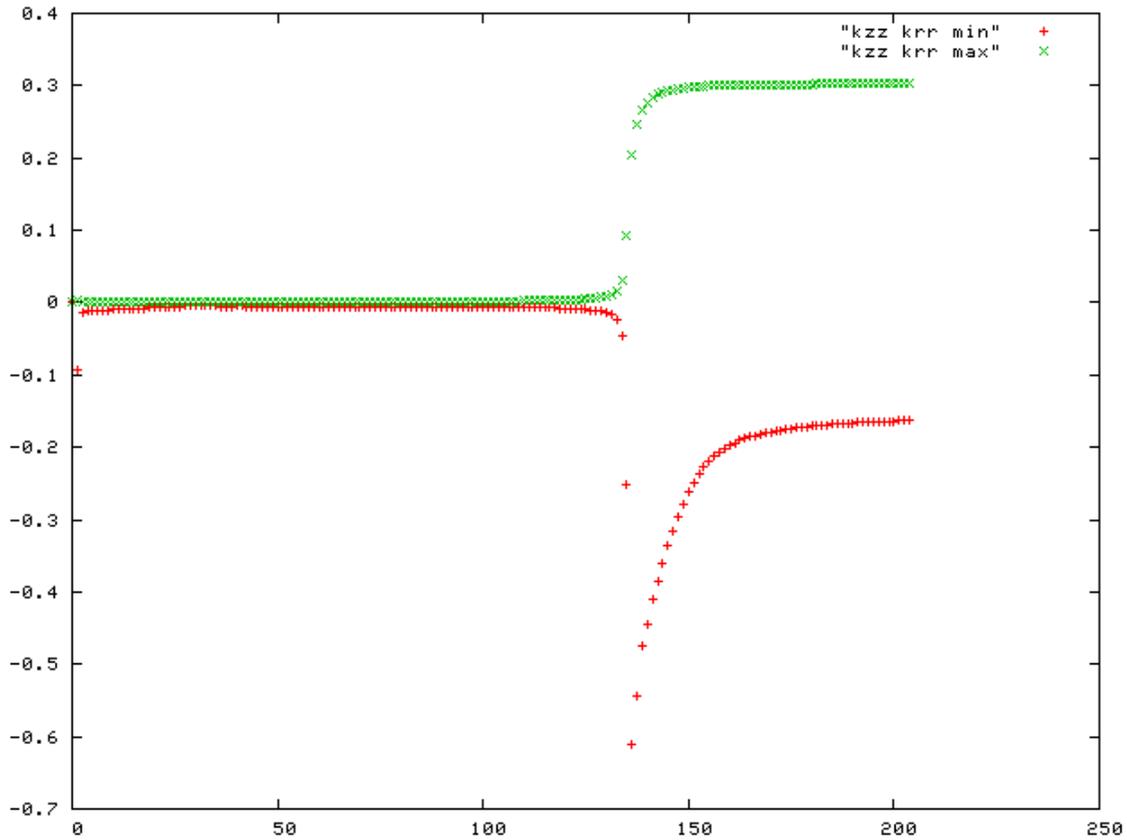
Figure 4.3: Looking at the evolution of the extrinsic curvature tensor for an inital data where $A_0 = 0.9$, there appears to be a problem around timestep 125. Like in the case of the ADM lapse, Figure 4.2, this rapid jump doesn't look natural. Based on the extrinsic curvature tensor and the ADM lapse, there appears to be a numerical instability in the code. The vertical axis is the amplitude of the extrinsic curvature tensor, the horizontal axis is the timestep.
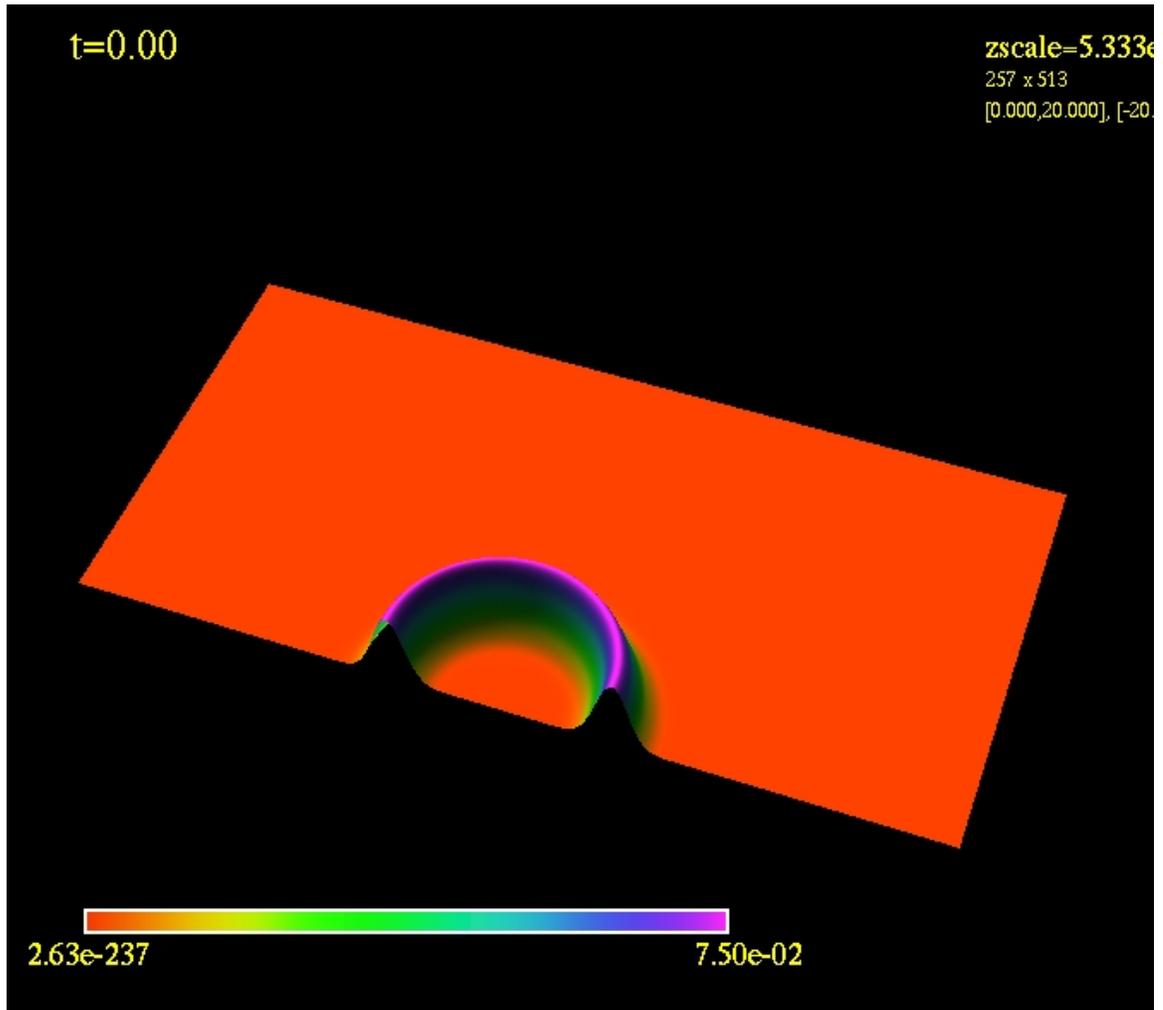
Figure 4.4: This initial data profile is an origin centered ring, with Gaussian fall-off. With the field initially concentrated off the origin, this provided a good initial profile. Additionally, because the initial data is time-symmetric this profile evolved outgoing and incoming waves. The incoming waves became our source of gravitational collapse.

Initially, it was thought that the concentration on the origin was the source of the problem seen in Section 4.1.1. To test this, the matter is moved away from the origin and into a shell. Unfortunately, this didn't fix the problem, it was, however, easier to see some dynamics happening. Because of the initial concentration of the field off the axis, but still symmetric about the origin, it was possible to track the evolution of an outgoing, dispersive portion, and a collapsing portion. Any black-hole formation would come from the initially collapsing portion of this profile. Again, the initial amplitude was varied with a change of behaviour happening between 0.07 and 0.075. The evolutions indicated that something odd was happening. Over the time range we looked at, which often amounted to thousands of time steps, larger amplitude fields would begin to disperse and then α would suddenly plummet as seen in Section 4.1.1.

Figure 4.5 shows the results of a family of evolutions. The early behaviour is what was expected, some dynamics in the lapse field that eventually lead to dispersion. Again, however, the lapse would suddenly collapse to values below 0.1. This appeared to be the same instability encountered in the first case (Section 4.1.1). Looking closely near the origin showed that the A_φ field was rapidly varying. Figure 4.6 shows a snap-shot of the A_φ field at a given time. Figure 4.7 is the next timestep, only 0.13 time-units later. The field is changing so rapidly between these two timesteps that the numerical code can't keep up and crashes. Another intriguing feature is the slight "bump" near the origin in Figure 4.7.

In order to push the instability to later times, we decided to lower the Courant factor, symbolized as λ in the code. The Courant factor represents the size of the discrete timestep. Because of the variation happening near the origin as the A_ϕ field collapsed (see Figures 4.6 and 4.7), we lowered the Courant factor to try and account for the rapid changes. If too much is changing within the timestep, the code will behave badly, leading to instabilities and spurious results. By decreasing the Courant factor from 0.4 to 0.2 and finally 0.1 the results improved, but at the cost of doubling or quadrupling the running time of the simulation. The results of the decreased λ are displayed in Figure 4.8. This improved the situation, but seemed to
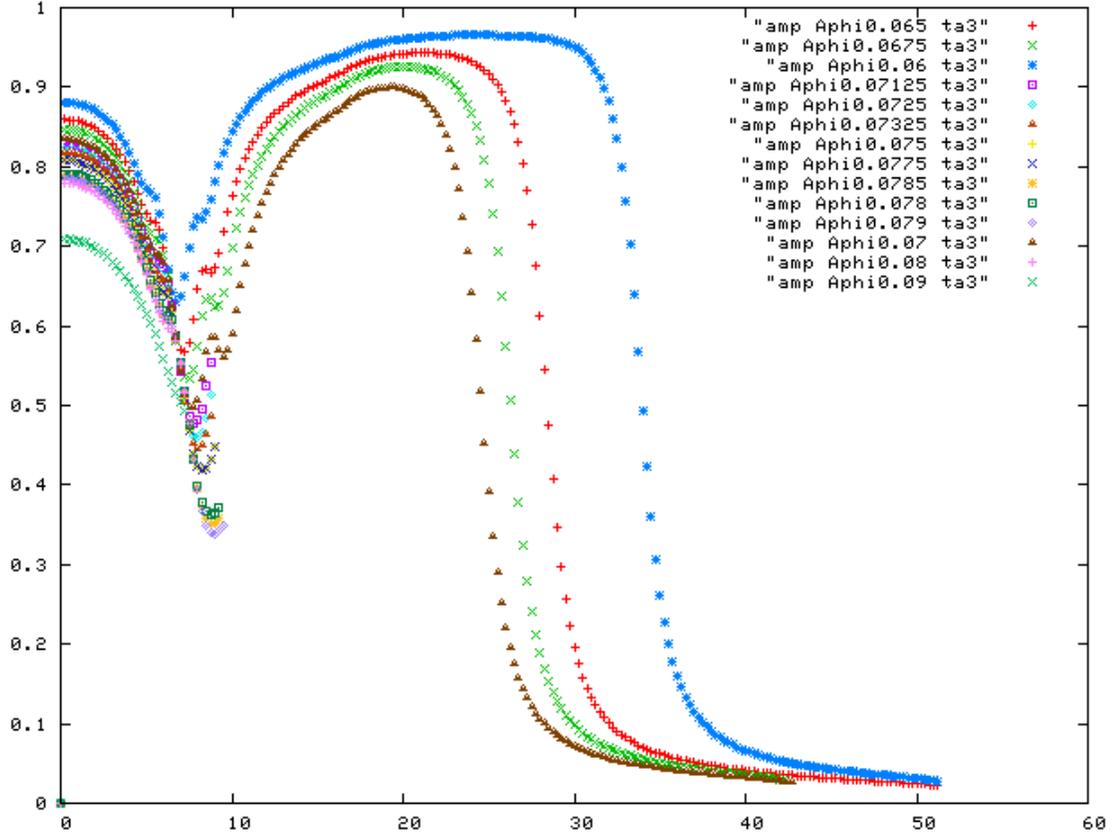
Figure 4.5: Time evolution of the ADM lapse for various initial amplitudes of A_φ from 0.065 to 0.09. Here we can see that most of the evolutions appear to be heading for a dispersive state, and suddenly crash to very low values of the lapse. The higher the amplitude, the faster this crash happens. Fields where the initial amplitude of A_φ is above 0.07 do not even finish the run. In these case the multigrid routine determines that the lapse is negative, and terminates with an error. The failure of the multigrid to find a value for the lapse is most likely associated with the rapid variations of the A_φ field near the origin (see Figures 4.6 and 4.6). The vertical axis is the minimum value of the lapse, the horizontal axis is the time.
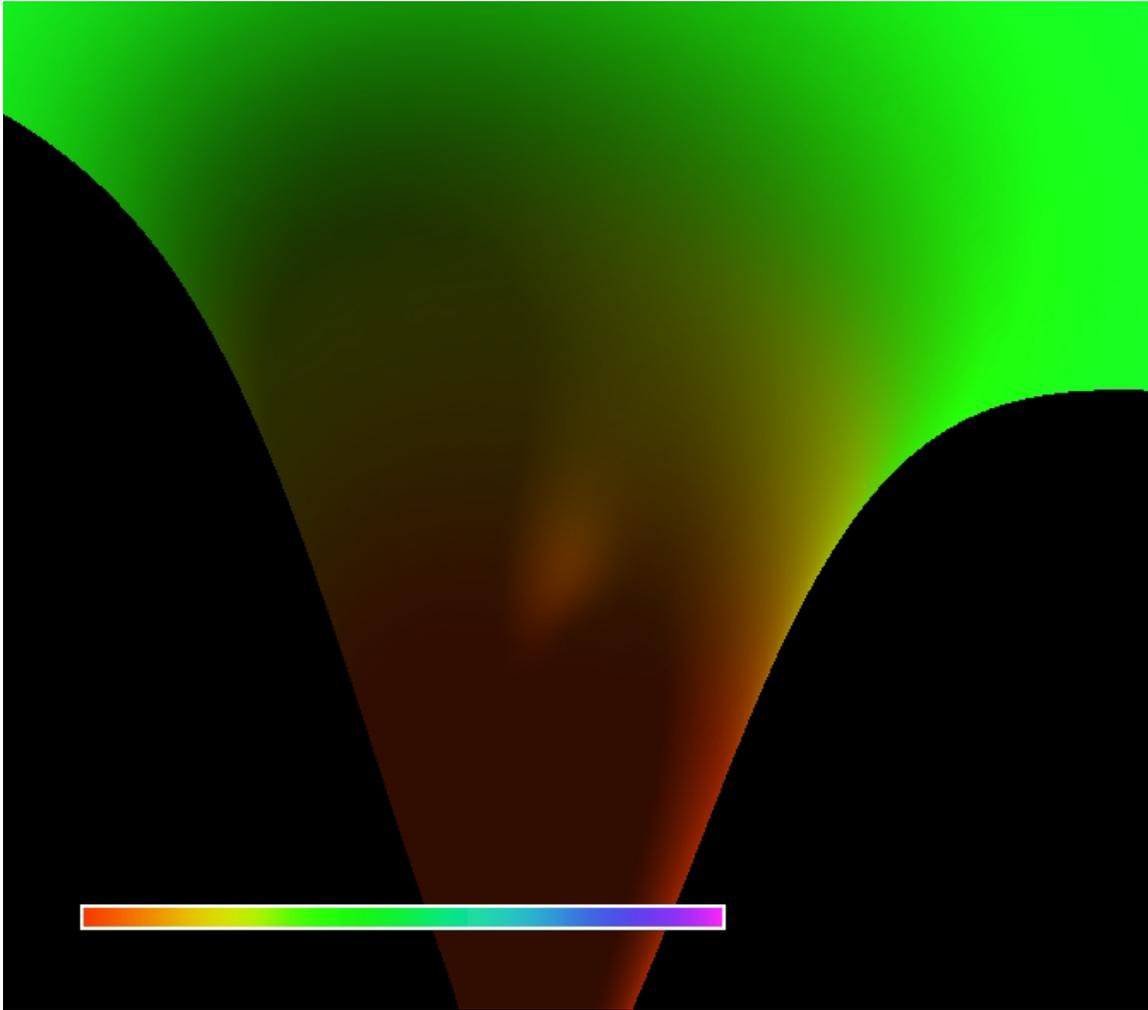
Figure 4.6: This figure displays the timestep before A_φ displayed in Figure 4.7. The scale for Figures 4.6 and 4.7 are the same.
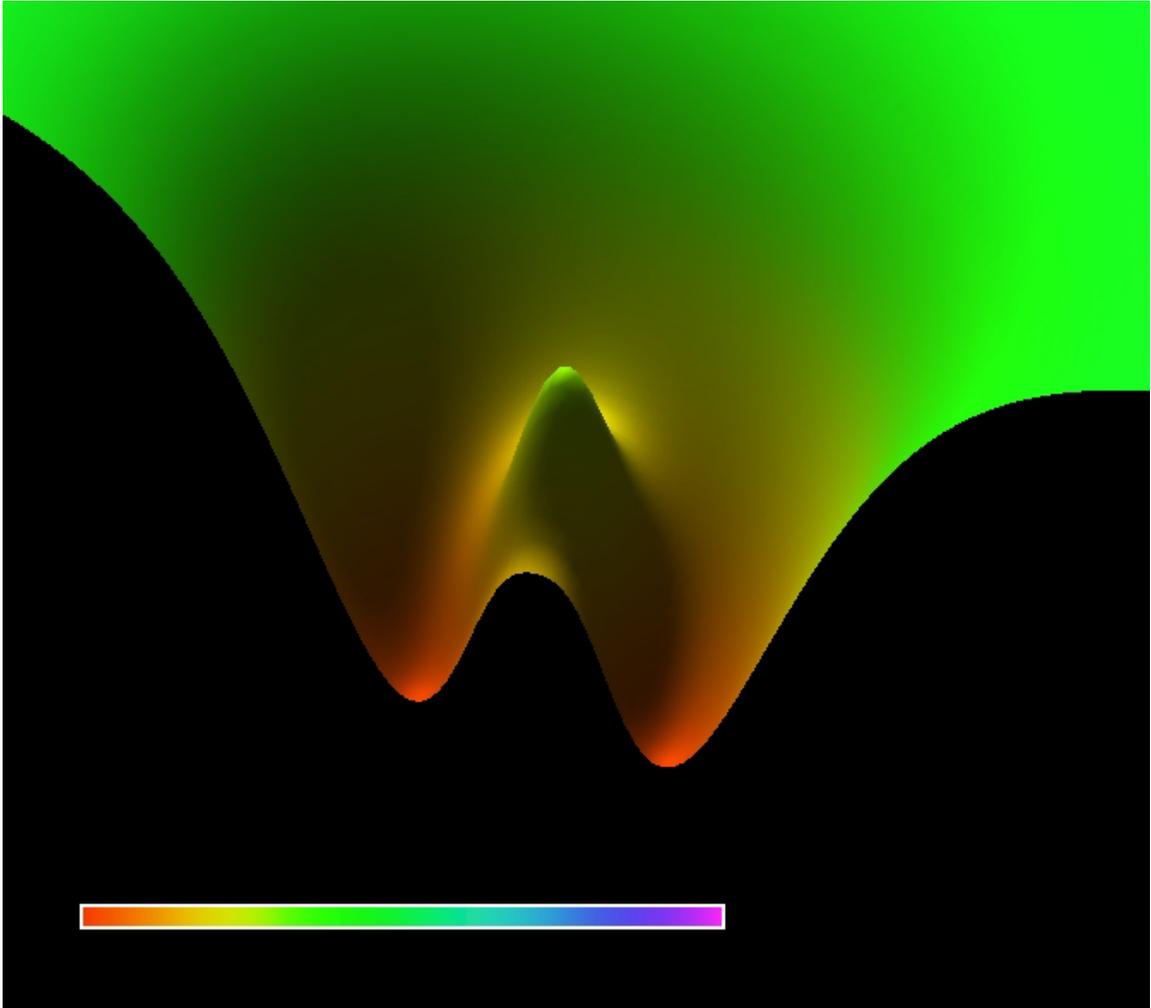
Figure 4.7: From Figure 4.6 to this figure there is only one timestep, and yet there is rapid variation in the field. This figure is from a run with the Courant factor set at 0.2, which is half the original Courant factor of 0.4. Even at this lower value of the Courant factor, there is rapid variation and change. Additionally, there seems to be some interesting structure that is noticable with this zoomed view. There seems to be a "crease" near the axis, with the central peak actually off the axis.
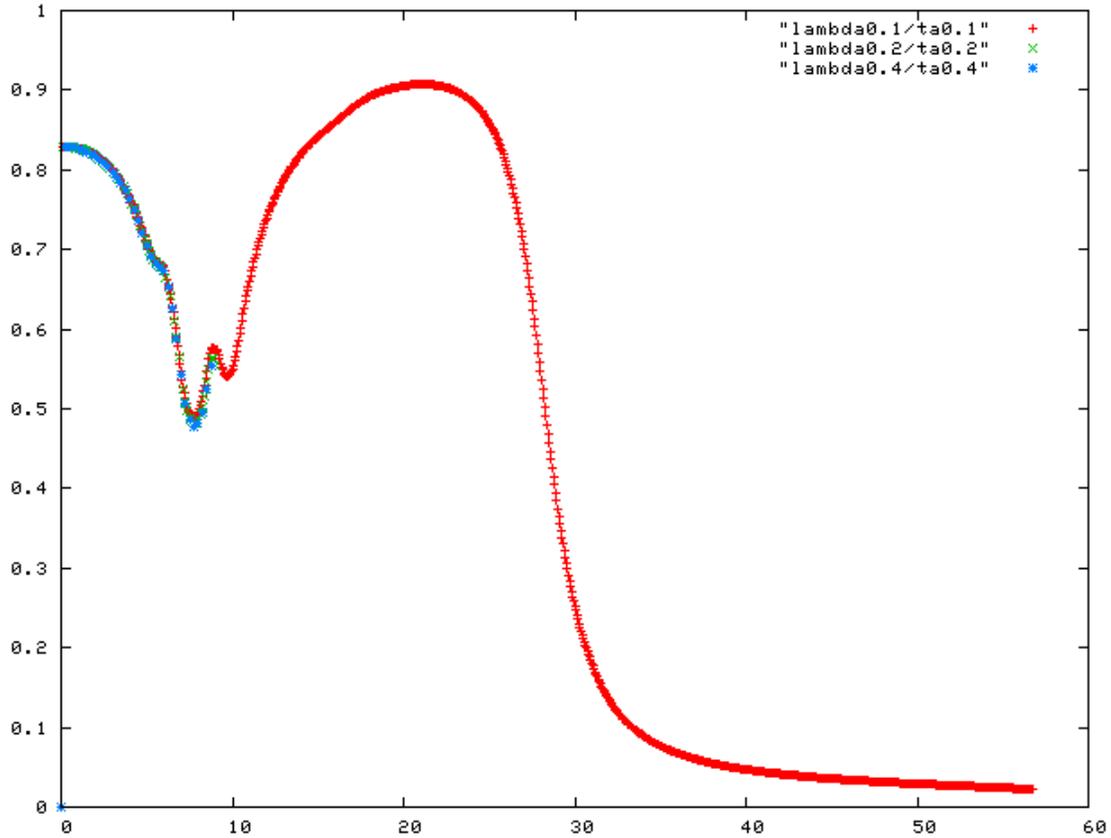
Figure 4.8: This figure displays the minimum value of the ADM lapse for three different values of the Courant factor: 0.4 (in blue), 0.2 (in green), 0.1 (in red). Lower Courant factors represented closer temporal spacing in the numerical code, but require the code to make more calculations. With a Courant factor of 0.1, the evolution completes, though the lapse again shows the crash behaviour. In the other two cases, the evolution terminates with an error, because in the next step the lapse is negative. Figure 4.9 shows a zoomed view of the region where the larger Courant factors fail.
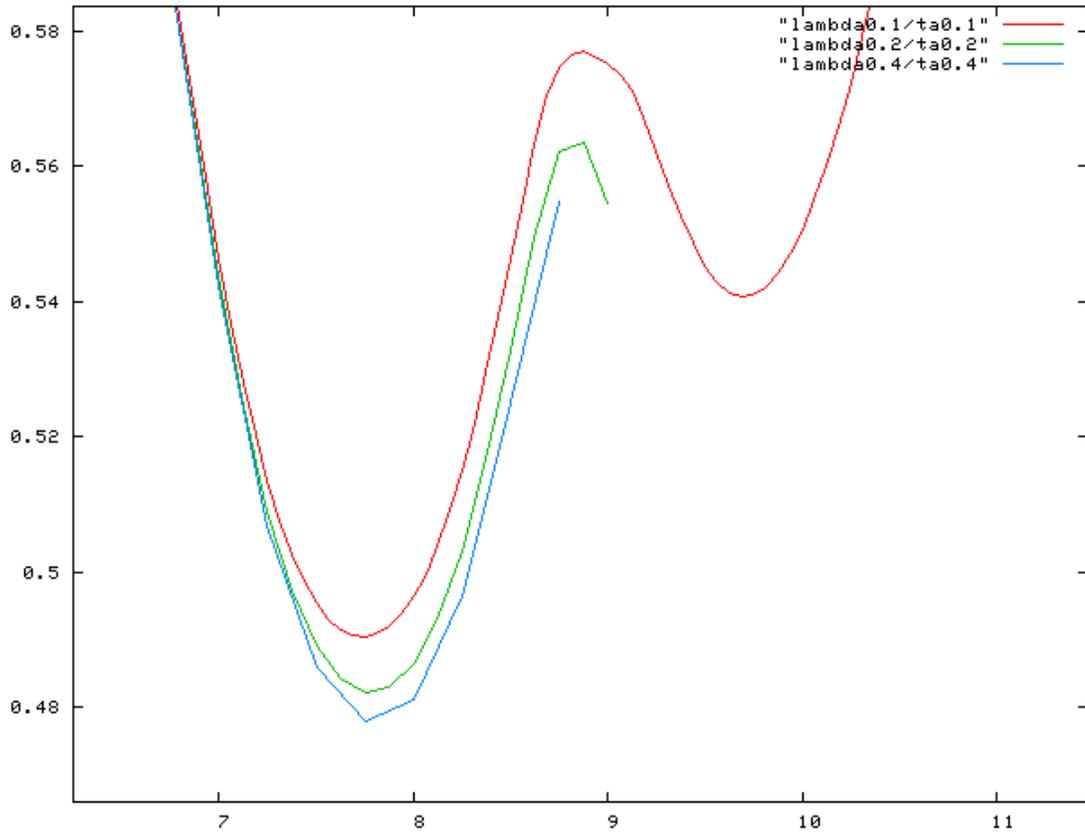
Figure 4.9: Zooming in on the region of interest from 4.8, shows that while the different Courant factors don't deviate too much from each other, the lower factor "survives" longer and doesn't experiance the crash of other factors. This plot uses lines, rather then points, to emphasis the curves. Again, the initial amplitude is still 0.07125. Notice that the runs with higher Courant factors, which are also "courser" in time steps, isn't able to handle the variation around 8.75-9.0

only delay the instabilty.

Adaptive Mesh Refinement [17, 6], AMR, may help solve some of the problems. An AMR algorithm monitors the simulation and adapts the the resolution of the grid as the simulation runs. The instability *may* signal critical behaviour, and if so then AMR would be able to determine this. On the other hand, there may be a fundimental problem with the code, in which case AMR would be unable to improve the results.

4.1.3   Initial data: oblate and prolate rings

$$A_\varphi = A_0 \exp^{\left(\sqrt{\rho^2 + 0.25z^2} - 5.0\right)^2} \tag{4.4}$$

$$A_\varphi = A_0 \exp^{\left(\sqrt{\rho^2 + 4.0z^2} - 5.0\right)^2} \tag{4.5}$$

The final subset of initial data is a prolate and oblate profile. An example of each is displayed here. This led to some very intriguing results: the apparent formation of two gravitational collapses. The way in which A_ϕ collapsed would lead to two points along the axis where α would begin to decrease. Figure 4.12 shows a case of this for $\beta = 4.0$ and $A_0 = 0.1$. However, in all the cases we looked at, the system ended up dispersive or the instability showed up again.

4.2   Future directions

There is still much to learn by studying the interaction of gravitation and electromagnetism. We have focused on a few simple cases. We've explored critical behaviour in some cases, and worked to demonstrate the accuracy of our numerical code. A few further directions including looking at the toroidal case, where $A_\varphi = 0$ and the other electromagnetic fields are non-zero. Of course, fully evolving all the electromagnetic fields is another option to pursue. If the full electromagnetic fields are allowed to evolve the scalar field can be re-coupled to the system. In the implementation for A_φ the scalar field was decoupled from the electromagnetic field to insure that the other Maxwell-related fields where not sourced. Finally, while
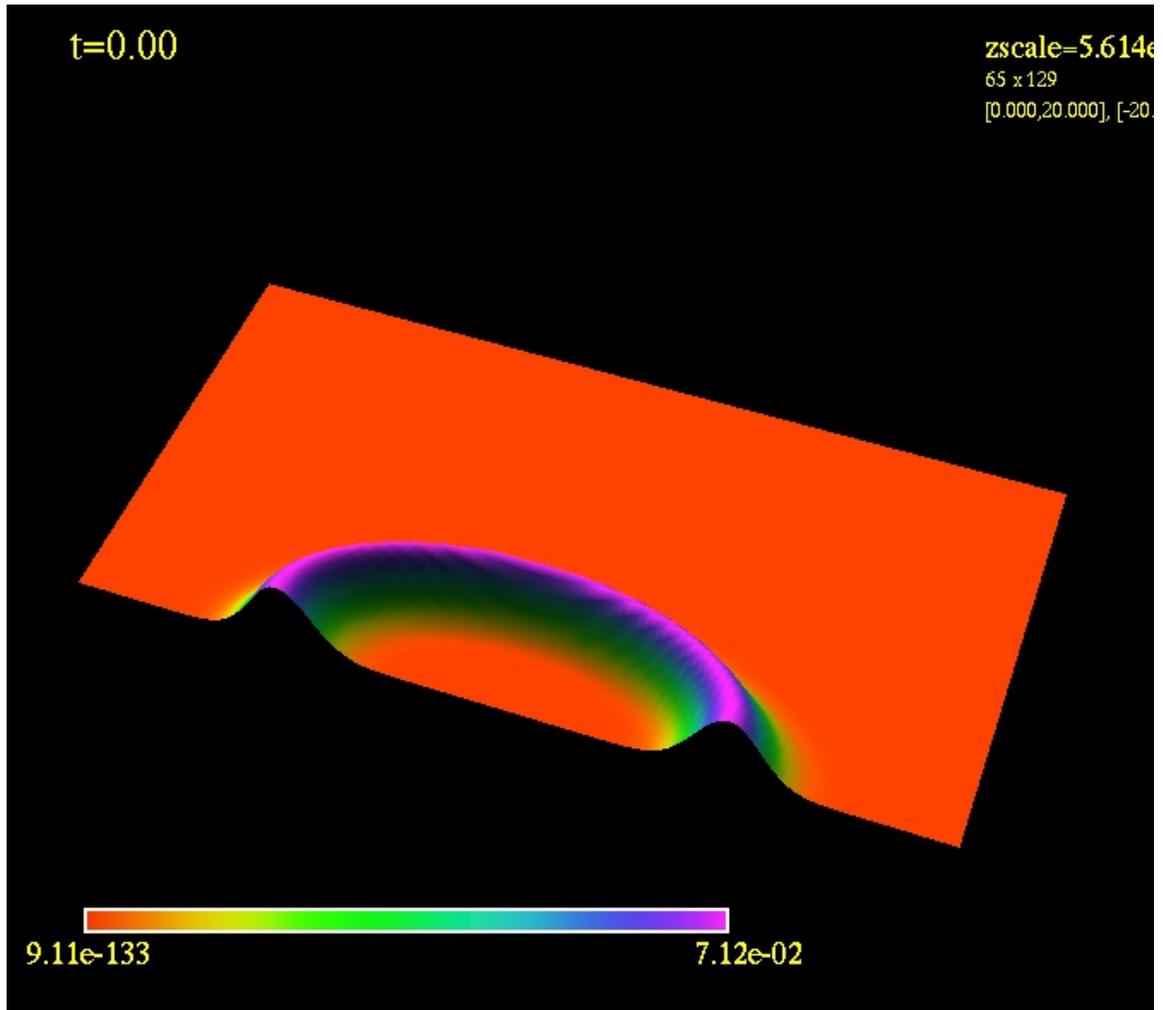
Figure 4.10: Initial data profile of an origin centered ring distorted into a prolate shape. This initial profile, along with the oblate case shown in Figure 4.11, show some interesting behaviour near the origin as the matter field collapses. There appears to be two regions on the axis where the ADM lapse is beginning to decrease, which can be seen in Figure 4.12.
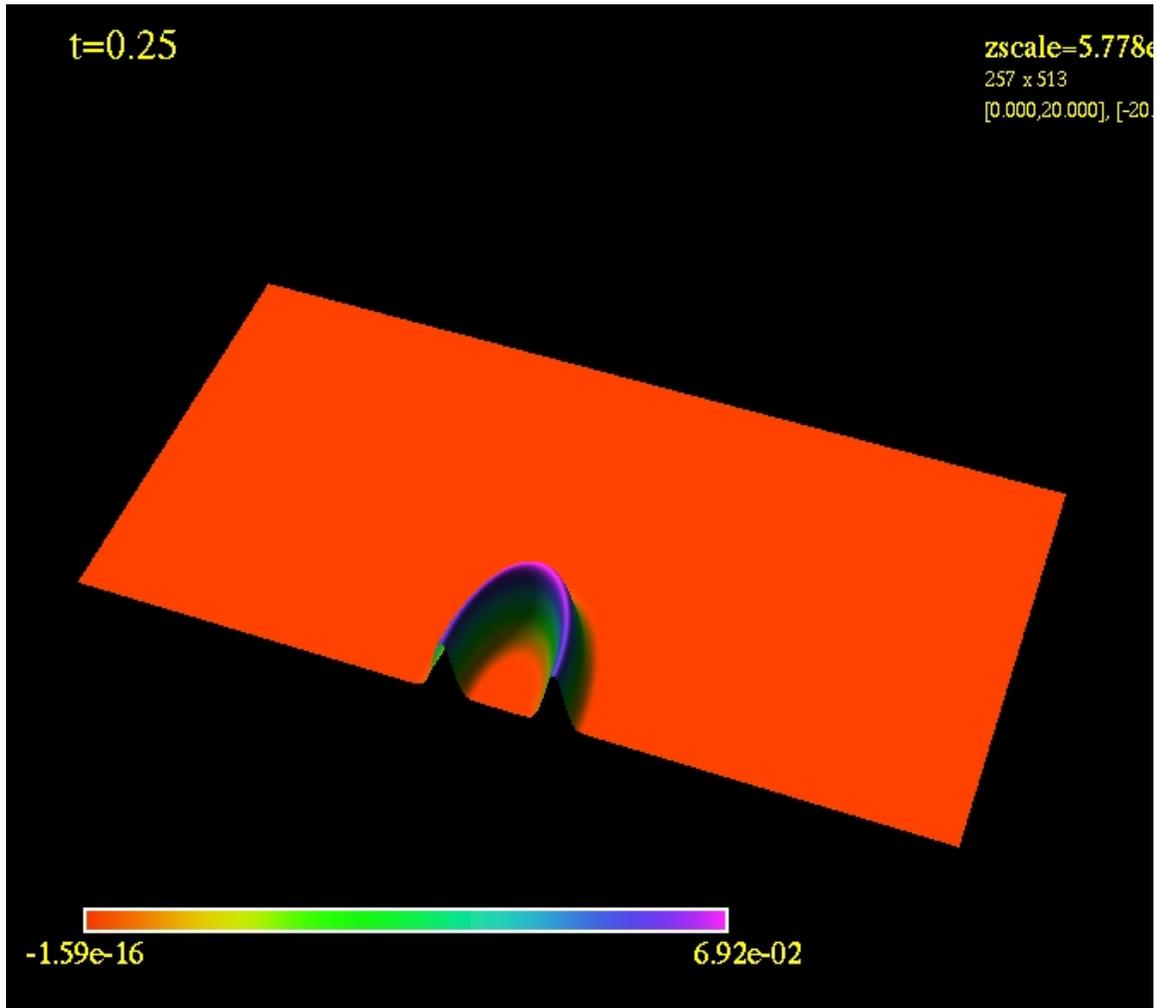
Figure 4.11: Initial data profile of an origin centered ring in a prolate shape. This shape, along with the oblate case in Figure 4.10 show a possible two-region collapse of the ADM lapse on the axis (see 4.12).
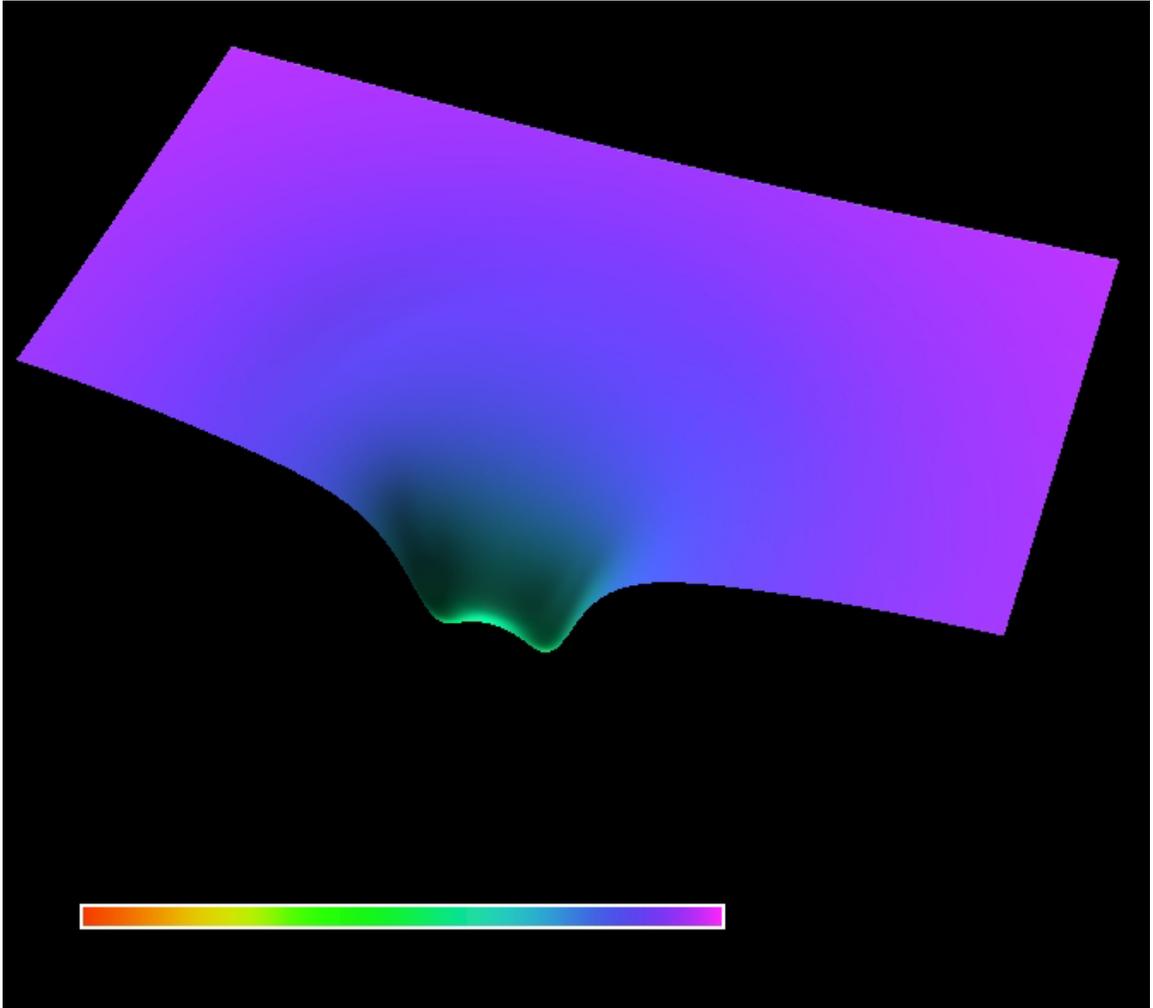
Figure 4.12: This figure shows two "dimples" along the ρ axis where the ADM lapse is decreasing. In the case of the evolution, the lapse evolved into a dispersive case (and then crashed via the instability). Assuming the code and its instability is fixed, this would be an interesting initial data set to explore more fully. It may be possible to form two black holes from a collapse started by this initial data set.

the full mathematical model includes rotation, the numerical implementation does not. Most conceptual models for gravitational collapse include rotation and angular momentum. Adding rotation to the implementation would allow for some exploration of these situations.

A persistent numerical instability was never adequately removed from this scenario. A future step to consider is a change in the gravitational "gauge". Rather then choosing the 2-dimensional conformal transformation, we could choose another gauge. This approach is motivated by some 1-dimensional work by Christensen and Hirschmann [18].

Another improvement would be a true adaptive mesh refinement (AMR) algorithm to handle the regions of gravitational collapse. Because we are looking at gravitational collapse, we necessarily expect to see most of the dynamics happening on a smaller and smaller region of the grid. Currently, the grid spacing is fixed at the beginning of the simulation run. Adding AMR would dramatically increase the complexity of the implemenation, though it should help deal with the collapse by providing a finer grid to analyze.

Another choice of the electromagnetism formulation may lead to a more stable code. This seems unlikely based on the flat space results, but perhaps given the complex non-linearity of Einstein's equation another formulation may work better. We are able to reproduce results from `GRAXI` when the electromagnetic fields are all initially zero so it seems that the source of the instability is in the equations governing electromagnetism.

4.3   Conclusions

The mathematical model developed appears to be good. Combining electromagnetism and gravitation in a way that allows for a dynamic spacetime is challenging, but rewarding. The numerical implementation has some issues, primarily the numerical instability. Any more progress with this code will need to deal with the instability.

Appendix A

Differential Geometry

Differential geometry is a branch of mathematics dealing with differential changes in geometry. This is not an introduction to the complex field of differential geometry. It is intended to summarize notation and definitions used throughout. For a much fuller introduction see [2, 11, 19].

A.1   Einstein Summation Convention

The Einstein summation convention assumes that a repeated subscript and superscript imply a summation. For instance (assuming 4 dimensions),

$$A_c B^c = \sum_{c=0}^{3} A_c B^c = A_0 B^0 + A_1 B^1 + A_2 B^2 + A_3 B^3.$$

This convention is used extensively throughout general relativity.

A.2   The metric g_{ab}

The metric is perhaps the most important tensor in differential geometry and general relativity. The metric can be used to determine distance in more complex geometries. In addition, it is used to define the inner produce of vectors. The line element, or the square of the differential distance, is defined as $ds^2 = g_{ab} dx^a dx^b$, where g_{ab} is the metric tensor. The elements of the metric are generally the "unknowns" when solving the Einstein equation.

A.2.1 Metric signature

A convention for specifying the relative "sign" of the magnitude of space-like or time-like vectors. A common signature is $(-, +, +, +)$ $(+2)$, meaning that magnitude of a purely time-like vector is negative. On the other hand, another common signature is $(+, -, -, -)$ (-2) which simply states that time-like vectors will have a positive magnitude.

A.2.2 Time-like

A time-like vector is a vector that can be the path of a physical body. The norm of a time-like vector will be - or +, depending on the signature of the metric. For instance, if the signature is -2 then $V^a V_a > 0$ for a timelike vector. For a signature $+2$, $V^a V_a < 0$. The sign of the norm will be opposite the sign of a space-like vector. Physical bodies follow paths which have

A.2.3 Space-like

The norm of a space-like vector is opposite that of a time-like vector. For a signature of -2 a space-like vector's norm will be $V^a V_a < 0$, while for $+2$ $V^a V_a > 0$.

A.2.4 Light-like or null

With an indefinite metric, as in general relativity, it is possible that a vector's norm is zero, $V^a V_a = 0$. In that case, the vector is called light-like or null.

A.3 Covariant derivative

The covariant derivative, ∇_μ, is a generalization of the partial derivative to curvilinear coordinate systems. The definition is

$$\nabla_c T^{a\cdots}_{b\cdots} = \partial_c T^{a\cdots}_{b\cdots} + \Gamma^a_{dc} T^{d\cdots}_{b\cdots} - \Gamma^d_{bc} T^{a\cdots}_{d\cdots}. \tag{A.1}$$

A.4 Metric Connection

The metric connection, usually denoted as Γ^a_{bc}, is defined as

$$\Gamma^a_{bc} = \frac{1}{2} g^{ad} (g_{dc,b} + g_{db,c} - g_{bc,d}). \tag{A.2}$$

This mathematical object is not a tensor, though the difference of two connections is a tensor. The connection used used in differentiation of tensor objects with respect to the covariant derivative.

A.5 The Lie derivative

The Lie derivative is a covariant differential operator. Unlike the covariant derivative, the Lie derivative does not use the metric connection. The Lie derivative is defined by measuring the difference in a tensor as it is "dragged" from point A to point B along the vector X, and taking the limit as A approaches B. For a vector V^a, the Lie derivative is

$$\mathcal{L}_X V^a = X^b V^a{}_{,b} - V^b X^a{}_{,b}. \tag{A.3}$$

A.6 Riemann tensor

The Riemann tensor is defined as

$$R^a{}_{bcd} = \partial_c \Gamma^a_{bd} - \partial_d \Gamma^a_{bc} + \Gamma^l_{bd} \Gamma^a_{lc} - \Gamma^l_{bc} \Gamma^a_{ld}. \tag{A.4}$$

This tensor is also called the curvature tensor. The curvature tensor is often derived when solving for parallel transport of a vector, and the commutator of covariant derivatives. In addition, the curvature tensor provides an important check on the relationship of a given space to Euclidean space. If $R^a{}_{bcd} = 0$ for all of space then the space *must* be flat or Euclidean.

The Riemann tensor is related to the commutator of covariant derivatives operating on a vector:

$$(\nabla_a \nabla_b - \nabla_b \nabla_a) V^c = \nabla_{[a} \nabla_{b]} V^c = \frac{1}{2} R^c{}_{dab} V^d. \tag{A.5}$$

Therefore, only in flat space, when $R^a{}_{bcd} = 0$, will covariant derivatives commutate.

A.7 Ricci tensor

The Ricci tensor is formed by contracting on the first and fourth indices of the Riemann tensor,

$$R_{bc} \equiv R^d{}_{bcd} = g_{ad} R^a{}_{bcd}. \tag{A.6}$$

This tensor is used extensively in general relativity, as it is part of the definition for the Einstein tensor.

A.7.1 Ricci scalar

The Ricci scalar is the contraction of the Ricci tensor on its two indices. As a scalar, this is an invariant measure of curvature. The Ricci scalar is

$$R \equiv R^a{}_a = g_{ab} R^b{}_a. \tag{A.7}$$

The Ricci scalar is also used in the definition of the Einstein tensor. As a scalar, the Ricci scalar is an invariant measure of curvature.

A.8 Killing vector

A Killing vector, K^a, is a solution to the following equation:

$$\mathcal{L}_K g_{ab} = 0, \tag{A.8}$$

which states that the Lie derivative along the vector K^a of the metric is zero. This vector K^a implies a constant of motion along a direction, and leads to symmetries in the spacetime itself. For instance, if K^a were a timelike vector, then this would imply that there is a conserved quantity which can be associated with the energy. A good choice of coordinates can leverage a Killing vector. Generally, this is called a set of coordinates adapted to the Killing vector, and the Killing vector can be written as $K^a = (0, 0, 0, 1)$.

Appendix B

Equations

B.1 (2+1)+1 form

$$n^a \, \partial_a \phi \;=\; -\Pi + ie(n^a A_a) \, \phi \tag{B.1}$$

$$n^c \partial_c \Pi \;=\; (K + \chi)\Pi - {}^2\!\Delta^a \, \Phi_a - \Phi^a \Big[{}^2\!\Delta_a \ln(\alpha s) - ieA_a \Big]$$
$$+ ie(n^a A_a) \, \Pi + \frac{e^2}{s^2} \, A_\varphi^2 \, \phi + \frac{2a_2}{a_0} \, \frac{\partial V}{\partial \phi^*} \tag{B.2}$$

$$n^a \partial_a s \;=\; -s\chi \tag{B.3}$$

$$n^a \partial_a \chi \;=\; (K + \chi)\chi - \frac{1}{\alpha s} \, {}^2\!\Delta^a (\alpha \cdot {}^2\!\Delta_a s) - \frac{a_0}{2} \frac{e^2}{s^2} \, A_\varphi^2 |\phi|^2 - \frac{a_2}{2} \, V$$
$$+ \frac{s^2}{4} \frac{1}{d^2} \Big\{ [u^2 \epsilon_{ab} - a_1 s A_\varphi \, {}^2\!F_{ab}]^2 - 2[{}^2 \epsilon_{ab} \, {}^2\!\Delta^b w + a_1 s A_\varphi E_a]^2 \Big\}$$
$$+ \frac{a_1}{8} \Big\{ \frac{1}{d^2} \Big[({}^2\!F_{ab} \, s^3 + u A_\varphi \, {}^2 \epsilon_{ab})^2 - 2({}^2\!E_a \, s^3 - A_\varphi \, {}^2 \epsilon_{ab} \, {}^2\!\Delta^b w)^2 \Big]$$
$$+ \frac{2}{s^2} \Big[({}^2\!\Delta_a A_\varphi)^2 - P^2 \Big] \Big\} \tag{B.4}$$

$$n^a \partial_a A_\varphi \;=\; -P \tag{B.5}$$

$$n^a \partial_a P \;=\; (K - \chi)P - \frac{s}{\alpha} {}^2\!\Delta^a \Big(\frac{\alpha}{s} \cdot {}^2\!\Delta_a A_\varphi \Big) + \frac{a_0}{a_1} \, e^2 A_\varphi |\phi|^2$$
$$- \frac{s^2}{2} \frac{1}{d^2} \Big\{ -2 \Big[a_1 \, s A_\varphi \cdot {}^2\!E_a + {}^2 \epsilon_{ab} \cdot {}^2\!\Delta^b w \Big] \cdot \Big[{}^2\!E^a \, s^3 - A_\varphi \cdot {}^2 \epsilon^{ac} \, {}^2\!\Delta_c w \Big]$$
$$\Big[a_1 \, s \, A_\varphi \, {}^2\!F_{ab} - u \, {}^2 \epsilon_{ab} \Big] \cdot \Big[{}^2\!F^{ab} \, s^3 + u A_\varphi \cdot {}^2 \epsilon^{ab} \Big] \Big\} \tag{B.6}$$

$$n^a \partial_a w \;=\; -u \tag{B.7}$$

$$n^a \partial_a u \;=\; Ku - \frac{d}{\alpha} {}^2\!\Delta^a \Big(\frac{\alpha}{d} \cdot {}^2\!\Delta_a w \Big) + \frac{u}{d} \cdot n^a \partial_a d$$
$$+ \frac{a_1}{2} \, d \Big\{ {}^2 \epsilon_{ab} {}^2\!F^{ab} \, n^c \partial_c \Big(\frac{s}{d} A_\varphi \Big) - 2 \cdot {}^2 \epsilon_{ab} {}^2\!E^a \cdot {}^2\!\Delta^b \Big(\frac{s}{d} A_\varphi \Big) \Big\} \tag{B.8}$$

73

$$
\begin{aligned}
0 \;=\;& {}^2\Delta_a\, {}^2E^a + {}^2\epsilon_{ab}\cdot {}^2\Delta^a w \cdot {}^2\Delta^b\!\Big(\frac{A_\varphi}{s^3}\Big) \\[4pt]
&+ \Big[\,{}^2E_a - {}^2\epsilon_{ab}\cdot\frac{A_\varphi}{s^3}\cdot {}^2\Delta^b w\,\Big]\cdot {}^2\Delta^a \ln\!\Big(\frac{s^4}{d}\Big) \\[4pt]
&- \frac{a_0}{a_1}\frac{ie}{2}\,[\phi\,\Pi^* - \phi^*\,\Pi]\,\frac{d}{s^3} \tag{B.9}
\end{aligned}
$$

$$
\begin{aligned}
h_{ab}\,n^c\partial_c E^b \;=\;& -\frac{1}{\alpha}\,h_{ab}\,{}^2E^c\partial_c\beta^b - h_{ab}\,\frac{1}{\alpha\sqrt{h}}\,\partial_c\big(\alpha\sqrt{h}\,{}^2F^{cb}\big) + K\cdot {}^2E_a \\[4pt]
&+ {}^2\epsilon_{ab}\,\frac{1}{s^3}\Big[(3\chi A_\varphi - P)\,{}^2\Delta^b w - (3A_\varphi\frac{1}{s}{}^2\Delta^b s - {}^2\Delta^b A_\varphi)\,u\Big] \\[4pt]
&+ \Big[\,{}^2F_{ab} + \frac{u}{s^3}\,A_\varphi\,{}^2\epsilon_{ab}\Big]\cdot {}^2\Delta^b \ln\!\Big(\frac{s^4}{d}\Big) \\[4pt]
&- \Big[\,{}^2E_a - \frac{A_\varphi}{s^3}\,{}^2\epsilon_{ab}\,{}^2\Delta^b w\,\Big]\cdot n^c\partial_c\!\Big(\frac{s^4}{d}\Big) \\[4pt]
&- \frac{a_0}{a_1}\frac{ie}{2}\Big[\phi\,\Phi_a^* - \phi^*\,\Phi_a\Big]\,\frac{d}{s^3} \tag{B.10}
\end{aligned}
$$

$$
{}^2\epsilon^{ab}\,n^c\partial_c\,{}^2F_{ab} \;=\; \frac{2}{\alpha}\,{}^2\epsilon^{ab}\,{}^2F_{ac}\partial_b\beta^c - 2\cdot {}^2\epsilon^{ab}\,\frac{1}{\alpha}\,{}^2\Delta_a(\alpha\,{}^2E_b) \tag{B.11}
$$

$$
0 \;=\; -{}^2F_{ab} + h_a{}^c h_b{}^d(\partial_c{}^2A_d - \partial_d{}^2A_c) \tag{B.12}
$$

$$
h_{ab}\cdot n^c\partial_c\,{}^2A^b \;=\; -h_{ab}\frac{1}{\alpha}\,{}^2A^c\partial_c\beta^b + 2\,K_{ab}\,{}^2A^b + \frac{1}{\alpha}\cdot {}^2\Delta_a(\alpha\cdot n^b A_b) - {}^2E_a \tag{B.13}
$$

$$
n^a\partial_a(n^b A_b) \;=\; (K+\chi)\,(n^a A_a) + \frac{1}{\alpha s}\,{}^2\Delta_a(\alpha s\cdot {}^2A^a) \tag{B.14}
$$

$$
\begin{aligned}
{}^2R - K_a{}^b K_b{}^a \;=\;& -(K+2\chi)K + \frac{2}{s}\,{}^2\Delta_a{}^2\Delta^a s \\[4pt]
&+ \frac{a_0}{2}\Big[|\Pi|^2 + |{}^2\Phi^a|^2 + \frac{e^2}{s^2}\,A_\varphi^2\,|\phi|^2\Big] + a_2\,V \\[4pt]
&+ \frac{s^2}{4d^2}\Big\{(a_1\,s\,A_\varphi\,{}^2F_{ab} - u\,{}^2\epsilon_{ab})^2 + 2\,(a_1\,s\,A_\varphi\,{}^2E_a + {}^2\epsilon_{ab}\,{}^2\Delta^b w)^2\Big\} \\[4pt]
&+ \frac{a_1}{4d^2}\Big\{({}^2F_{ab}\,s^3 + uA_\varphi\,{}^2\epsilon_{ab})^2 + 2\,({}^2E_a\,s^3 - A_\varphi\,{}^2\epsilon_{ab}\,{}^2\Delta^b w)^2\Big\} \\[4pt]
&+ \frac{a_1}{2}\frac{1}{s^2}\Big[({}^2\Delta_a A_\varphi)^2 + P^2\Big] \tag{B.15}
\end{aligned}
$$

$$
\begin{aligned}
{}^2\Delta_a K_b{}^a \;=\;& {}^2\Delta_b(K+\chi) + \chi\,{}^2\Delta_b\ln s - \frac{1}{s}\,{}^2\Delta_a s\cdot K^a{}_b \\[4pt]
&+ \frac{a_0}{4}\Big[\Pi\,\Phi_b^* + \Pi^*\,\Phi_b\Big] + \frac{a_1}{2s^2}\,P\cdot {}^2\Delta_b A_\varphi \\[4pt]
&+ \frac{s^2}{2d^2}\Big[a_1\,s\,A_\varphi\,{}^2F_{bc} - u\,{}^2\epsilon_{bc}\Big]\Big[a_1\,s\,A_\varphi\,{}^2E^c + {}^2\epsilon^{cd}\,{}^2\Delta_d w\Big] \\[4pt]
&+ \frac{a_1}{2d^2}\Big[{}^2E_a\,s^3 - A_\varphi\,{}^2\epsilon_{ac}\,{}^2\Delta^c w\Big]\Big[{}^2F_b{}^a\,s^3 + uA_\varphi\,{}^2\epsilon_b{}^a\Big] \tag{B.16}
\end{aligned}
$$

$$
{}^2\Delta_a\,{}^2\Delta^a\alpha \;=\; \alpha\Bigg\{ -n^a\partial_a(K+\chi) + (K+\chi)^2 + {}^2R - \frac{2}{s}\,{}^2\Delta_a{}^2\Delta^a s - {}^2\Delta_a\ln s\,{}^2\Delta^a\ln\alpha
$$
$$
-\frac{a_0}{2}\,|{}^2\Phi_a|^2 - \frac{a_0}{2}\frac{e^2}{s^2}\,A_\varphi^2\,|\phi|^2 - \frac{3}{2}\,a_2\,V
$$
$$
-\frac{a_1}{8\,d^2}\Big[({}^2F_{ab}\,s^3 + uA_\varphi\,{}^2\epsilon_{ab})^2 + 2\,({}^2E_a\,s^3 - A_\varphi\,{}^2\epsilon_{ab}\,{}^2\Delta^b w)^2\Big]
$$
$$
-\frac{a_1}{4}\Big[({}^2\Delta_a A_\varphi)^2 + P^2\Big] - \frac{s^2}{4d^2}\Big[a_1\,s\,A_\varphi\cdot{}^2F_{ab} - u\,{}^2\epsilon_{ab}\Big]^2\Bigg\} \qquad (\text{B.17})
$$

$$
\partial_t h_{ab} \;=\; \beta^c\partial_c h_{ab} + h_{ac}\partial_b\beta^c + h_{bc}\partial_a\beta^c - 2\alpha\,h_{bc}K_a{}^c \qquad\qquad\qquad (\text{B.18})
$$

$$
\partial_t K_a{}^b \;=\; \beta^c\partial_c K_{ab} + K_c{}^b\partial_a\beta^c - K_a{}^c\partial_c\beta^b + \alpha\,(K+\chi)K_a{}^b + \alpha\cdot{}^2R_a{}^b - {}^2\Delta_a\,{}^2\Delta^b\alpha
$$
$$
-\frac{\alpha}{s}\,{}^2\Delta_a\,{}^2\Delta^b s - \frac{a_0\alpha}{4}\Big[{}^2\Phi_a\cdot({}^2\Phi^b)^* + ({}^2\Phi_a)^*\cdot{}^2\Phi^b\Big] - \frac{a_2\alpha}{2}\,h_a{}^b\,V
$$
$$
-\frac{\alpha s^2}{2\,d^2}\Big[\,({}^2\epsilon_{ac}\,u - a_1\,s\,A_\varphi\cdot{}^2F_{ac})({}^2\epsilon^{bc}\,u - a_1\,s\,A_\varphi\cdot{}^2F^{bc})
$$
$$
-({}^2\epsilon_{ac}\cdot{}^2\Delta^c w + a_1\,s\,A_\varphi\cdot{}^2E_a)({}^2\epsilon^{bd}\cdot{}^2\Delta_d w + a_1\,s\,A_\varphi\cdot{}^2E^b)\,\Big]
$$
$$
-\frac{a_1\alpha}{2\,s^2}\Big[{}^2\Delta_a A_\varphi\,{}^2\Delta^b A_\varphi - \frac{1}{2}\,h_a{}^b\big(({}^2\Delta_c A_\varphi)^2 - P^2\big)\Big]
$$
$$
-\frac{a_1\alpha}{2\,d^2}\Big[\,({}^2F_{ac}\,s^3 + uA_\varphi\,{}^2\epsilon_{ac})({}^2F^{bc}\,s^3 + uA_\varphi\,{}^2\epsilon^{bc})
$$
$$
-({}^2E_a\,s^3 - A_\varphi\,{}^2\epsilon_{ac}\,{}^2\Delta^c w)({}^2E^b\,s^3 - A_\varphi\,{}^2\epsilon^{bd}\,{}^2\Delta_d w)
$$
$$
-\frac{1}{4}\,h_a{}^b\big(({}^2F_{cd}\,s^3 + uA_\varphi\,{}^2\epsilon_{cd})^2
$$
$$
-2\,({}^2E_c\,s^3 - A_\varphi\,{}^2\epsilon_{cd}\,{}^2\Delta^d w)^2\big)\,\Big] \qquad\qquad (\text{B.19})
$$

B.2 Scalar form

$$\dot{\phi} \;=\; \beta^\rho \phi_{,\rho} + \beta^z \phi_{,z} + ie\,\alpha(n^a A_a)\,\phi - \alpha\,\Pi \tag{B.20}$$

$$\begin{aligned}
\dot{\Pi} \;=\;& \beta^\rho \Pi_{,\rho} + \beta^z \Pi_{,z} + \alpha\,(K+\chi)\Pi \\
& -\frac{1}{sa^2}\Big[(\alpha s(\phi_{,\rho} - ieA_\rho\phi))_{,\rho} + (\alpha s(\phi_{,z} - ieA_z\phi))_{,z} \\
& \qquad\qquad -ie\alpha s A_\rho(\phi_{,\rho} - ieA_\rho\phi) - ie\alpha s A_z(\phi_{,z} - ieA_z\phi) \Big] \\
& +ie(nA)\,\alpha\Pi + \frac{e^2}{s^2}\,\alpha A_\phi^2\,\phi + \frac{2a_2}{a_0}\,\alpha\,\frac{\partial V}{\partial \phi^*}
\end{aligned} \tag{B.21}$$

$$\dot{s} \;=\; \beta^\rho s_{,\rho} + \beta^z s_{,z} - \alpha s\chi \tag{B.22}$$

$$\begin{aligned}
\dot{\chi} \;=\;& \beta^\rho \chi_{,\rho} + \beta^z \chi_{,z} + \alpha(K+\chi)\chi - \frac{1}{a^2 s}\Big[(\alpha s_{,\rho})_{,\rho} + (\alpha s_{,z})_{,z} \Big] - \frac{a_0}{2}\frac{e^2}{s^2}\,\alpha A_\varphi^2\,|\phi|^2 \\
& -\frac{a_2}{2}\,\alpha\,V + \frac{\alpha s^2}{2\,d^2}\Big[(a_1\,s\,A_\varphi\,{}^2F_\rho{}^z - u)^2 - \frac{1}{a^2}(a_1\,s\,A_\varphi\,{}^2E^\rho a^2 + w_{,z})^2 \\
& \qquad\qquad\qquad\qquad\qquad\qquad -\frac{1}{a^2}(a_1\,s\,A_\varphi\,{}^2E^z a^2 - w_{,\rho})^2 \Big] \\
& +\frac{a_1}{4\,d^2}\,\alpha\,\Big[({}^2F_\rho{}^z\,s^3 + uA_\varphi)^2 - \frac{1}{a^2}({}^2E^\rho\,a^2 s^3 - A_\varphi w_{,z})^2 + \frac{d^2}{s^2}\,P^2 \\
& \qquad\qquad -\frac{1}{a^2}({}^2E^z\,a^2 s^3 + A_\varphi w_{,\rho})^2 - \frac{d^2}{a^2 s^2}((A_{\varphi,\rho})^2 + (A_{\varphi,z})^2) \Big] \tag{B.23}
\end{aligned}$$

$$\dot{A}_\phi \;=\; \beta^\rho A_{\varphi,\rho} + \beta^z A_{\varphi,z} - \alpha P \tag{B.24}$$

$$\begin{aligned}
\dot{P} \;=\;& \beta^\rho P_{,\rho} + \beta^z P_{,z} + \alpha(K-\chi)P \\
& -\frac{s}{a^2}\Big[\Big(\frac{\alpha}{s}A_{\varphi,\rho}\Big)_{,\rho} + \Big(\frac{\alpha}{s}A_{\varphi,z}\Big)_{,z} \Big] + \frac{a_0}{a_1}\,e^2\,|\phi|^2\,A_\varphi \\
& -\frac{\alpha s^2}{d^2}\Big[(a_1\,s\,A_\varphi \cdot {}^2F_\rho{}^z - u)({}^2F_\rho{}^z\,s^3 + uA_\varphi) \\
& \qquad\qquad -\frac{1}{a^2}(a_1\,s\,A_\varphi \cdot {}^2E^\rho\,a^2 + w_{,z})({}^2E^\rho\,a^2 s^3 - A_\varphi w_{,z}) \\
& \qquad\qquad -\frac{1}{a^2}(a_1\,s\,A_\varphi \cdot {}^2E^z\,a^2 - w_{,\rho})({}^2E^z\,a^2 s^3 + A_\varphi w_{,\rho}) \Big] \tag{B.25}
\end{aligned}$$

$$\dot{w} \;=\; \beta^\rho w_{,\rho} + \beta^z w_{,z} - \alpha u \tag{B.26}$$

$$\begin{aligned}
\dot{u} \;=\;& \beta^\rho u_{,\rho} + \beta^z u_{,z} + \alpha(K-3\chi)u - \frac{d}{a^2}\Big[\Big(\frac{\alpha}{d}w_{,\rho}\Big)_{,\rho} + \Big(\frac{\alpha}{d}w_{,z}\Big)_{,z} \Big] \\
& +2a_1\,\alpha\,\frac{s}{d}\,A_\varphi(A_\varphi(\chi) - P)\,u \\
& +a_1\,\alpha d\,\Big[{}^2F_\rho{}^z \cdot \frac{s^2}{d^2}\Big(2s^2 A_\varphi\chi - P(s^2 - a_1 A_\varphi^2) \Big) \\
& \qquad\qquad -{}^2E^\rho \cdot \Big(\frac{s}{d}A_\varphi\Big)_{,z} + {}^2E^z \cdot \Big(\frac{s}{d}A_\varphi\Big)_{,\rho} \Big] \tag{B.27}
\end{aligned}$$

$$
^2\dot{E}^\rho = \beta^\rho\,^2E^\rho_{,\rho} + \beta^z\,^2E^\rho_{,z} - (^2E^\rho\beta^\rho_{,\rho} + {}^2E^z\beta^\rho_{,z}) + \alpha K\,^2E^\rho + \frac{1}{a^2}\left(\alpha\,^2F_\rho{}^z\right)_{,z}
$$
$$
+ \frac{\alpha}{a^2 s^3}\Big[\, w_{,z}(3A_\varphi\chi - P) + u\Big(A_{\varphi,z} - 3A_\varphi\,\frac{s_{,z}}{s}\Big)
$$
$$
+ (^2F_\rho{}^z\, s^3 + uA_\varphi)\Big(\frac{4s_{,z}}{s} - \frac{d_{,z}}{d}\Big)
$$
$$
+ (^2E^\rho\, a^2 s^3 - A_\varphi w_{,z})\Big(\chi + 2a_1\frac{s}{d}A_\varphi(A_\varphi\chi - P)\Big)
$$
$$
- \frac{a_0}{a_1}\frac{ie}{2}\, d(\phi\cdot\Phi^*_\rho - \phi^*\cdot\Phi_\rho)\,\Big] \tag{B.28}
$$

$$
^2\dot{E}^z = \beta^\rho\,^2E^z_{,\rho} + \beta^z\,^2E^z_{,z} - (^2E^\rho\beta^z_{,\rho} + {}^2E^z\beta^z_{,z}) + \alpha K\,^2E^z - \frac{1}{a^2}\left(\alpha\,^2F_\rho{}^z\right)_{,\rho}
$$
$$
- \frac{\alpha}{a^2 s^3}\Big[\, w_{,\rho}(3A_\varphi\chi - P) + u\Big(A_{\varphi,\rho} - 3A_\varphi\,\frac{s_{,\rho}}{s}\Big)
$$
$$
+ (^2F_\rho{}^z\, s^3 + uA_\varphi)\Big(\frac{4s_{,\rho}}{s} - \frac{d_{,\rho}}{d}\Big)
$$
$$
- (^2E^z\, a^2 s^3 + A_\varphi w_{,\rho})\Big(\chi + 2a_1\frac{s}{d}A_\varphi(A_\varphi\chi - P)\Big)
$$
$$
+ \frac{a_0}{a_1}\frac{ie}{2}\, d(\phi\cdot\Phi^*_z - \phi^*\cdot\Phi_z)\,\Big] \tag{B.29}
$$

$$
^2\dot{F}_{\rho z} = \beta^\rho\,^2F_{\rho z,\rho} + \beta^z\,^2F_{\rho z,\rho} + {}^2F_{\rho z}(\beta^\rho_{,\rho} + \beta^z_{,z}) - (\alpha\,^2E^z a^2)_{,\rho}
$$
$$
+ (\alpha\,^2E^\rho a^2)_{,z} \tag{B.30}
$$

$$
(n^b A_b)^{\cdot} = \beta^\rho(n^b A_b)_{,\rho} + \beta^z(n^b A_b)_{,z} + \alpha(K + \chi)(n^b A_b)
$$
$$
+ \frac{1}{a^2 s}\Big[(\alpha s\cdot{}^2A_\rho)_{,\rho} + (\alpha s\cdot{}^2A_z)_{,z}\Big] \tag{B.31}
$$

$$
^2\dot{A}^\rho = \beta^\rho\,^2A^\rho_{,\rho} + \beta^z\,^2A^\rho_{,z} - (^2A^\rho\beta^\rho_{,\rho} + {}^2A^z\beta^\rho_{,z}) + 2\alpha(K_\rho{}^\rho\,^2A^\rho + K_\rho{}^z\,^2A^z)
$$
$$
+ \frac{1}{a^2}\Big[(\alpha\,(n^b A_b))_{,\rho} - \alpha^2 E^\rho a^2\Big] \tag{B.32}
$$

$$
^2\dot{A}^z = \beta^\rho\,^2A^z_{,\rho} + \beta^z\,^2A^z_{,z} - (^2A^\rho\beta^z_{,\rho} + {}^2A^z\beta^z_{,z}) + 2\alpha(K_\rho{}^z\,^2A^\rho + K_z{}^z\,^2A^z)
$$
$$
+ \frac{1}{a^2}\Big[(\alpha\,(n^b A_b))_{,z} - \alpha^2 E^z a^2\Big] \tag{B.33}
$$

$$
0 = \frac{1}{a^2}(^2E_{\rho,\rho} + {}^2E_{z,z}) - \frac{1}{a^2}\Big[\Big(\frac{A_\varphi}{s^3}\Big)_{,\rho} w_{,z} - \Big(\frac{A_\varphi}{s^3}\Big)_{,z} w_{,\rho}\Big]
$$
$$
+ \Big[^2E^\rho - \frac{A_\varphi}{a^2 s^3} w_{,z}\Big]\Big[\frac{4s_{,\rho}}{s} - \frac{d_{,\rho}}{d}\Big]
$$
$$
+ \Big[^2E^z + \frac{A_\varphi}{a^2 s^3} w_{,\rho}\Big]\Big[\frac{4s_{,z}}{s} - \frac{d_{,z}}{d}\Big] \tag{B.34}
$$

$$
0 = -^2F_{\rho z} + {}^2A_{z,\rho} - {}^2A_{\rho,z} \tag{B.35}
$$

$$
\begin{aligned}
0 \;=\; & \frac{1}{a^2}(\ln a^2)_{,\rho\rho} + \frac{1}{a^2}(\ln a^2)_{,zz} + \frac{2}{a^2 s}(s_{,\rho\rho} + s_{,zz}) \\[4pt]
& + K_\rho{}^{\rho 2} + 2\,K_\rho{}^{z2} + K_z{}^{z2} - (K+2\chi)K \\[4pt]
& + \frac{a_0}{2}\Big[\,|\Pi|^2 + \frac{1}{a^2}|\Phi_\rho|^2 + \frac{1}{a^2}|\Phi_z|^2 + \frac{e^2}{s^2}A_\varphi^2\,|\phi|^2\,\Big] + a_2 V \\[4pt]
& + \frac{s^2}{2\,d^2}\Big[\,(a_1\,s\,A_\varphi{}^2 F_\rho{}^z - u)^2 + \frac{1}{a^2}(a_1\,s\,A_\varphi{}^2 E^\rho a^2 + w_{,z})^2 \\[4pt]
& \hspace{5cm} + \frac{1}{a^2}(a_1\,s\,A_\varphi{}^2 E^z a^2 - w_{,\rho})^2\,\Big] \\[4pt]
& + \frac{a_1}{2\,d^2}\Big[\,({}^2F_\rho{}^z s^3 + uA_\varphi)^2 + \frac{1}{a^2}({}^2E^\rho\,a^2 s^3 - A_\varphi w_{,z})^2 \\[4pt]
& \hspace{5cm} + \frac{1}{a^2}({}^2E^z\,a^2 s^3 + A_\varphi w_{,\rho})^2\,\Big] \\[4pt]
& + \frac{a_1}{2}\,\frac{1}{s^2}\Big[\,\frac{1}{a^2}\big((A_{\varphi,\rho})^2 + (A_{\varphi,z})^2\big) + P^2\,\Big] \hspace{2cm} \text{(B.36)} \\[12pt]
K_\rho{}^\rho{}_{,\rho} + K_\rho{}^z{}_{,z} \;=\; & (K+\chi)_{,\rho} - \frac{a_{,\rho}}{a}(K_\rho{}^\rho - K_z{}^z) + \frac{s_{,\rho}}{s}(\chi - K_\rho{}^\rho) - \Big(\frac{2a_{,z}}{a} + \frac{s_{,z}}{s}\Big)K_\rho{}^z \\[4pt]
& + \frac{a_0}{4}[\Pi\Phi_\rho^* + \Pi^*\Phi_\rho] + \frac{a_1}{2s^2}\,P\,A_{\varphi,\rho} \\[4pt]
& + \frac{s^2}{2\,d^2}(a_1\,s\,A_\varphi{}^2 F_\rho{}^z - u)(a_1\,s\,A_\varphi{}^2 E^z a^2 - w_{,\rho}) \\[4pt]
& + \frac{a_1}{2\,d^2}\,({}^2E^z\,a^2 s^3 + A_\varphi w_{,\rho})({}^2F_\rho{}^z s^3 + uA_\varphi) \hspace{1.5cm} \text{(B.37)} \\[12pt]
K_\rho{}^z{}_{,\rho} + K_z{}^z{}_{,z} \;=\; & (K+\chi)_{,z} + \frac{a_{,z}}{a}(K_\rho{}^\rho - K_z{}^z) + \frac{s_{,z}}{s}(\chi - K_z{}^z) - \Big(\frac{2a_{,\rho}}{a} + \frac{s_{,\rho}}{s}\Big)K_\rho{}^z \\[4pt]
& + \frac{a_0}{4}[\Pi\Phi_z^* + \Pi^*\Phi_z] + \frac{a_1}{2s^2}\,P\,A_{\varphi,z} \\[4pt]
& - \frac{s^2}{2\,d^2}(a_1\,s\,A_\varphi{}^2 F_\rho{}^z - u)(a_1\,s\,A_\varphi{}^2 E^\rho a^2 + w_{,z}) \\[4pt]
& - \frac{a_1}{2\,d^2}\,({}^2E^\rho\,a^2 s^3 - A_\varphi w_{,z})({}^2F_\rho{}^z s^3 + uA_\varphi) \hspace{1.5cm} \text{(B.38)} \\[12pt]
\alpha_{,\rho\rho} + \alpha_{,zz} \;=\; & \alpha a^2 \Big\{ -n^a\partial_a(K+\chi) + (K+\chi)^2 - \frac{1}{a^2}\big[(\ln a^2)_{,\rho\rho} + (\ln a^2)_{,zz}\big] \\[4pt]
& - \frac{2}{a^2 s}(s_{,\rho\rho} + s_{,zz}) - \frac{1}{a^2}\Big(\frac{s_{,\rho}}{s}\frac{\alpha_{,\rho}}{\alpha} + \frac{s_{,z}}{s}\frac{\alpha_{,z}}{\alpha}\Big) \\[4pt]
& - \frac{a_0}{2}\frac{1}{a^2}[|\Phi_\rho|^2 + |\Phi_z|^2] - \frac{a_0}{2}\frac{e^2}{s^2}A_\varphi^2\,|\phi|^2 - \frac{3}{2}a_2 V \\[4pt]
& - \frac{s^2}{2\,d^2}(a_1\,s\,A_\varphi{}^2 F_\rho{}^z - u)^2 \\[4pt]
& - \frac{a_1}{4\,d^2}\Big[\,({}^2F_\rho{}^z s^3 + uA_\varphi)^2 + \frac{1}{a^2}({}^2E^\rho\,a^2 s^3 - A_\varphi w_{,z})^2 \\[4pt]
& \hspace{5cm} + \frac{1}{a^2}({}^2E^z\,a^2 s^3 + A_\varphi w_{,\rho})^2\,\Big] \\[4pt]
& - \frac{a_1}{4\,s^2}\Big[\,\frac{1}{a^2}\big((A_{\varphi,\rho})^2 + (A_{\varphi,z})^2\big) + P^2\,\Big]\Big\} \hspace{1.5cm} \text{(B.39)}
\end{aligned}
$$

$$\frac{\dot{a}}{a} = \beta^\rho \frac{a_{,\rho}}{a} + \beta^z \frac{a_{,z}}{a} + \beta^\rho_{,\rho} - \alpha\, K_\rho{}^\rho \tag{B.40}$$

$$\frac{\dot{a}}{a} = \beta^\rho \frac{a_{,\rho}}{a} + \beta^z \frac{a_{,z}}{a} + \beta^z_{,z} - \alpha\, K_z{}^z \tag{B.41}$$

$$0 = \beta^\rho_{,z} + \beta^z_{,\rho} - 2\alpha\, K_\rho{}^z \tag{B.42}$$

$$
\begin{aligned}
\dot{K}_\rho{}^\rho =\ & \beta^\rho K_\rho{}^\rho{}_{,\rho} + \beta^z K_\rho{}^\rho{}_{,z} + K_\rho{}^z(\beta^z_{,\rho} - \beta^\rho_{,z}) + \alpha(K+\chi)K_\rho{}^\rho \\
& -\frac{\alpha}{2\,a^2}\Big[(\ln a^2)_{,\rho\rho} + (\ln a^2)_{,zz}\Big] - \alpha\frac{a_2}{2}\,V \\
& -\frac{1}{a^2}\Big[\alpha_{,\rho\rho} - \frac{a_{,\rho}}{a}\,\alpha_{,\rho} + \frac{a_{,z}}{a}\,\alpha_{,z}\Big] - \frac{\alpha}{a^2 s}\Big[s_{,\rho\rho} - \frac{a_{,\rho}}{a}\,s_{,\rho} + \frac{a_{,z}}{a}\,s_{,z}\Big] \\
& -\frac{\alpha}{a^2}\left\{ \frac{s^2}{2\,d^2}\Big[a^2(u - a_1\,s\,A_\varphi\,{}^2F_\rho{}^z)^2 - (a_1\,s\,A_\varphi\,{}^2E^\rho a^2 + w_{,z})^2\Big] \right. \\
& \qquad\qquad + \frac{a_1}{4\,d^2}\Big[a^2({}^2F_\rho{}^z\,s^3 + uA_\varphi)^2 - ({}^2E^\rho\,a^2 s^3 - A_\varphi w_{,z})^2 \\
& \qquad\qquad\qquad\qquad\qquad + ({}^2E^z\,a^2 s^3 + A_\varphi w_{,\rho})^2\Big] \\
& \qquad\qquad \left. + \frac{a_0}{2}\,|\,\Phi_\rho|^2 + \frac{a_1}{4\,s^2}\Big[(A_{\varphi,\rho})^2 - (A_{\varphi,z})^2 + P^2 a^2\Big] \right\}
\end{aligned}
\tag{B.43}
$$

$$
\begin{aligned}
\dot{K}_z{}^z =\ & \beta^\rho K_z{}^z{}_{,\rho} + \beta^z K_z{}^z{}_{,z} - K_\rho{}^z(\beta^z_{,\rho} - \beta^\rho_{,z}) + \alpha(K+\chi)K_z{}^z \\
& -\frac{\alpha}{2\,a^2}\Big[(\ln a^2)_{,\rho\rho} + (\ln a^2)_{,zz}\Big] - \alpha\frac{a_2}{2}\,V \\
& -\frac{1}{a^2}\Big[\alpha_{,zz} + \frac{a_{,\rho}}{a}\,\alpha_{,\rho} - \frac{a_{,z}}{a}\,\alpha_{,z}\Big] - \frac{\alpha}{a^2 s}\Big[s_{,zz} + \frac{a_{,\rho}}{a}\,s_{,\rho} - \frac{a_{,z}}{a}\,s_{,z}\Big] \\
& -\frac{\alpha}{a^2}\left\{ \frac{s^2}{2\,d^2}\Big[a^2(u - a_1\,s\,A_\varphi\,{}^2F_\rho{}^z)^2 - (a_1\,s\,A_\varphi\,{}^2E^z a^2 - w_{,\rho})^2\Big] \right. \\
& \qquad\qquad + \frac{a_1}{4\,d^2}\Big[a^2({}^2F_\rho{}^z\,s^3 + uA_\varphi)^2 + ({}^2E^\rho\,a^2 s^3 - A_\varphi w_{,z})^2 \\
& \qquad\qquad\qquad\qquad\qquad - ({}^2E^z\,a^2 s^3 + A_\varphi w_{,\rho})^2\Big] \\
& \qquad\qquad \left. + \frac{a_0}{2}\,|\,\Phi_z|^2 + \frac{a_1}{4\,s^2}\Big[(A_{\varphi,z})^2 - (A_{\varphi,\rho})^2 + P^2 a^2\Big] \right\}
\end{aligned}
\tag{B.44}
$$

$$
\begin{aligned}
\dot{K}_\rho{}^z =\ & \beta^\rho K_\rho{}^z{}_{,\rho} + \beta^z K_\rho{}^z{}_{,z} + K_\rho{}^z(\beta^\rho_{,\rho} - \beta^z_{,z}) - \beta^z_{,\rho}(K_\rho{}^\rho - K_z{}^z) + \alpha(K+\chi)K_\rho{}^z \\
& -\frac{1}{a^2}\Big[\alpha_{,\rho z} - \frac{a_{,z}}{a}\,\alpha_{,\rho} - \frac{a_{,\rho}}{a}\,\alpha_{,z}\Big] - \frac{\alpha}{a^2 s}\Big[s_{,\rho z} - \frac{a_{,z}}{a}\,s_{,\rho} - \frac{a_{,\rho}}{a}\,s_{,z}\Big] \\
& -\frac{\alpha}{a^2}\left\{ \frac{s^2}{2\,d^2}(w_{,z} + a_1\,s\,A_\varphi\,{}^2E^\rho a^2)(w_{,\rho} - a_1\,s\,A_\varphi\,{}^2E^z a^2) \right. \\
& \qquad\qquad - \frac{a_1}{2\,d^2}\,({}^2E^\rho\,a^2 s^3 - A_\varphi w_{,z})({}^2E^z\,a^2 s^3 + A_\varphi w_{,\rho}) \\
& \qquad\qquad \left. + \frac{a_0}{4}\Big[\Phi_\rho\,(\Phi_z)^* + (\Phi_\rho)^*\,\Phi_z\Big] + \frac{a_1}{4\,s^2}\,A_{\varphi,\rho}\,A_{\varphi,z} \right\}
\end{aligned}
\tag{B.45}
$$

Appendix C

Origin ring evolution

Figure C.1 displays a complete evolution of the A_φ field where the initial amplitude is $A_0 = 0.07$, and the profile is a ring. The first frames show the field as it propagates outward and inward. The colourmap and "vertical" scale are auto-adjusting to keep the data visible, but the final scale is an order of magnitude smaller. This evolution is another case where the numerical code terminated with an error. It is possible to see some collection of matter near the origin, but recall that the scale is an order of magnitude smaller.

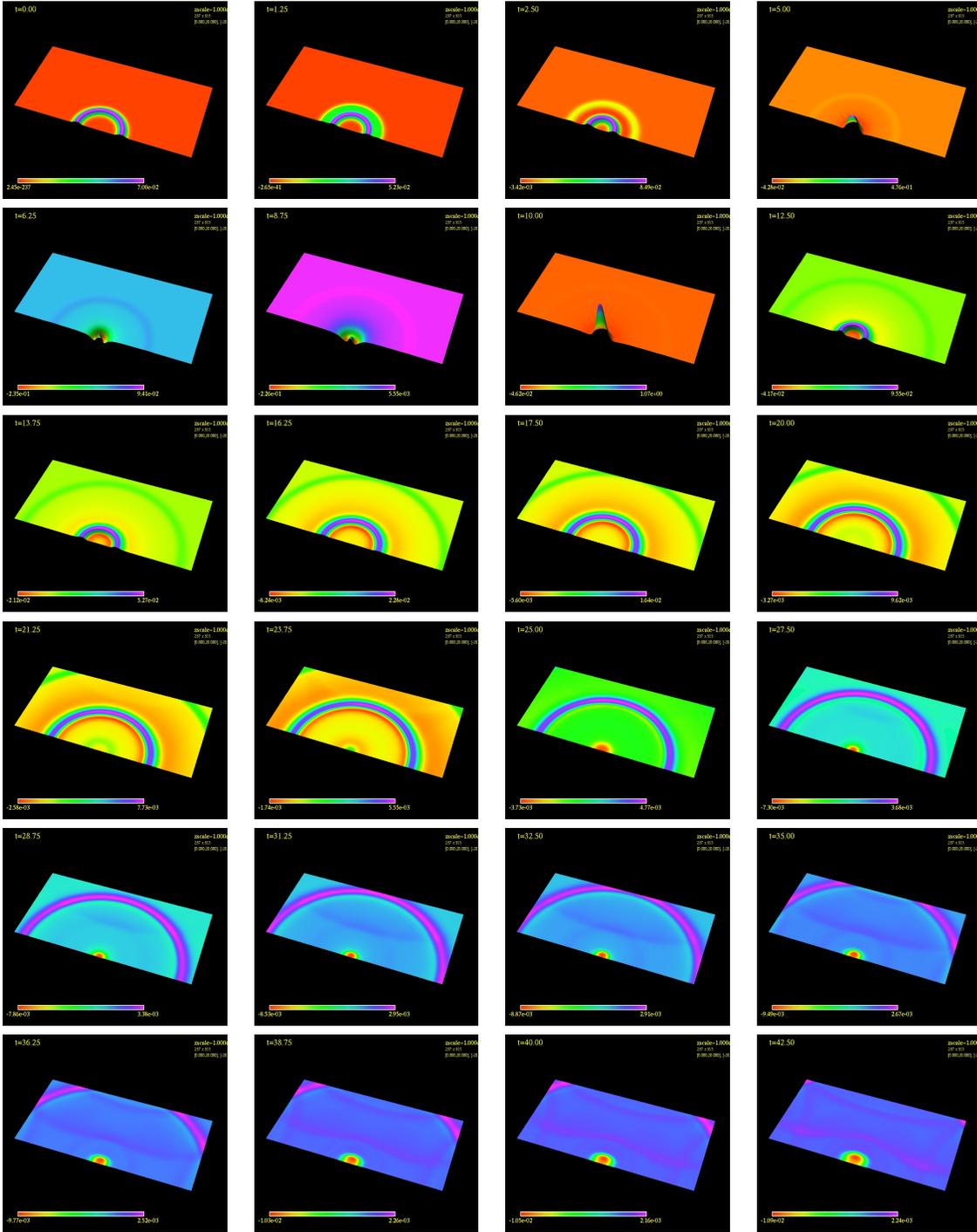This table of images should be read left-to-right, top-to-bottom.

Figure C.1: The evolution of the A_ϕ field with an initial amplitude of 0.07. This table should be read left-to-right, top-to-bottom.

Bibliography

[1] M. W. Choptuik, E. W. Hirschmann, S. L. Liebling, and F. Pretorius, Classical and Quantum Gravity **20**, 1857 (2003).

[2] R. D'Inverno, *Introducing Einstein's Relativity*, Oxford University Press, 2000.

[3] R. D. Blandford and R. L. Znajek, Royal Astronomical Society, Monthly Notices **179**, 433 (1977).

[4] T. W. Baumgarte and S. L. Shapiro, Astrophysical Journal **585**, 921 (2003).

[5] T. W. Baumgarte and S. L. Shapiro, Astrophysical Journal **585**, 930 (2003).

[6] M. Choptuik, Physical Review Letters **70**, 9 (1993).

[7] E. W. Hirschmann and D. M. Eardley, Physical Review D **51**, 4198 (1995).

[8] S. Hod and T. Piran, Physical Review D **55**, 3485 (1997).

[9] A. M. Abrahams and C. R. Evans, Physical Review Letters **70**, 2980 (1993).

[10] C. Gundlach, Living Rev. Rel. **2**, 4 (1999).

[11] E. Poisson, *A Relativist's Toolkit: The Mathematics of Black-Hole Mechanics*, Cambridge University Press, 2004.

[12] R. Arnowitt, S. Deser, and C. W. Misner, *The dynamics of general relativity*, Wiley, 1962.

[13] A. Garcia, *Numerical Methods for Physics (2nd Edition)*, Prentice Hall, 1999.

[14] M. C. Robert Marsa, The rnpl reference manual, `http://laplace.physics.ubc.ca/People/marsa/rnpl/refman/refman.html`.

[15] L. C. Evans, *Partial Differential Equations*, American Mathematical Society, 1998.

[16] A. Pasini, European Journal of Physics **9**, 289 (1988).

[17] M. W. Choptuik, *Experiences with an Adaptive Mesh Refinement Algorithm in Numerical Relativity*, pages 206–+, Frontiers in Numerical Relativity, 1989.

[18] M. Christiansen, Black spaghetti: A numerical model of gravitational collapse in 4 + 1 spacetime, Master's thesis, Brigham Young University, 2005.

[19] M. Dalarsson and N. Dalarsson, *Tensors, Relativity, and Cosmology*, Elsevier Academic Press, 2005.